Short Circuit Modeling of Wind Turbine Generators

A Thesis Submitted

to the College of Graduate Studies and Research

in

Partial Fulfillment of the Requirements

for the M.Sc. Degree

in the Department of Electrical and Computer Engineering
University of Saskatchewan

by

Sriram Chandrasekar

Saskatoon, Saskatchewan, Canada

© Copyright Sriram Chandrasekar, August, 2013. All rights reserved.

Permission to Use

In presenting this thesis in partial fulfillment of the requirements for a Postgraduate degree from the University of Saskatchewan, it is agreed that the Libraries of this University may make it freely available for inspection. Permission for copying of this thesis in any manner, in whole or in part, for scholarly purposes may be granted by the professors who supervised this thesis work or, in their absence, by the Head of the Department of Electrical and Computer Engineering or the Dean of the College of Graduate Studies and Research at the University of Saskatchewan. Any copying, publication, or use of this thesis, or parts thereof, for financial gain without the written permission of the author is strictly prohibited. Proper recognition shall be given to the author and to the University of Saskatchewan in any scholarly use which may be made of any material in this thesis.

Request for permission to copy or to make any other use of material in this thesis in whole or in part should be addressed to:

Head of the Department of Electrical and Computer Engineering
57 Campus Drive
University of Saskatchewan
Saskatoon, Saskatchewan, Canada
S7N 5A9

Acknowledgments

First of all, I would like to acknowledge and extend my heartfelt gratitude to Prof. Rama Gokaraju for his patient and thoughtful guidance and support that motivated and inspired me to successfully complete my research work and thesis. I would like to thank Prof. Rama Gokaraju and Prof. Mohindar Singh Sachdev for providing funding from their NSERC Discovery Grants.

I would like to thank the faculty of the Department of Electrical and Computer Engineering at the University of Saskatchewan for providing the foundation for my research work through courses and for the Department scholarship. I am thankful to Dean Miller, Chair of the C17 joint working group (Fault current contributions from wind plants) of the IEEE Power System Relaying Committee for providing me with utility wind farm fault data. I owe special thanks to the engineers from Electranix Corporation, Winnipeg, Canada for their invaluable support and discussions while modeling the Type 3 wind farm. I am thankful to Prof. Ramamoorty Mylavarapu (Retired. Formerly with IIT, Kanpur and Central Power Research Institute, India) for his suggestions and critical review of the research work. I would also like to thank Dr. Dharshana Muthumani from the Manitoba HVDC Research Centre, Winnipeg, Canada for his valuable input during the course of the research work with respect to validating the developed wind generator models against their models.

I thank all of the students from the Power Systems Simulation Laboratory for a pleasant working atmosphere and the continuous support they gave me. I also thank my family and friends, without whom this would not have been possible. I especially thank my brother Arvind Vyas for always being an inspiration to me.

—Sriram Chandrasekar

Dedicated

to my

late father

Abstract

Modeling of wind farms to determine their short circuit contribution in response to faults is a crucial part of system impact studies performed by power utilities. Short circuit calculations are necessary to determine protective relay settings, equipment ratings and to provide data for protection coordination.

The plethora of different factors that influence the response of wind farms to short circuits makes short circuit modeling of wind farms an interesting, complex, and challenging task. Low voltage ride through (LVRT) requirements make it necessary for the latest generation of wind generators to be capable of providing reactive power support without disconnecting from the grid during and after voltage sags. If the wind generator must stay connected to the grid, a facility has to be provided to by-pass the high rotor current that occurs during voltage sags and prevent damage of the rotor side power electronic circuits. This is done through crowbar circuits which are of two types, namely active and passive crowbars, based on the power electronic device used in the crowbar triggering circuit. Power electronics-based converters and controls have become an integral part of wind generator systems like the Type 3 doubly fed induction generator based wind generators. The proprietary nature of the design of these power electronics makes it difficult to obtain the necessary information from the manufacturer to model them accurately. Also, the use of power electronic controllers has led to phenomena such as sub-synchronous control interactions (SSCI) in series compensated Type 3 wind farms which are characterized by non-fundamental frequency oscillations. SSCI affects fault current magnitude significantly and is a crucial factor that cannot be ignored while modeling series compensated Type 3 wind farms.

These factors have led to disagreement and inconsistencies about which techniques are appropriate for short circuit modeling of wind farms. Fundamental frequency models like voltage behind transient reactance model are incapable of representing the majority of critical wind generator fault characteristics such as sub-synchronous interactions. The Detailed time domain models, though accurate, demand high levels of computation and modeling expertise. Voltage dependent current source modeling based on look up tables are not stand-alone

models and provide only a black-box type of solution.

The short circuit modeling methodology developed in this research work for representing a series compensated Type 3 wind farm is based on the generalized averaging theory, where the system variables are represented as time varying Fourier coefficients known as dynamic phasors. The modeling technique is also known as dynamic phasor modeling. The Type 3 wind generator has become the most popular type of wind generator, making it an ideal candidate for such a modeling method to be developed.

The dynamic phasor model provides a generic model and achieves a middle ground between the conventional electromechanical models and the cumbersome electromagnetic time domain models. The essence of this scheme to model a periodically driven system, such as power converter circuits, is to retain only particular Fourier coefficients based on the behavior of interest of the system under study making it computationally efficient and inclusive of the required frequency components, even if non-fundamental in nature. The capability to model non-fundamental frequency components is critical for representing sub-synchronous interactions. A 450 MW Type 3 wind farm consisting of 150 generator units was modeled using the proposed approach. The method is shown to be highly accurate for representing faults at the point of interconnection of the wind farm to the grid for balanced and unbalanced faults as well as for non-fundamental frequency components present in fault currents during sub-synchronous interactions. Further, the model is shown to be accurate also for different degrees of transmission line compensation and different transformer configurations used in the test system.

Table of Contents

List of Tables

List of Figures

List of Symbols and Abbreviations

C	Capacitance of the DC-link capacitor
C_{line}	Series compensation
$DFIG$	Doubly fed induction generator
EMT	Electromagnetic transient
$ERCOT$	Electric reliability council of Texas
f_m	Frequency of rotation of the rotor
$FACTS$	Flexible AC transmission systems
FFT	Fast Fourier transform
f_r	Rotor field frequency
f_s	Stator field frequency
GSC	Grid side converter
H	Inertia constant
i_{dc}	Current through the DC-link capacitor
$i_{g,d}, i_{g,q}$	d and q components of grid side converter current
$i_{r,d}, i_{r,q}$	d and q components of rotor side converter current
$i_{s,d}, i_{s,q}$	d and q components of stator current
i_d, i_q	d and q axis currents in the transmission line
$i_{t,d}, i_{t,q}$	d and q axis transformer current

$IGBT$	Insulated gate bipolar transistor
I_L	Lower limit of fault current at inception of fault
${i_{r,d}}^*, {i_{r,q}}^*$	Reference d and q components of rotor side converter current
${i_{g,d}}^*, {i_{g,q}}^*$	Reference d and q components of grid side converter current
I_s	Stator current
I_sc	Short circuit current
I_U	Upper limit of fault current at inception of fault
K_I	Integral time constants
K_P	Proportional controller gains
K	Set of Fourier coefficients
L_{line}	Inductance of the transmission line
l	Leakage factor
$LVRT$	Low voltage ride through
L_m	Mutual inductance between stator and rotor
L_s, L_r	Stator and rotor leakage inductance
L_t	Transformer inductance
m_d, m_q	Modulation indices of the PWM converter
$MISO$	Midwest independent transmission system operator
ω_r	Rotor speed
ω_s	Synchronous speed
$POCC$	Point of common coupling

POI	Point of interconnection
P_r, P_g	Real power flow at rotor side and grid side converters
P_s, Q_s	Stator real and reactive power
$P_s{}^*, Q_s{}^*$	Stator real and reactive power references
$R_{IGBT-ON}$	IGBT ON resistance
$R_{IGBT-OFF}$	IGBT OFF resistance
$R_{IGBT-ON-GSC}$	IGBT ON resistance - GSC side
$R_{IGBT-ON-RSC}$	IGBT ON resistance - RSC side
R_{line}	Resistance of the transmission line
$R_{r_{ext}}$	Rotor external resistance
$R_{crowbar}$	Rotor crowbar resistance
RSC	Rotor side converter
RMS	Root mean square
R_s, R_r	Stator and rotor resistance
R_t	Transformer resistance
R_L	Transmission line resistance
$\psi_{s,d}, \psi_{s,q}$	d and q components of stator flux linkage
$\psi_{r,d}, \psi_{r,q}$	d and q components of rotor flux linkage
$SCIG$	Squirrel cage induction generator
$SSCI$	Sub-synchronous control interaction
$STATCOM$	Static compensator

SSR	Sub synchronous resonance
σ	Slip
T_e	Electrical torque
T_m	Mechanical torque
T_r	Rotor damping time constant
T_s	Stator damping time constant
$TCSC$	Thyristor controlled series capacitor
$TSAT$	Transient security assessment tool
$UPFC$	Unified power flow controller
$V_{s,d}, V_{s,q}$	d and q components of stator voltage
$V_{r,d}, V_{r,q}$	d and q components of rotor voltage
$v_{s,d} v_{s,q}$	d and q axis stator voltages
$v_{c,d}, v_{c,q}$	d and q axis voltages across the series capacitor compensation
$v_{b,d}, v_{b,q}$	d and q axis infinite bus voltages
$v_{pri,d}, v_{pri,q}$	d and q axis primary side transformer voltage
$v_{sec,d}, v_{sec,q}$	d and q axis secondary side transformer voltage
V_∞	Infinite bus voltage
V_{dc-LL}	Lower threshold limit of DC-link voltage
${V_{r,d}}^*, {V_{r,q}}^*$	Reference d and q components of rotor voltage
${V_{dc}}^*$	Reference DC-link capacitor voltage
V_{dc-UL}	Upper threshold limit of DC-link voltage

V_{dc}	Voltage across the DC-link capacitor
VSC	Voltage source converter
VSG	Voltage sag generator
VBR	Voltage behind transient reactance
$WRIG$	Wound rotor induction generator
$WECS$	Wind energy conversion system
$x(\tau)$	Complex time domain periodic signal
X_k	k^{th} Fourier coefficient
$\langle x \rangle_k(t), X_k(t)$	k^{th} dynamic phasor
X_m	Mutual reactance
X_r	Rotor reactance
X_C	Reactance of series compensating capacitor
X_s	Stator reactance
X'	Transient reactance
X_L	Transmission line reactance
Z'	Transient impedance

Chapter 1

Introduction

1.1 Background

The global integration of renewable sources of power into the power grid has been growing significantly. A number of renewable energy technologies like wind power, photovoltaics, hydro power, and biomass have become widely installed. This trend has been driven by growing concerns over climate change, ever increasing power consumption, and the need to reduce dependence on fossil fuels, which as of 2010 provide about 80 percent of the world's energy (Figure 1.1). Figure 1.2 shows the power supply distribution for the USA for the year 2009. From 2006 to 2011, solar photovoltaics and wind power grew at annual average rates of 58 and 26 percent, respectively, which are very high when compared to growth rates for fossil fuel power generation for the same period [2].

Advances in technology for optimal extraction of power from renewable sources, along with the associated decrease in cost and government policies with fiscal incentives supporting the growth of renewable power, have factored into the marked integration of renewable power sources. For instance, a new energy agreement was reached in Denmark in March 2012 that contains initiatives to bring Denmark closer to a target of 100 percent renewable energy in the energy and transport sector by 2050. Ontario's Green Energy and Green Economy Act of 2009 established a feed-in-tariff programme that offers payments for renewable energy power generation above market prices [1].

As important as it is to integrate renewable sources of energy into the grid, it is equally important to ensure that the reliable operation of the system is maintained, considering the

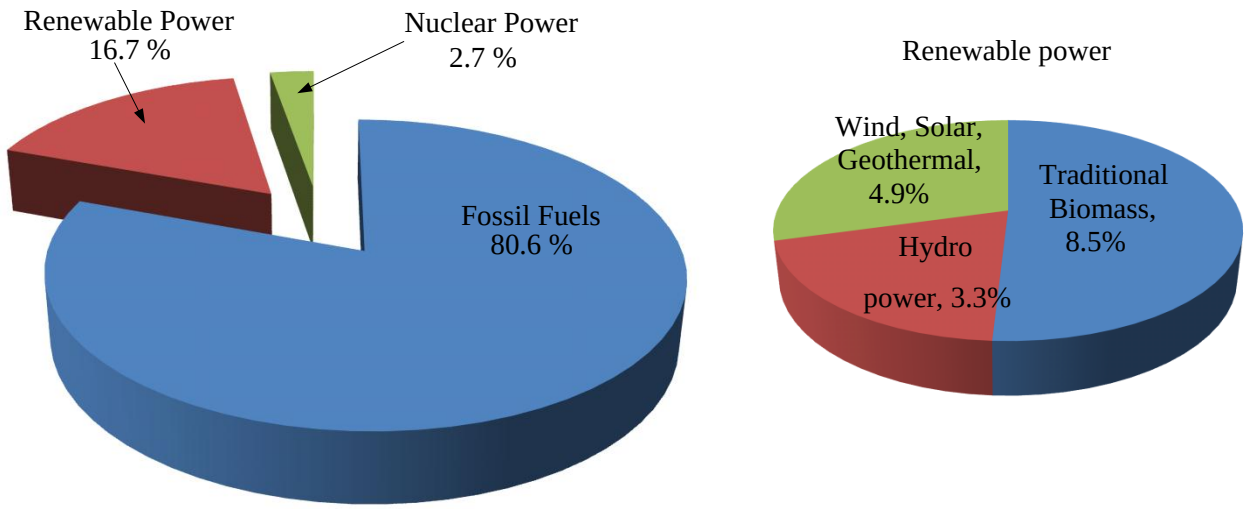

Figure 1.1: Renewable energy contribution to global power production, 2010 [1]

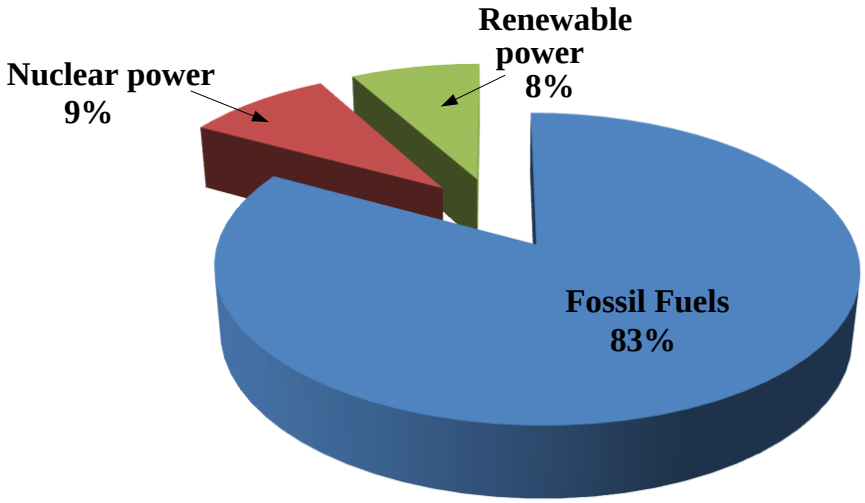

Figure 1.2: Renewable energy contribution to power production in the USA, 2009

intermittent nature of renewable sources such as wind power. This necessitates being able to accurately model their behavior to perform valid system impact studies.

1.2 Wind Power

1.2.1 Wind Power Trends

Wind power underwent significant growth from 2000 to 2012, as shown in Figure 1.3. Global wind power capacity by the end of 2012 was approximately 282 GW, with the largest capacity addition of approximately 45 GW in 2012. Figure 1.4 shows the installed wind power in different regions of the world up to the end of 2011 and in 2012. This growth trend has continued with many countries setting targets to increase the wind energy contribution to as high as 20 percent by 2020.

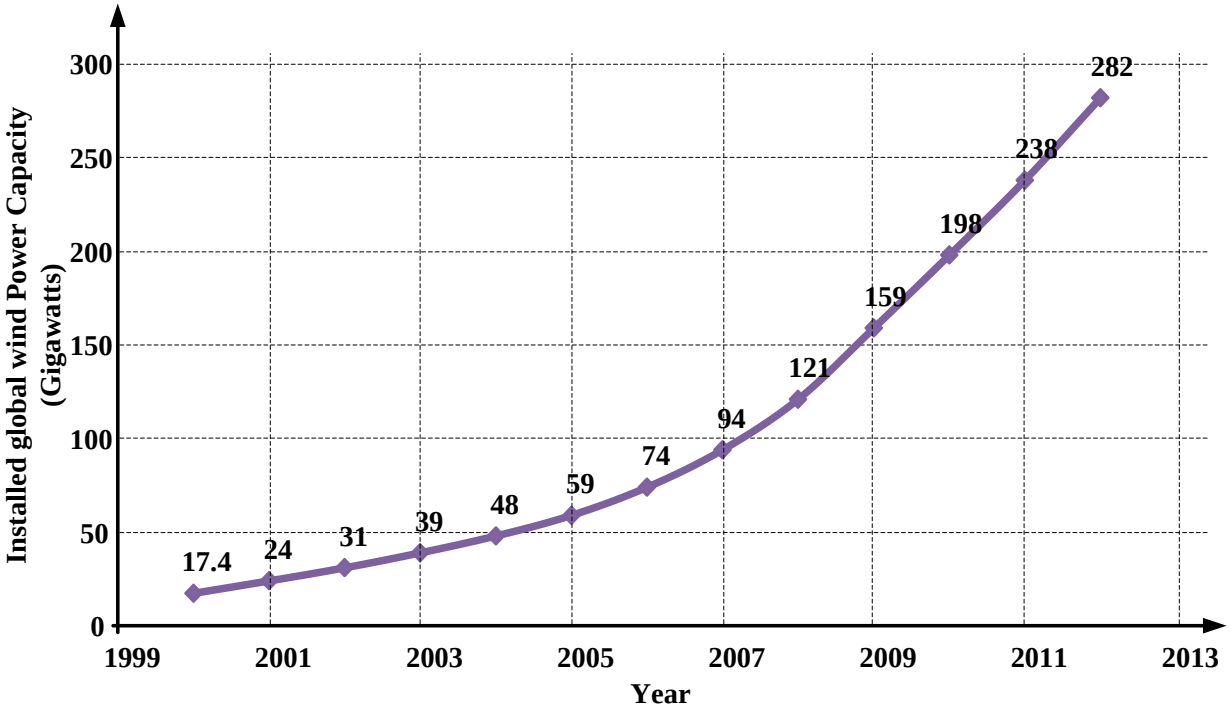

Figure 1.3: Growth of wind power installed capacity from 2000 to 2012(GW)

Wind is an intermittent source of power with a low capacity factor (the amount of output a power plant produces divided by the amount it would have produced, had it been in operation 24 hours/day, 365 days/year) of 20 to 40 percent [3]. Apart from blade pitch angle control, which varies the pitch of the blade according to the speed of the wind, wind generators (except Type 1 wind generators) utilize power electronics to deal with wind variability.

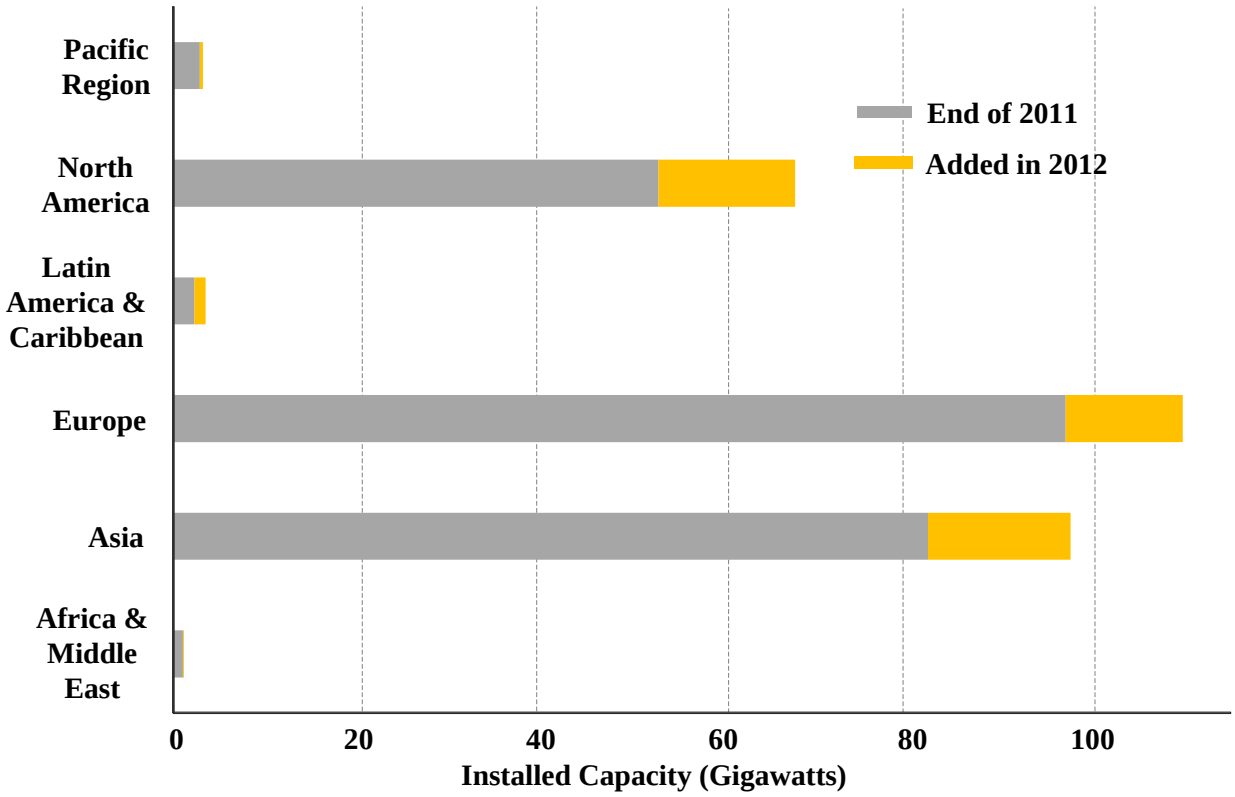

Figure 1.4: Growth of wind power installed capacity in 2012(GW)

Wind turbine generators are classified into four types based on the control strategies that are used to deal with wind variability, namely Type 1 (Squirrel cage induction generator), Type 2 (Wound rotor induction generator), Type 3 (Doubly fed induction generator), and Type 4 (Full converter based wind generator).

With respect to market penetration of a particular type of wind generator, Type 3 wind turbine generators have gained the highest popularity among the different types. Figure 1.5 shows the global trend in market penetration of the four types of wind generators [4] as well as the wind generator types used in the Electric Reliability Council of Texas (ERCOT) system [5]. Type 3 wind generator technology, which was introduced in 1996, has been and continues to be the most installed type among the four wind generator types. This factor, along with the need to model the complex behavior of the Type 3 wind generator and its controls, make it an ideal candidate for performing modeling studies.

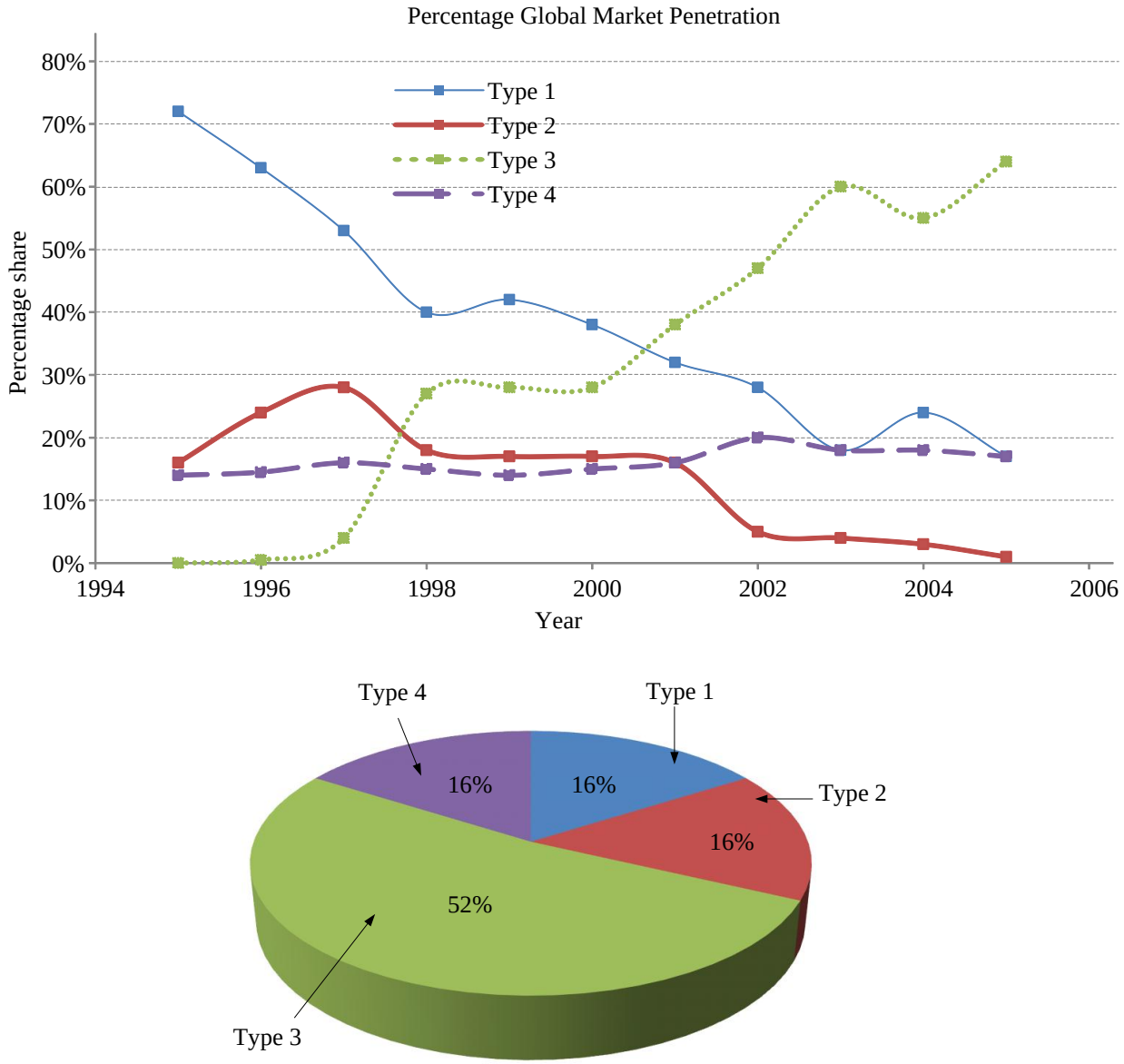

Figure 1.5: Trend in market penetration of different types of wind generators

1.2.2 Short Circuit Modeling of Wind Generators and Challenges

It is crucial that system impact studies are done before integrating any new generation into the existing power grid, with studies of the short circuit contribution being a critical task. Short circuit levels must be assessed to accurately design protective relay settings, determine equipment ratings, and for protection coordination. As the accuracy of relay

settings is crucial to prevent the mal-operation of relays, it is important for short circuit levels, and hence the short circuit models, to be accurate. In order to assess the behavior of wind generators and their response to system faults, appropriate models of these wind generators have to be developed.

Short circuit faults can occur in the power system due to different reasons, the single line to ground fault being the most commonly occurring. Short circuit characteristics of synchronous machines are well defined, as the technology has existed for several years and accurate models are available to predict their short circuit contribution. However, this is not the case for wind generator technology, which is relatively new and is constantly evolving.

Of the existing types of wind turbine generators, the Type 3 wind generator and its short circuit modeling are the main focus of this thesis. As will be discussed in Chapter 2, it is relatively less complex to model the short circuit behavior of the other types of wind generators as compared to the Type 3 wind generator. The short circuit modeling of a Type 3 wind generator is more complex than even the Type 4 wind generator, as the usage of a full power converter in the latter implies that the fault current is limited by the rating of the converter.

The influence of many factors, including LVRT (low voltage ride through) defined by grid codes, wind farm aggregation, and control algorithms used by different manufacturers, contribute to the increased complexity of the Type 3 wind generator. The need to add series compensation on transmission lines that deliver power from remote high wind locations to load centers has also led to undesired interactions [6] that affect the short circuit behavior of wind farms, particularly the Type 3 wind farm. The proprietary nature of information about wind generators also makes it difficult to obtain this information from manufacturers.

The focus of this thesis is to develop short circuit models to allow the design of accurate protection for wind generators with the ability to also design controls. The model is generic and does not need detailed models for all of the exact internals of the wind generators. The model could be used by protection engineers in utilities to design protection and control settings for wind farms without the need to model the wind farm in detail. Various short

circuit modeling techniques have been developed and utilized to model the short circuit behavior of the different types of wind generators. The choice of the appropriate modeling technique for a particular wind generator depends on the extent to which that technique can accurately represent the complexities unique to that wind generator.

Recent practice in the power industry has been to study the behavior of wind farms and model them with fundamental frequency synchronous generator equivalents. This is a simplified method of modeling the wind farm's behavior and does not ensure a high level of accuracy. Due to power electronic converters employed in the energy conversion systems of wind generators, it is very difficult to accurately represent short circuit behavior with these fundamental frequency representations.

Electromagnetic transient (EMT) modeling, which models power system components in the form of time domain dq0 equations, is the modeling technique used as a benchmark model to validate the other modeling techniques. This is due to the fact that electromagnetic transient modeling has the ability to model every component of the test system in detail and includes all of the associated frequency components. Even though EMT modeling is highly accurate and detailed, it is a cumbersome process for modeling a large and complex system, such as a type 3 wind farm consisting of multiple wind generators, and is computationally demanding.

Developing a model that is accurate, instead of compromising with fundamental frequency representations, and at the same time not as cumbersome as the detailed EMT model is crucial. Simplifying the modeling of power systems yet retaining the essential system characteristics based on the purpose of the study in hand [7–9] is needed. This calls for developing a middle ground between the detailed EMT and fundamental frequency models; this is the main focus of the modeling technique proposed in this research work.

1.3 Literature Review

1.3.1 Short Circuit Modeling of Type 1 and Type 2 Generators

1.3.1.1 Type 1 Wind Generator

Several techniques have been proposed in the literature to model the short circuit behavior of wind turbine generators. This section summarizes such efforts to model Type 1 and Type 2 wind generators. The first generation of utility-sized wind turbine generators was Type 1 wind generators based on a squirrel cage induction generator [10] with blade pitch angle control as the only wind power control mechanism. This design has the advantages of mechanical simplicity, high efficiency, and low maintenance requirements [11].

Induction motors have significant fault current contributions and the fault current contribution of induction motors can be characterized by performing a series of tests [12].The typical fault behavior of an induction motor can be described in terms of the symmetrical and DC components present in the stator fault current. The DC component is a significant part of the fault current and should be included for protection design purposes [12].

The instantaneous peak fault current at the application of the fault is the most important quantity to be obtained, as this determines the rating of the protective relaying [13]. An expression for the short circuit current as a function of rotor and stator time constants is derived and compared with the results from tests on real induction machines, indicating that the model provides adequate representation. A similar approach is defined in [14] where the short circuit contribution is derived in the form of an analytical expression for an induction machine. In [15] and [16], the analytical expression modeling is used for short circuit modeling of Type 1 wind generators. These works show that the short circuit current of a Type 1 wind generator can be accurately obtained from the analytical expression of the stator fault current.

A technique based on voltage behind transient reactance (VBR) representation is presented in [17] to model the short circuit behavior for Type 1 wind generators for symmetrical

and unsymmetrical fault conditions. The modeling is based on developing a VBR representation by using sequence component networks and solving for the fault current at the inception of the fault. The results are verified against an EMT simulation model of the test system and show a high level of accuracy for the Type 1 wind generator.

1.3.1.2 Type 2 Wind Generator

The Type 2 wind generator utilizes a wound rotor induction generator (WRIG) in which the electrical characteristics of the rotor can be externally controlled by connecting a variable resistance [11]. Though the Type 2 wind generator is more expensive and power is dissipated as losses in the external resistance, it provides an improved operating speed range compared to the Type 1 wind generator configuration.

In [18] and [19], the short circuit behavior of a Type 2 wind generator and equivalencing of the wind farm collector system are discussed. The external rotor resistance value affects the damping of the short circuit current, with higher rotor resistance contributing to more damping. Further, a Type 2 wind farm model is built both with and without inclusion of the impedances of the cables connecting the individual wind generators to the main transformer at the substation and the fault behavior observed. The cable impedances can be completely neglected for short circuit studies on Type 2 wind farms for faults outside the wind farm. However, this is not true for faults within the wind farm.

1.3.2 Short Circuit Modeling of Type 3 Generators

1.3.2.1 Modeling Complexities

Type 3 wind generators like the Type 2 wind generators utilize a wound rotor induction generator. However, the rotor winding in a Type 3 wind generator is connected to the stator side by means of a bi-directional back-to-back voltage source converter (VSC). The different modeling complexities of Type 3 wind generators are discussed in the literature with an objective to simplify their representation yet not compromise the accuracy of the developed

model.

Wind Farm Aggregation:

A wind farm typically consists of tens of wind turbine generators arranged in a manner to maximize wind capture and connected to the main substation through cables forming the collector system. The wind generators are mostly the same type within a wind farm; however, the length of the cables from each unit to the common point of coupling may vary. This is an important modeling complexity not only for studying the transient behavior of Type 3 wind farms but also for all other wind farms in general. The recent trend has been towards an aggregated model for assessing the transient behavior of a wind farm as a whole because it is a cumbersome task to create a detailed model.

References [20], [21] and [22] discuss the impact of aggregating all of the wind turbine generators in a Type 3 wind farm and representing their collective behavior by a single equivalent generator. It is assumed in these studies that all of the generators in the wind farm are of the same type and that all of the wind turbines see the same wind speed. It is also assumed that all units in the wind farm trip for a fault outside it, whereas in reality not all of the units could trip.

These works conclude that, even with these assumptions, the aggregated model provides a good enough approximation of the performance of the wind farm for faults outside the wind farm but is inaccurate for faults inside the wind farm. Due to these reasons, an aggregated model of the Type 3 wind farm is used for the purpose of fault studies to represent the collective behavior [23].

LVRT (Low voltage ride through) Requirements:

In the past, wind farms were allowed to trip and disconnect from the grid during disturbances where the conventional generation units would provide the voltage support. However, this is not acceptable when considering the large amount of wind power generation that has been integrated into the grid in recent times. LVRT requirements defined by utilities make it necessary for wind farms to stay connected to the grid and support the system for normally

cleared disturbances [20]. This is necessary to enable more integration of wind energy into the existing grid and for wind generators to support the voltage and frequency of the grid during and immediately following grid failure due to faults.

Voltage dips due to faults and other disturbances cause a rise in the stator current of the wind generator and also lead to high rotor current through induction. If the wind generator must stay connected to the grid, a facility has to be provided to by-pass this high rotor current and prevent damage of the rotor side power electronic circuits. This is done through crowbar circuits, which give the wind generators the ability to stay connected to the grid during voltage dips [24].

In order to study such voltage dip behaviors, a voltage sag generator is to be modeled and used to apply voltage sags. [25] describes the commonly used voltage sag generator topologies from which the one based on a variable autotransformer is utilized in this research work due to its less complex and cost effective nature.

Reference [24] describes a dq0 model for the Type 3 wind generator where the short circuit behavior is discussed with and without the crowbar circuit in place. With the crowbar included, the wind generator had the ability to stay connected to the grid. A scheme to inject reactive power into the grid for voltage support during the sag is discussed. As soon as the voltage recovers, the crowbar is removed and normal operation is re-established. Even though the crowbar action is described in this work, its relevance to LVRT characteristics and wind generator protection is not sufficiently explained; this thesis describes this in detail. A protection scheme where the unit breaker trips based on the LVRT characteristic defined and the crowbar triggers based on the DC-link voltage value is utilized in this research work.

Reference [26] insists upon the need for LVRT feature and voltage profile maintenance in new wind turbine generator installations as well as retrofitting older generators. It describes the LVRT requirements that wind generators are required to have based on grid codes and also to optimize the active and reactive power support during and immediately after the fault. It is suggested that tripping of the unit is reasonable only for voltages that remain low for longer than 1.5 s.

The research work in this thesis takes into account the LVRT capability for modeling and analyzes its impact on fault behavior of Type 3 wind generators.

Sub-synchronous Control Interactions:

The nature of most wind farms being located far from load centers has made long transmission lines necessary. In order to reduce the impedance of these lines, they are required to be series compensated. Reference [6] shows that un-damped sub-synchronous oscillations, termed sub-synchronous control interactions (SSCI), could potentially occur in Type 3 wind turbine generators with power electronic converters and controls that operate near series compensated transmission lines. SSCI is a control interaction between any power electronic device (such as the converter in Type 3 wind turbines) and a series capacitor.

An analysis of sub-synchronous interactions in a series compensated Type 3 wind farm is done in [27] in order to identify the cause of these interactions. The eigen value analysis performed concludes that the network and the generator have significant participation in the sub-synchronous oscillatory mode.

References [28], [29] and [30] describe different techniques to identify the frequency of the sub-synchronous interactions and also the elements in the system causing them. The analytical method of frequency scanning, where the driving point impedance over the frequency range of interest is calculated when looking into the system from the generator terminals is utilized in this research.

Reference [31] discusses that the control algorithms of power electronics used in wind generators, especially Type 3 wind generators, play a significant role in the occurrence of SSCI. If left unmitigated, these oscillations can cause severe over voltages, current distortion, and damage to the wind farm control circuits, such as in the case of the Texas event in 2009 [32].

Reference [23] recommends that the controller gains of a Type 3 wind generator controls be kept in a particular range to avoid SSCI. The major control loops in the converter controller are identified and an SSCI damping controller proposed in [6] as a mitigation. Other

works to mitigate Type 3 wind farm sub-synchronous control interaction issues are discussed in references [33], [34], and [35].

The above works show the growing importance of the issue of SSCI with respect to assessing the interaction of a Type 3 wind farm with a series compensated transmission line. SSCI introduces sub-synchronous oscillations. This thesis shows that these sub-synchronous oscillations distort the fault current waveforms and therefore impact the short circuit current levels of Type 3 wind farms. This research work studies this effect in detail and a short circuit model that is inclusive of these conditions is developed.

1.3.2.2 Modeling Methods

Reference [14] obtains the fault current contribution of a conventional induction machine in terms of an analytical expression for the short circuit current and then extends its application to a Type 3 wind generator with crowbar protection. Even though this approach includes the crowbar resistance in calculating the short circuit contribution of the Type 3 wind generator, it does not include LVRT based protection. This leads to the assumption that the crowbar is activated throughout the fault duration. It also does not include non-fundamental frequencies as part of the modeling, which means the approach is limited to representing balanced faults.

Reference [36] describes the basic voltage and flux linkage equations of an induction machine. It further transforms the equations to the dq0 reference frame and describes a model that can be used to represent balanced and unbalanced conditions. The transformation to the dq0 reference frame helps eliminate the time varying coefficients that appear in the voltage equations due to mutual inductances and vary as a function of rotor angle. These equations in the dq0 reference frame are used as a basis to develop the EMT model of the generator used in the test system in this thesis.

A voltage dependent current source model is developed in [37] to represent Type 3 and Type 4 wind generator short circuit behavior. This modeling method is a black-box approach and is capable of generating short circuit current characteristics in the form of upper and

lower envelopes of fault currents. The accuracy of this model depends on the level of accuracy of the model used to obtain the fault current envelopes. A detailed EMT model is used in this case to obtain the fault current values. Thus, this method is not a standalone model, as it requires the short circuit current values to be obtained from detailed EMT models or from the wind generator manufacturer, and does not give insight into phenomena such as crowbar activation or sub-synchronous behavior.

Though capable of representing balanced fault conditions fairly accurately, fundamental frequency simplifications are viewed as non-inclusive of other essential non-fundamental frequency components required to represent sub-synchronous interactions, such as in the case of Type 3 wind farms. Detailed EMT models based on dq0 equations of the machine are highly capable of representing the short circuit behavior of a Type 3 wind farm. However, they are computationally demanding as they include all of the frequency components and also provide little insight into control interactions. Also, developing a detailed EMT model would require manufacturer proprietary information, such as control algorithms, which are difficult or impossible to obtain.

Generalized Averaging Theory (or Dynamic Phasor Modeling):

An understanding of the short circuit modeling complexities of a Type 3 wind farm and of the existing modeling techniques is followed by developing a model with the following features:

- It should be capable of representing fault current behavior for balanced faults, unbalanced faults, and faults with sub-synchronous interactions for a Type 3 wind farm.
- This model should be more sophisticated than fundamental frequency models and at the same time simpler than a detailed EMT model. It should also provide insight into designing both protection and controls for wind farms.
- In order for this model to be more computationally efficient than an EMT model, it should have the capacity to selectively model only the required frequency components to accurately represent the desired fault behavior of a Type 3 wind farm.

- The model should be generic in nature, meaning it should not require exact manufacturer proprietary information. A power utility engineer should be able to use the model to design the protection and controls of a Type 3 wind farm without the need to know the exact modeling details.

The generalized averaging scheme which is also currently referred to by some authors as dynamic phasor modeling, was developed by an MIT researcher in 1991 for modeling power converter circuits [38]. It is capable of accommodating arbitrary types of waveforms and is based on time varying Fourier series representation for a sliding time window of a given waveform. The essence of this scheme to model a periodically driven system, such as power converter circuits, is to retain only particular Fourier coefficients based on the behavior of interest of the system under study. Simplifying approximations are made by omitting insignificant terms from the series.

Reference [39] discusses the application of generalized averaging model to large synchronous machines for symmetrical and unsymmetrical fault analysis. It shows that by the choice of appropriate harmonics (Fourier coefficients), the averaged model is capable of accurately capturing faulted dynamics of a synchronous machine.

Reference [40] extends the application of the generalized averaging model to represent the dynamic behavior of a thyristor-controlled series capacitor (TCSC) in a simple yet accurate manner that is faster than detailed time domain simulation. It shows that simply choosing the fundamental frequency harmonic for modeling is not accurate enough to represent TCSC behavior when it is close to resonance, as there is a significant presence of other higher order harmonic components. Other flexible AC transmission systems (FACTS) devices, such as the unified power flow controller (UPFC) in [41], the static VAR compensator (SVC) in [34], and the synchronous static compensator (STATCOM) in [42], have been modeled using dynamic phasors.

References [43] and [44, 45] utilize the generalized averaging scheme to model Type 1 and Type 3 wind generators, respectively, for short circuit modeling. These models dealt with fundamental frequency based modeling and were not sophisticated enough to represent

sub-synchronous frequency control interactions.

The above works in the literature show that there has been a good amount of work on machine modeling of DFIG wind generators but not much research has been done on developing accurate models for fault analysis, including both fundamental and non-fundamental sub-synchronous frequency effects. As discussed above, the generalized averaging scheme using dynamic phasors is a very powerful concept for accurately modeling the Type 3 wind generator and its power electronics. In this thesis, a dynamic phasor model was developed for a Type 3 wind farm, including fundamental and non-fundamental frequencies.

1.3.3 Short Circuit Modeling of Type 4 Generators

Type 4 wind generators utilize an induction machine or a synchronous generator connected to the grid through a full power converter. This makes Type 4 wind generators the most expensive of all types due to the requirement for a power converter that is rated as high as the wind generator itself. Reference [46] shows that the short circuit current of a Type 4 wind generator is regulated and limited to the rating of the power converter. Reference [37] goes further to show that Type 4 wind generators can be represented by a current source with an upper and lower limit based on the power converter rating for short circuit analysis. For these reasons, this thesis does not analyze short circuit modeling Type 4 wind generators in detail.

1.4 Objective of the Thesis

Wind power integration is ever increasing, with the market penetration of Type 3 wind farms far exceeding the other types. Short circuit modeling is a crucial step in understanding the fault behavior of wind generators in order to determine protective relay settings, protection coordination, and equipment ratings. The short circuit modeling of wind generators is affected by a number of factors. This has created inconsistencies in modeling techniques used for wind farm models and there is a need to address this issue by developing an accurate

generic model. The following are the objectives of this thesis in brief:

1. Identify the short circuit modeling complexities unique to each type of wind generator and their degree of influence on short circuit behavior.

2. Determine the accuracy of representing wind generators using conventional short circuit modeling techniques and their shortcomings.

3. Develop an accurate method of modeling the short circuit behavior of wind generators including the identified complexities and test the developed model's capacity to represent different fault behavior.

1.5 Organization of the Thesis

The thesis is organized into six chapters. Chapter 1 sets the background with a discussion of the present scenario of wind power integration and its inevitable nature in today's power supply and demand scenario. Following this, the significance of short circuit modeling of wind generators and the various challenges unique to each type of wind generator are identified. Approaches to wind generator short circuit modeling in the literature are briefly discussed, along with their capabilities and limitations. This is followed by a discussion of the motivation behind the development of a modeling technique that is capable of representing the previously discussed complexities, and which is the primary objective of the thesis.

Chapter 2 explains the types of wind generators and their principles of operation, then characterizes their short circuit behavior. The short circuit modeling complexities and their degree of influence on the short circuit behavior are also discussed for these wind generators.

Chapter 3 provides a critical review of the commonly used techniques for modeling short circuit behavior of wind generators and discusses the results of application of these methods for the different wind generator types. From the obtained results, the accuracy and applicability of these techniques along with their advantages and disadvantages for particular wind generator types are discussed.

In Chapter 4, the critical modeling complexity of Type 3 wind generators namely the sub-synchronous control interactions with series compensated transmission lines is discussed for symmetrical and unsymmetrical fault scenarios along with the frequency analysis of the fault behavior.

In Chapter 5, the dynamic phasor model of a Type 3 wind farm connected to a series compensated transmission line is developed and the accuracy of the model to represent the short circuit behavior is illustrated.

Chapter 6 provides a summary, thesis contributions, and suggestions for future work.

Appendix A gives the parameters of the test systems modeled in this thesis.

Chapter 2

Wind Turbine Generators and their Short Circuit Behavior

2.1 Introduction

The evolution of wind power conversion technology has led to the development of different types of wind turbine configurations that make use of a variety of electric generators. A classification of most common generators used in large wind energy conversion systems (WECS) [47] is presented in Figure 2.1 below.

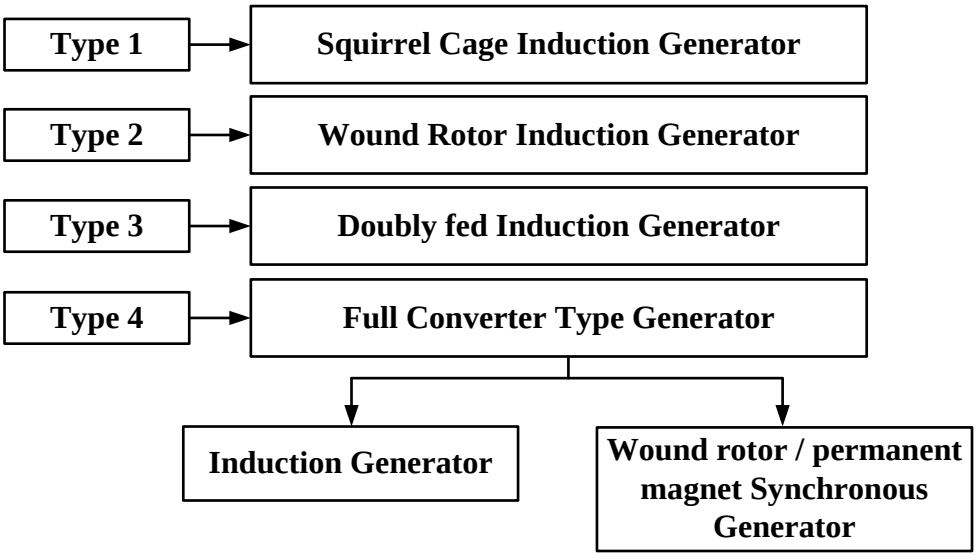

Figure 2.1: Types of wind turbine generators

Section 2.2 discusses the working principles of the different wind generator types and Section 2.3 explains the behavior of wind generators for symmetrical and unsymmetrical

faults.

2.2 Types of Wind Turbine Generators

2.2.1 Type 1 Squirrel Cage Induction Generator

Type 1 wind turbine generators are the first generation and hence the oldest type of wind generators. They consist of a squirrel cage rotor connected to the turbine through a gear box, as shown in Figure 2.2. They operate in the generating mode when driven above synchronous speed, which implies a negative slip. The normal operating slip range is between 0 and -1 percent [46]. Pitch angle control is used to regulate the turbine shaft speed to nearly a constant speed.

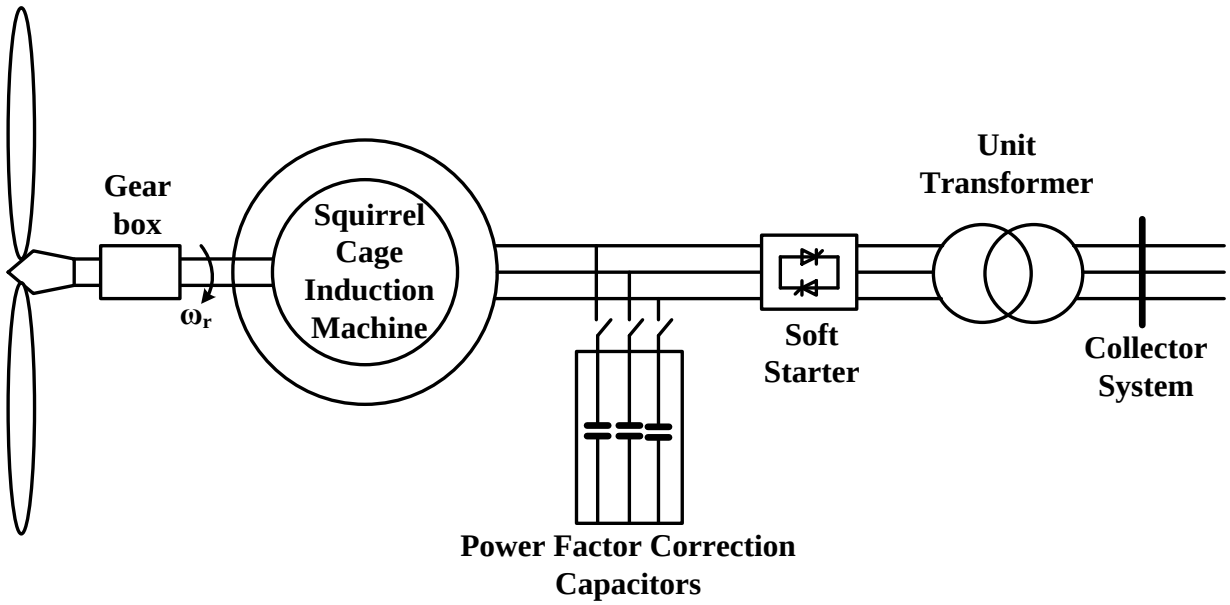

Figure 2.2: Type 1 wind turbine generator

The generator is connected to the wind farm collector system through a soft-starter and a step-up transformer. The soft-starter is employed because the start-up current is very high. Power factor correction capacitors are included at the base of the turbine tower and these serve the purpose of reactive power compensation [48].

2.2.2 Type 2 Wound Rotor Induction Generator

Type 2 wind turbine generators consist of a wound rotor induction generator, which makes connecting external resistances to the rotor winding possible. This provides the ability to operate at a higher range of slip (10 percent) as compared to a Type 1 wind generator [46]. This external resistance can be controlled by a high-frequency switch as shown in Figure 2.3, based on the speed of the wind. The rotor external resistance control is used in combination with pitch angle control to achieve variable slip operation. These controls are employed in such a manner so as to keep the resistive losses due to the external rotor resistance within acceptable limits [46]. This method of control necessitates including the external rotor resistance in fault calculations [48].

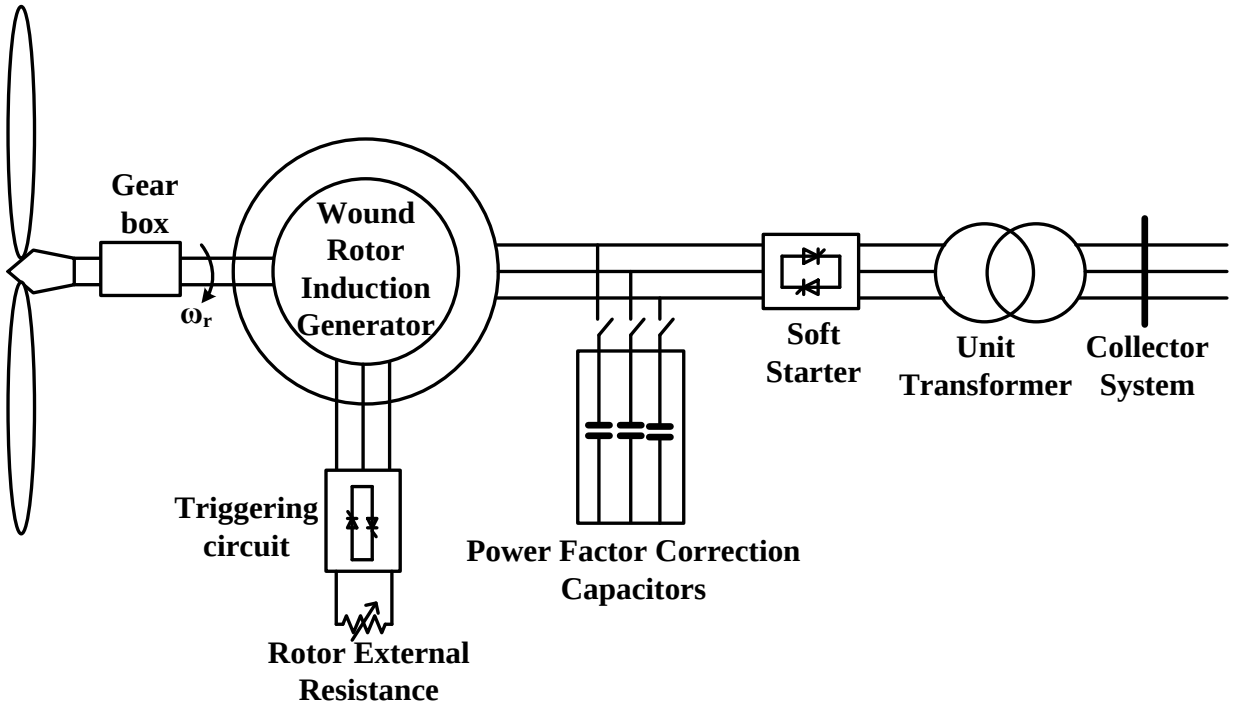

Figure 2.3: Type 2 wind turbine generator

Similar to the Type 1 generator, power factor correction is done using shunt capacitor banks on the generator terminals. The induction machine is connected to the wind farm collector system through a soft-starter and a step-up transformer.

2.2.3 Type 3 Doubly Fed Induction Generator

There has been a fast growing demand for the application of DFIG based wind generators in wind power plants in recent years. Currently, Type 3 wind generators dominate the market due to cost-effective provision of variable-speed operation. A Type 3 wind turbine generator consists of a wound rotor induction generator in which the rotor excitation is supplied by a back-to-back power converter [48]. The rotor speed is allowed to vary within a slip range of $\pm$ 30 percent. This implies that the power converter is rated for about 30 percent of the rated power [46].

As shown in Figure 2.4, the stator is connected directly to the collector system and then to the grid. The rotor is connected to the stator side through a back-to-back power converter that is capable of supplying a rotor excitation of variable magnitude and frequency. The power converter also makes rotor excitation of reversible phase rotation possible, where positive or negative sequence excitation is applied for sub-synchronous and super-synchronous operations, respectively. This variable rotor excitation is applied in such a manner that the net rotor magnetic field is at synchronous speed. The application of such an excitation results in the apparent rotation of the rotor magnetic field with respect to the rotor. The net magnetic field induced in the stator has a frequency f_s given by

$$f_s = f_r \pm f_m \tag{2.1}$$

where f_r is the rotor field frequency and f_m is the frequency of rotation of rotor.

During sub-synchronous operation when the wind speed is lower than the rated wind speed, a positive sequence rotor field excitation is applied so that it is in the same direction as mechanical rotation of the rotor i.e. $f_s = f_r + f_m$. The flow of real power is from the stator to the rotor as shown in Figure 2.4.

During super-synchronous operation when the wind speed is higher than the rated wind speed, a negative sequence rotor field excitation is applied so that it is in the opposite direction as the mechanical rotation of the rotor, i.e., $f_s = f_r - f_m$. In this mode of operation, there is a flow of real power out of the rotor that is converted to grid frequency. This is

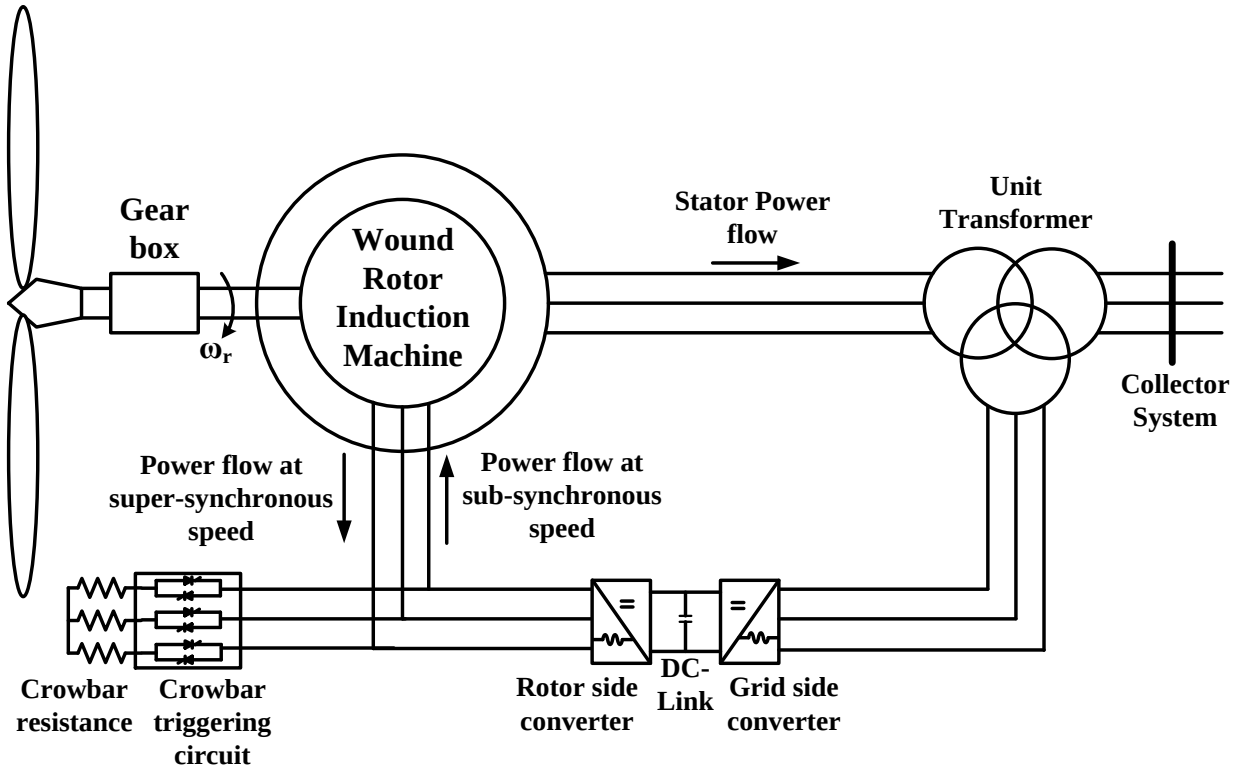

Figure 2.4: Type 3 wind turbine generator

added to the stator power and the net power supplied to the grid is the sum of the rotor and the stator real power outputs [48].

The back-to-back converter enables the Type 3 wind generator to have fast control over the real and reactive power output by controlling the phase angle and the magnitude of the rotor excitation, respectively. The back-to-back converter consists of a rotor side converter (RSC), a grid side converter (GSC), and a DC capacitor. The RSC provides an independent control of the stator side active and reactive power by controlling the q-axis and d-axis rotor current ($i_{r,q}$ and $i_{r,d}$) components, respectively. The RSC needs a DC power supply, which is usually generated by the GSC. A DC capacitor is used to remove the ripple and keep the DC bus voltage relatively smooth [49]. The objective of the GSC is to keep the DC-link voltage at a constant value by controlling the d-axis current ($i_{g,d}$) and regulate the reactive power exchange between the GSC and the grid by controlling the q-axis current ($i_{g,q}$).

The components of the power converter are designed to handle only normal currents and

normal DC bus voltage [46]. When a fault occurs on the stator side of the Type 3 wind generator, high voltages are in turn induced in the rotor, which causes high currents to flow in the power converter. In order to by-pass this high current and to protect the power converter from damage, a crowbar circuit is employed. There are two types of crowbar configurations, namely active and passive crowbars, based on the power electronic device used in the crowbar triggering circuit. The passive crowbar triggering circuit is constructed with thyristors and allows the circuit to close, but does not allow it to open until the crowbar current is extinguished. The active crowbar triggering circuit is constructed with insulated gate bipolar transistors (IGBT) and allows the circuit to open in forced commutation. Though different, both schemes use a resistor to bypass the excessive rotor current [50]. The value of the bypass resistor is of importance but not critical. It should be sufficiently low to avoid too large of a voltage on the converter terminals. On the other hand, it should be high enough to limit the current [24]. Different measures may be used for the crowbar activation, such as rotor AC current or DC bus voltage, as well as different magnitude thresholds for each of these measures [48].

Figure 2.4 shows the passive crowbar configuration; however, both the passive and active crowbar configurations were tested for a temporary three phase fault at the terminals of the generator. Figure 2.5 below shows the difference between how these two schemes operate with respect to activating and deactivating the crowbar circuit during and after the fault occurrence.

Active crowbar control allows the Type 3 wind generator to have LVRT capability, i.e., to reconnect the back-to-back converter as soon as possible after the fault occurrence. LVRT is discussed in detail in Section 2.3. The type of crowbar circuit and the LVRT based protection strategies used affect the short circuit behavior of the Type 3 wind generator and are important complexities that are considered for modeling in this thesis.

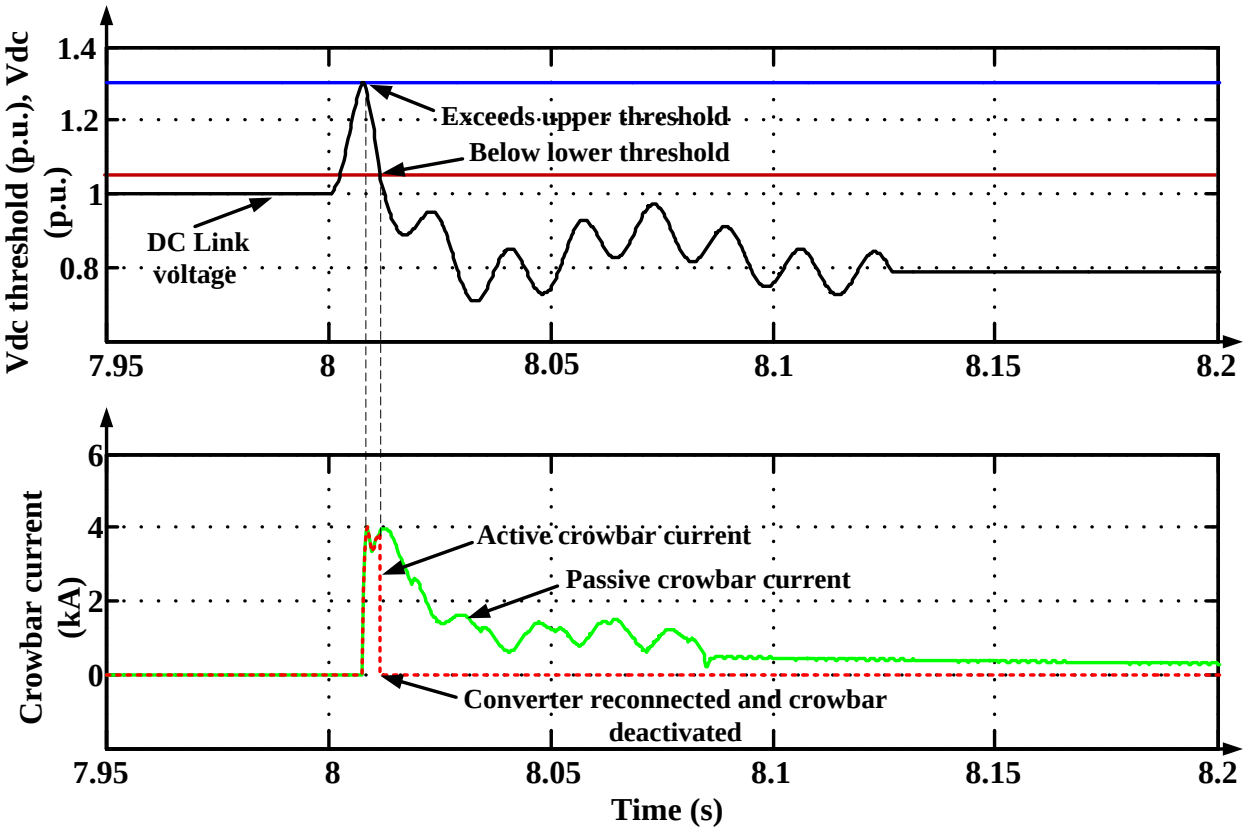

Figure 2.5: Active and passive crowbar operation

2.2.4 Type 4 Full Converter Wind Turbine Generator

The Type 4 wind generator, also known as the full power converter type wind generator, is shown in Figure 2.6, where the wind generator is connected to the grid using a converter having a rating equal to the generator itself. It is common to design a power converter for a Type 4 wind turbine with an overload capability of 10 percent above rated. The converter provides decoupling between the wind generator, which produces a variable frequency current based on the varying wind speed, and the grid operating at nominal frequency. Thus, while the grid is at 60 Hz, the stator winding of the generator may operate at variable frequencies [46]. Due to this reason, the response of the Type 4 wind generator is virtually independent of the type of generator used.

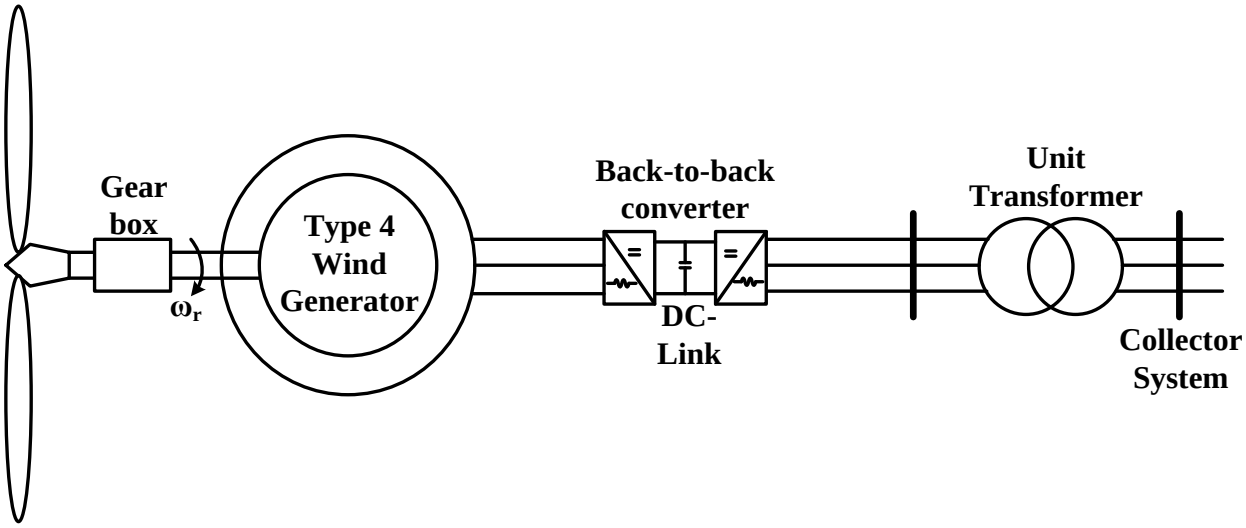

Figure 2.6: Type 4 wind turbine generator

2.3 Short Circuit Behavior of Wind Generators

The short circuit current contribution is important to know with respect to the coordination of network protection and the maximum currents that are allowed in a network [14]. This necessitates accurate short circuit models of the wind generators to be developed that take into account the different factors that influence the short circuit current behavior. This section discusses the typical short circuit behavior of the four different types of wind generators and their respective short circuit modeling complexities.

The typical short circuit behaviors of these wind generators are obtained by building detailed EMT simulation models of their test systems. This is used to assess the degree of influence of different complexities on the short circuit behavior of these wind generator systems. This understanding will be used as a basis to develop short circuit models and also to validate the developed models. PSCAD/EMTDC^{TM}[1] is an useful tool for performing detailed time domain simulations and for transient analysis of power system components.

[1]PSCAD/EMTDC^{TM} - Power System Computer Aided Design/Electromagnetic Transients DC is a registered trademark of Manitoba HVDC Research Centre Inc., Winnipeg, Canada. PSCAD/EMTDC^{TM} provides the ability to perform detailed time domain simulations and electromagnetic transient analysis where machines and the other network elements are represented using time-domain differential equations.

2.3.1 Type 1 Wind Turbine Generator

The test system shown below in Figure 2.7 is simulated. The induction generator is a GE Type 1, 1.5 MW squirrel cage machine [51], the parameters of which are given in Appendix A.1. The test system represents a typical wind generator set up connected to the collector system through a step up transformer. The transformer is a delta-wye configuration with the wye grounded. The power factor correction capacitors and soft starter are not shown for convenience.

The cable impedance up to the unit transformer is represented using a series impedance (RL) circuit. The circuit beyond the collector system is represented as an infinite bus. The wind speed is assumed to be constant and the generator is operating at 2 percent slip (turbine shaft speed of 1.02 pu).

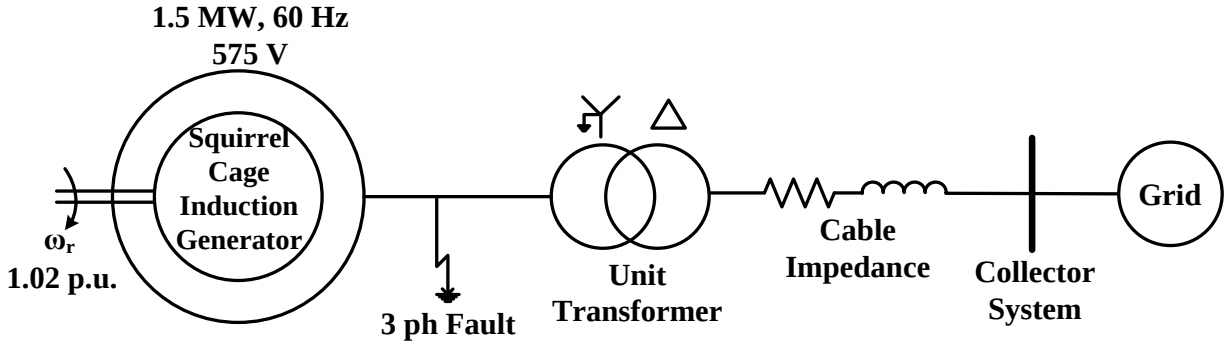

Figure 2.7: Type 1 wind generator test system

A three phase permanent fault is applied at the terminals of the generator 6.0 s after the start of the simulation and the short circuit behavior of the generator is observed. The three phase stator currents both before and after the application of the fault are shown in Figure 2.8 and the phase A fault current in Figure 2.9 below.

There is a rapid increase in the stator currents at the moment of application of the fault. The stator currents eventually decay as the source of excitation for the stator is removed. The fault current is asymmetrical due to the presence of DC offset. The moment of application of the fault, i.e., whether the fault is applied at the voltage zero crossing or the voltage

peak, determines the amount of DC offset in the fault current. For a purely inductive or highly inductive circuit with a high X/R ratio, the largest DC offset is produced when the fault occurs at the moment when the current is at or near its peak value as the voltage goes through a zero crossing [52]. The DC offset is negligible if the moment of fault occurrence coincides with the zero crossing of current. Thus, it is important to consider the effect of DC offset while performing short circuit calculations.

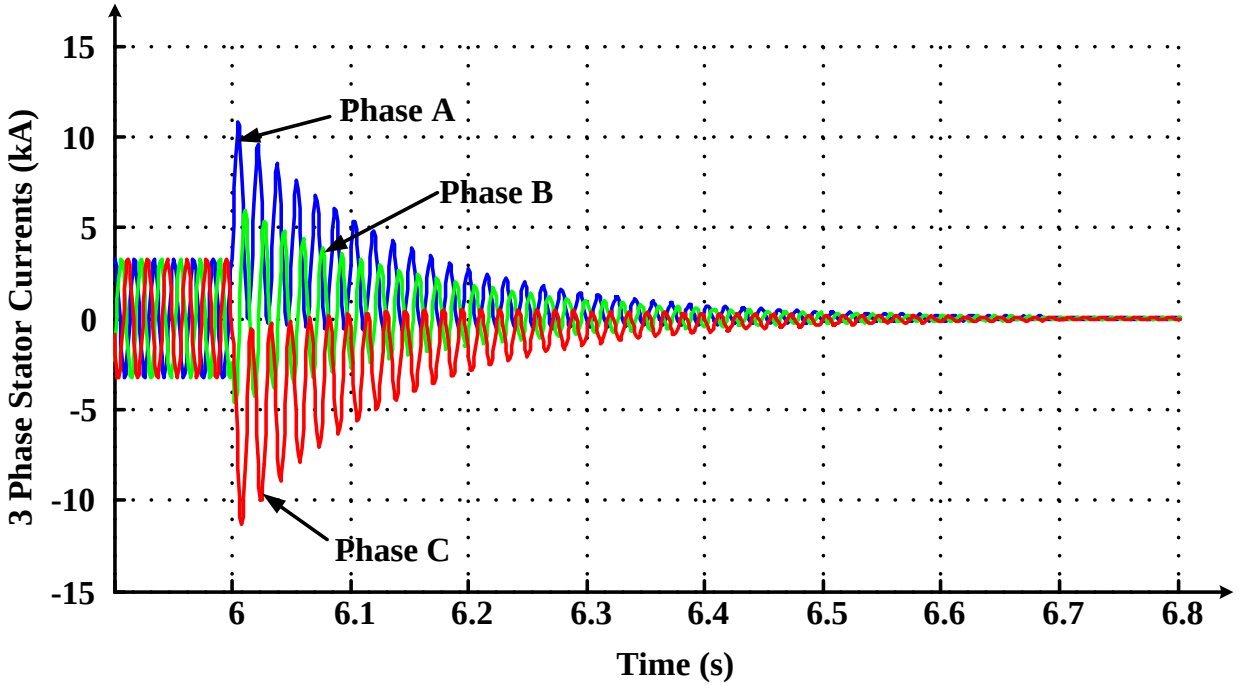

Figure 2.8: Type 1 wind generator three phase fault stator currents

The same test system was used to simulate a single line to ground unsymmetrical fault condition. A Phase A to ground permanent fault is applied at 6.0 s and the Phase A fault current waveform shown in Figure 2.10 is obtained. Unlike a symmetrical fault, where the short circuit current decays and goes to zero due to collapse of the air-gap magnetic field, the fault current for an unsymmetrical fault is sustained by the remaining two healthy phases. The post-fault current is sustained and settles at a magnitude of 5 kA peak to peak, which is lower than the steady state value of 6 kA peak to peak.

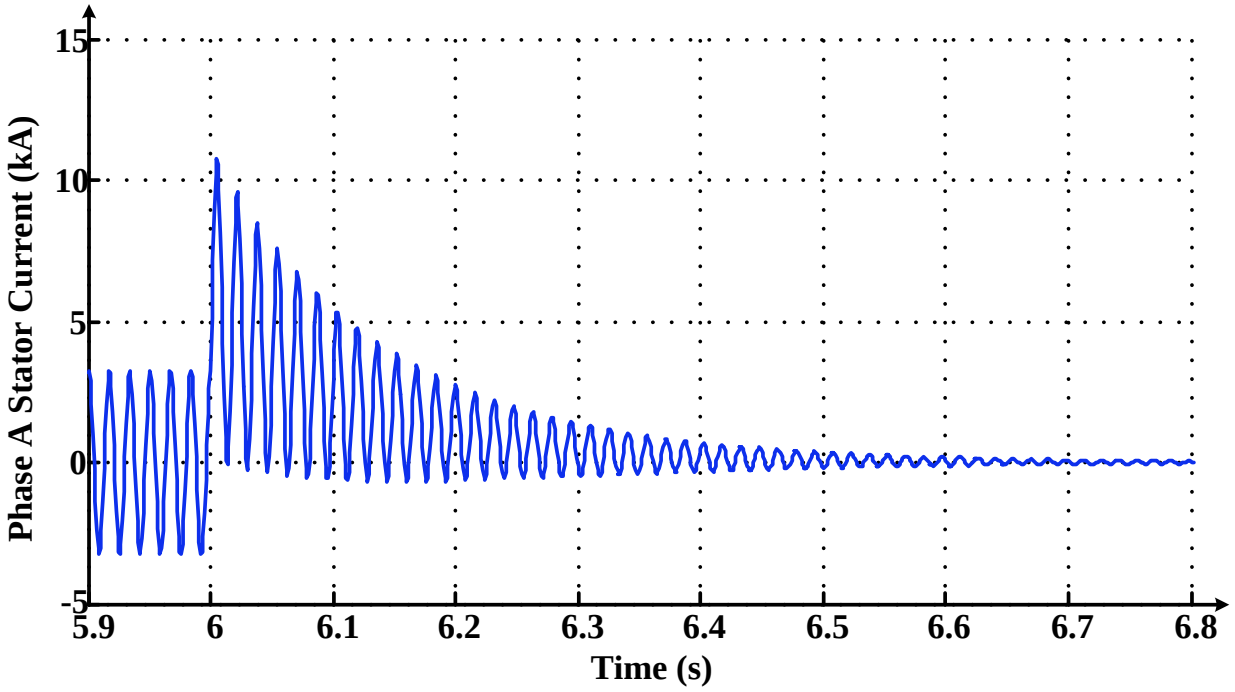

Figure 2.9: Type 1 wind generator three phase fault phase A stator current

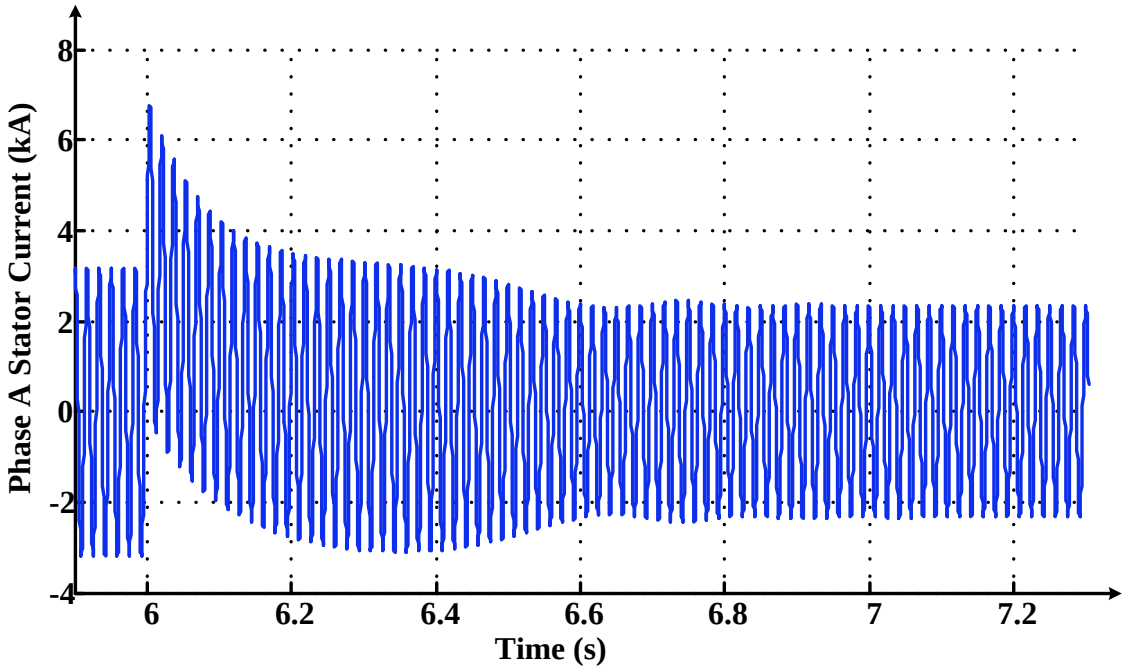

Figure 2.10: Type 1 wind generator phase A-G fault phase A stator current

The Figure 2.11 below shows the effect of the moment at which the fault is applied, on

the fault current, as it determines the amount of DC offset present in the current. If the fault is applied at the voltage zero crossing, maximum DC offset occurs. When the fault is applied at the voltage peak, the DC offset is negligible. There is still some DC offset present as the circuit is not purely inductive in nature.

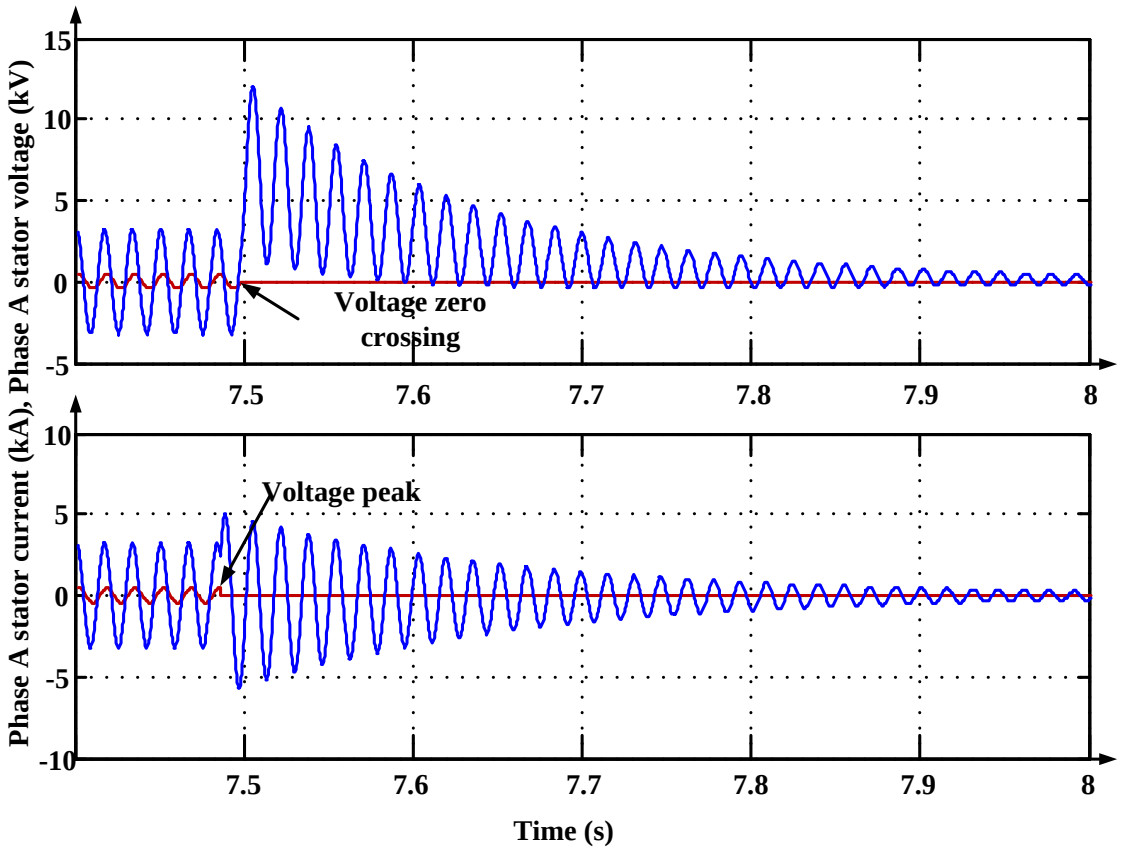

Figure 2.11: Type 1 wind generator - three phase fault - phase A stator current for different instants of fault application

2.3.2 Type 2 Wind Turbine Generator

A test system similar to the Type 1 wind generator is modeled and the short circuit characteristics are observed. The Type 2 wound rotor induction generator used is a Suzlon 2.1 MW wind generator [18, 53], the parameters of which are given in Appendix A.2. To study the fault behavior under symmetrical fault conditions, a three phase permanent fault is applied at the generator terminals. The impact of the variable slip operation (enabled by

variable rotor resistance control) on the fault current behavior is studied by simulating two different wind speeds and the corresponding values of external rotor resistances.

Figure 2.12 shows the three phase stator fault currents while operating at a slip of 6 percent. Similar to the Type 1 wind generator, the AC and DC components of the stator fault currents decay at a rate determined by the rotor and the stator decay time constants, respectively. However, unlike the Type 1 generator, the rotor decay time constant depends not only on the rotor winding resistance but also on the value of the external rotor resistance.

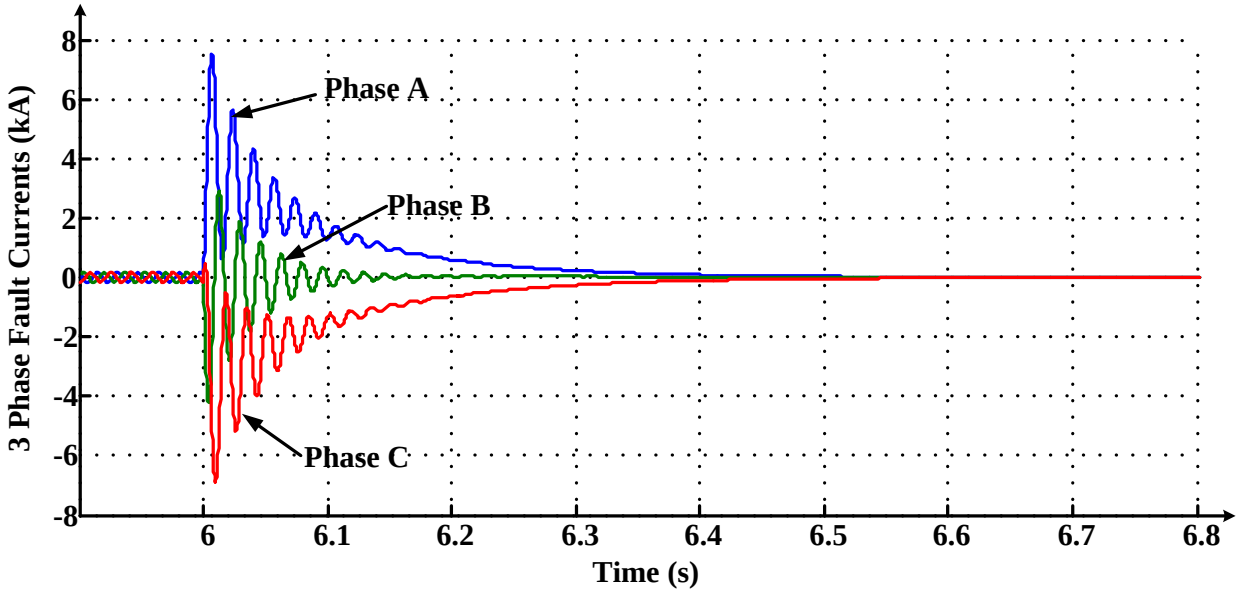

Figure 2.12: Type 2 wind generator three phase fault stator currents

For the given power output (2.283 MVA), voltage (600 V L-L), and slip (6 and 8 percent) values, the value of the external rotor resistance to be added to the rotor terminals can be determined from the equivalent circuit [18] shown in Figure 2.13. This value of resistance (0.0075 ohms for 6 percent slip and 0.0096 ohms for 8 percent slip) is used by the external rotor control circuit to maintain constant power output from the wind generator.

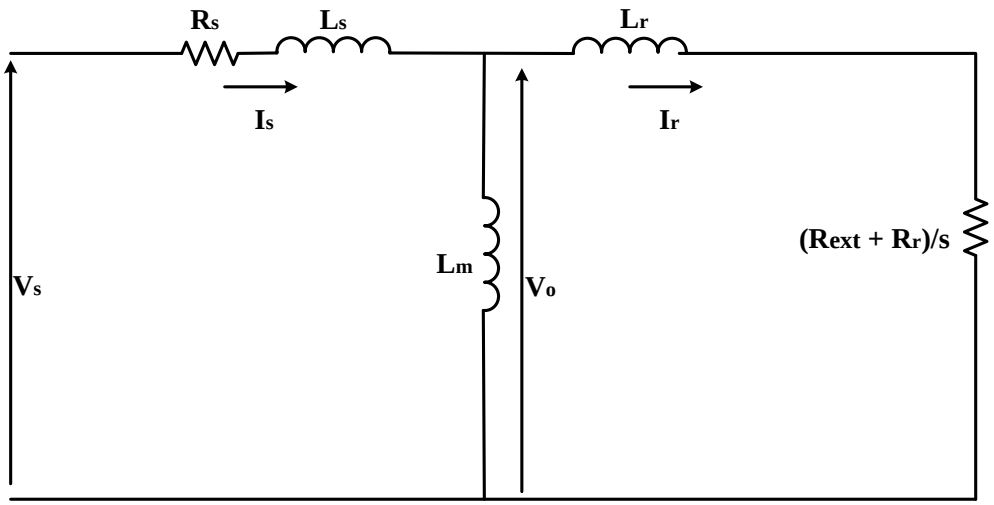

Figure 2.13: Equivalent circuit of Type 2 induction machine

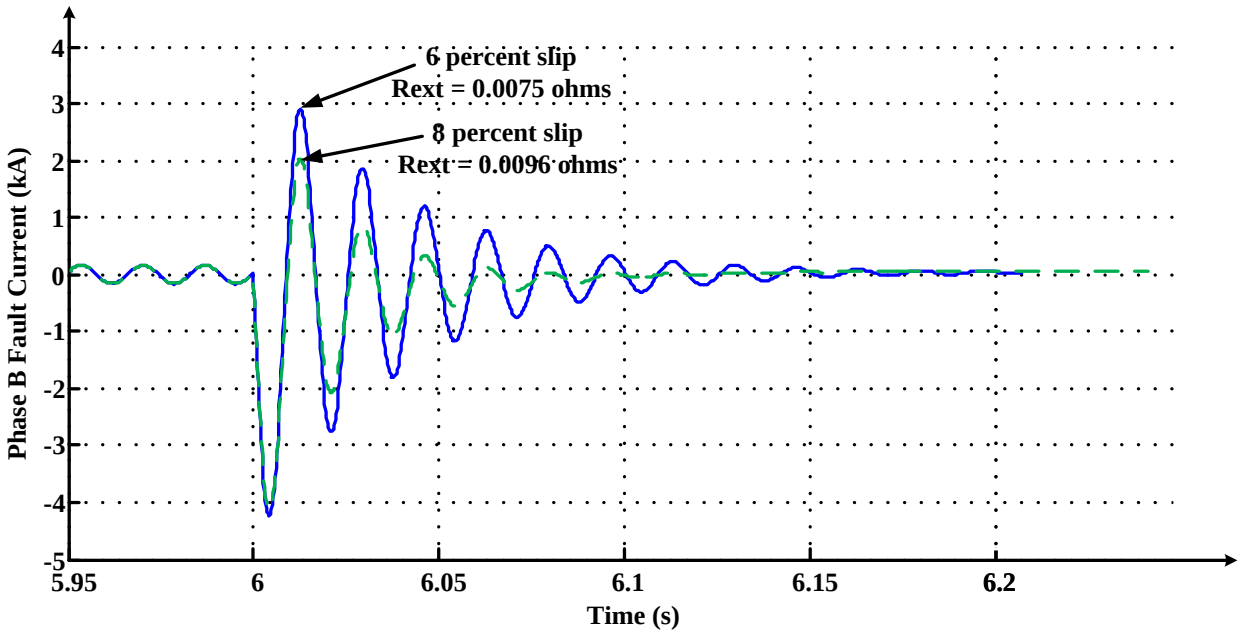

Figure 2.14: Effect of external rotor resistance control on short circuit current

For the same three phase fault condition, the short circuit response, specifically the phase B fault current, is observed for two different wind speeds (6 percent and 8 percent slips) in order to understand the effect of varying the external rotor resistance on the short circuit current. The higher the value of slip, the higher the external rotor resistance to be used. Figure 2.14 shows that the root mean square (RMS) fault current is 3 kA for 6 percent slip

and lower rotor resistance of 0.0075 ohms compared to 2.65 kA for 8 percent slip and higher rotor resistance of 0.0096 ohms.

The behavior of the Type 2 wind generator under unsymmetrical fault conditions is very similar to the Type 1 generator except for the influence of the external rotor resistance on the short circuit current. Figure 2.15 shows the three phase stator currents for a phase A to ground permanent fault at the terminals of the generator operating at a slip of 6 percent.

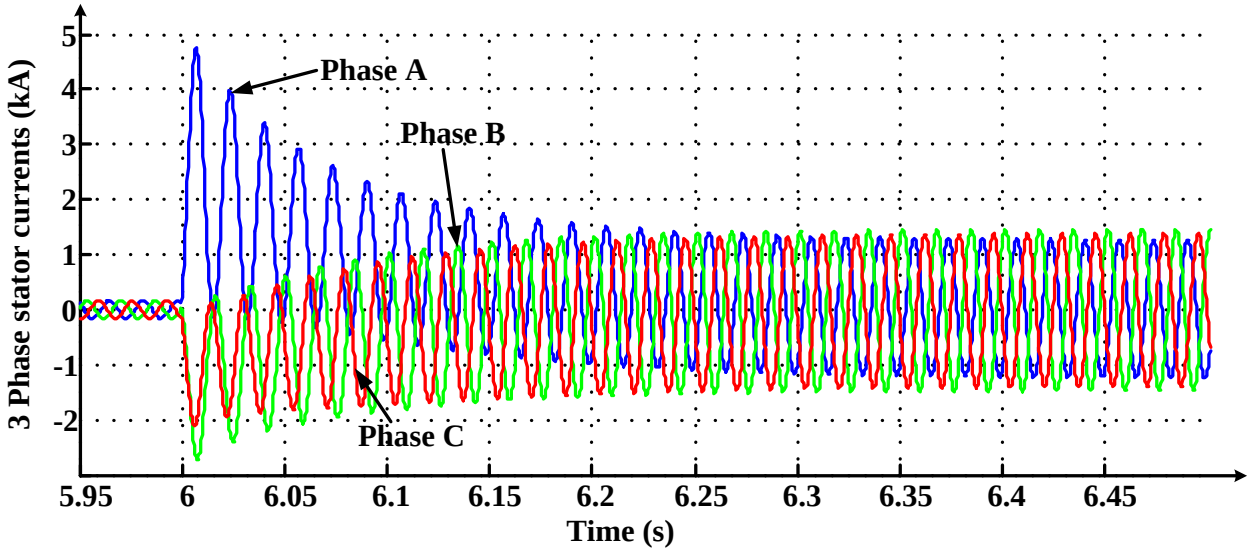

Figure 2.15: Type 2 wind generator phase A-G fault stator currents

2.3.3 Type 3 Wind Turbine Generator

This section introduces the Type 3 wind generator test system that was used to perform short circuit studies. The dq0 equations behind the test system's detailed EMT model are also discussed. This is followed by a discussion on the different modeling complexities that are crucial for the accurate short circuit representation of the Type 3 wind generator. However, for the purpose of clarity the discussion of an important modeling complexity, namely the presence of sub-synchronous components in fault currents due to control interactions, is presented in Chapter 4.

2.3.3.1 Test System

The test system shown in Figure 2.16 for studying the short circuit behavior of a Type 3 wind turbine generator consists of the wound rotor induction generator, the back-to-back converter (RSC, GSC, and DC-Link), unit transformer, and controllers that are modeled using dq0 time domain differential equations [45]. The system consists of a 3 MW Type 3 wind generator connected to the collector system through a unit transformer and then to the grid through a feeder line.

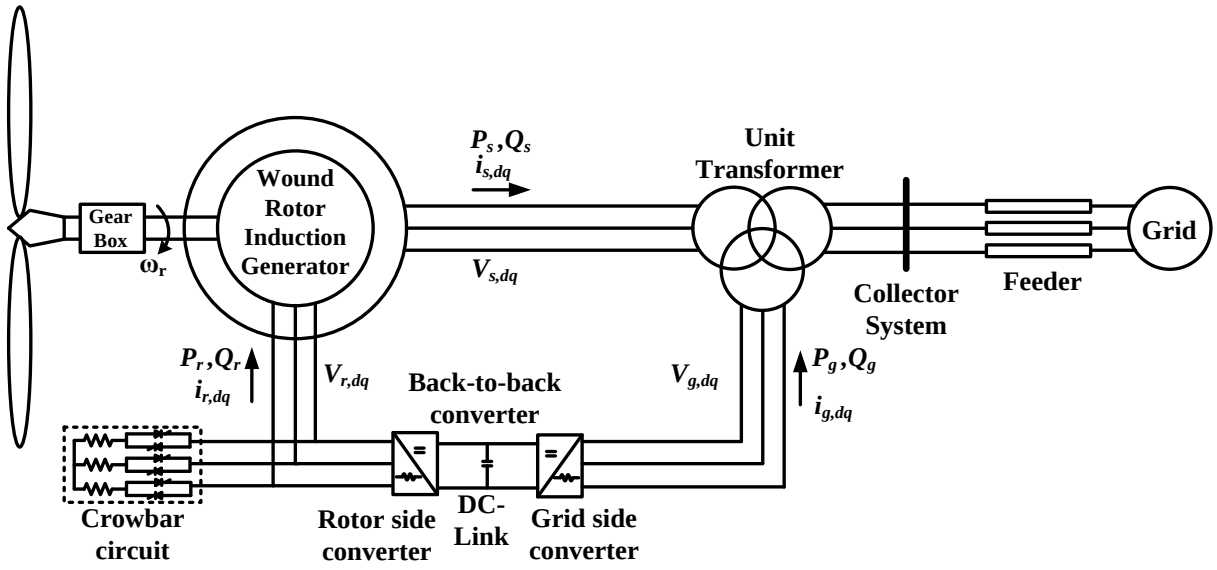

Figure 2.16: Type 3 wind generator test system

2.3.3.2 Modeling of the Test System

The differential equations representing the various components of the test system are discussed below. The equations are expressed in the dq0-reference frame rotating at synchronous speed ω_s. The test system is modeled based on the system parameters [6], which are given in detail in Appendix A.3.

Drive Train:

The turbine, shaft, and gear box are all lumped together as a single equivalent mass

(angular moment of inertia, $J = 2H$ =1.856 s). A multi-mass model would be required for studying phenomena such as sub-synchronous resonance. For studying sub-synchronous control interactions, the equivalent mass model is sufficient. The mechanical torque (T_m) is assumed to be constant as the wind speed during the duration of the fault is assumed to be constant. The equivalent mass model is represented by the classical swing equation

$$\frac{d\omega_r}{dt} = \frac{T_m - T_e}{2H} \tag{2.2}$$

where T_m and T_e are the mechanical and electrical torque of the generator with a rotor speed of ω_r. The electrical torque is given by

$$T_e = \psi_{r,q} i_{r,d} - \psi_{r,d} i_{r,q} \tag{2.3}$$

where $\psi_{r,d}$ and $\psi_{r,q}$ are the d and q axis components of the rotor flux linkages and $i_{r,d}$ and $i_{r,q}$ are the d and q axis components of the rotor current, respectively. In the following expressions,

$$X_{dq} = \begin{bmatrix} X_d \\ X_q \end{bmatrix} \tag{2.4}$$

is used to represent the d and q axis flux linkages, current, and voltages.

Stator Voltages:

The stator flux linkage due to the self-inductance of the stator circuit, L_s, and the mutual inductance between the stator and rotor circuits, L_m, is given by

$$\psi_{s,dq} = L_{ss} i_{s,dq} + L_{sr} i_{r,dq} \tag{2.5}$$

where the inductance matrices are defined as

$$L_{ss} = \begin{bmatrix} L_s + L_m & 0 \\ 0 & L_s + L_m \end{bmatrix}, L_{sr} = \begin{bmatrix} L_m & 0 \\ 0 & L_m \end{bmatrix} \tag{2.6}$$

and the stator voltage ($V_{s,dq}$) equation in terms of the flux linkage ($\psi_{s,dq}$) and stator current ($i_{s,dq}$) is expressed as

$$V_{s,dq} = R_{ss} i_{s,dq} + J\omega_s \psi_{s,dq} + \frac{d\psi_{s,dq}}{dt} \tag{2.7}$$

where the stator resistance matrix is given by

$$R_{ss} = \begin{bmatrix} R_s & 0 \\ 0 & R_s \end{bmatrix} \tag{2.8}$$

and

$$J = \begin{bmatrix} 0 & -1 \\ 1 & 0 \end{bmatrix} \tag{2.9}$$

Rotor Voltages:

Similarly, the rotor flux linkage due to the self-inductance of the rotor circuit, L_r, and the mutual inductance between the stator and rotor circuits, L_m, is given by

$$\psi_{r,dq} = L_{rr} i_{r,dq} + L_{rs} i_{s,dq} \tag{2.10}$$

with the inductance matrices defined by

$$L_{rr} = \begin{bmatrix} L_r + L_m & 0 \\ 0 & L_r + L_m \end{bmatrix}, L_{rs} = \begin{bmatrix} L_m & 0 \\ 0 & L_m \end{bmatrix}. \tag{2.11}$$

The rotor voltage ($V_{r,dq}$) equation in terms of the flux linkage ($\psi_{r,dq}$) and rotor current ($i_{r,dq}$) is expressed as

$$V_{r,dq} = R_{rr} i_{r,dq} + J\sigma\omega_s \psi_{r,dq} + \frac{d\psi_{r,dq}}{dt} \tag{2.12}$$

where the rotor resistance matrix is

$$R_{rr} = \begin{bmatrix} R_r & 0 \\ 0 & R_r \end{bmatrix}. \tag{2.13}$$

The relative speed between the rotor rotating at a speed of ω_r and the synchronously rotating stator magnetic field at ω_s is defined as the slip speed given by $\omega_s - \omega_r$. The slip, σ, which is the normalized slip speed, is defined as

$$\sigma = \frac{\omega_s - \omega_r}{\omega_s}. \tag{2.14}$$

Back to Back Converter:

The back-to-back converter consists of detailed model of pulse width modulated IGBT based VSCs, namely the RSC and the GSC with a DC Link capacitor configuration, as shown in Figure 2.17 below.

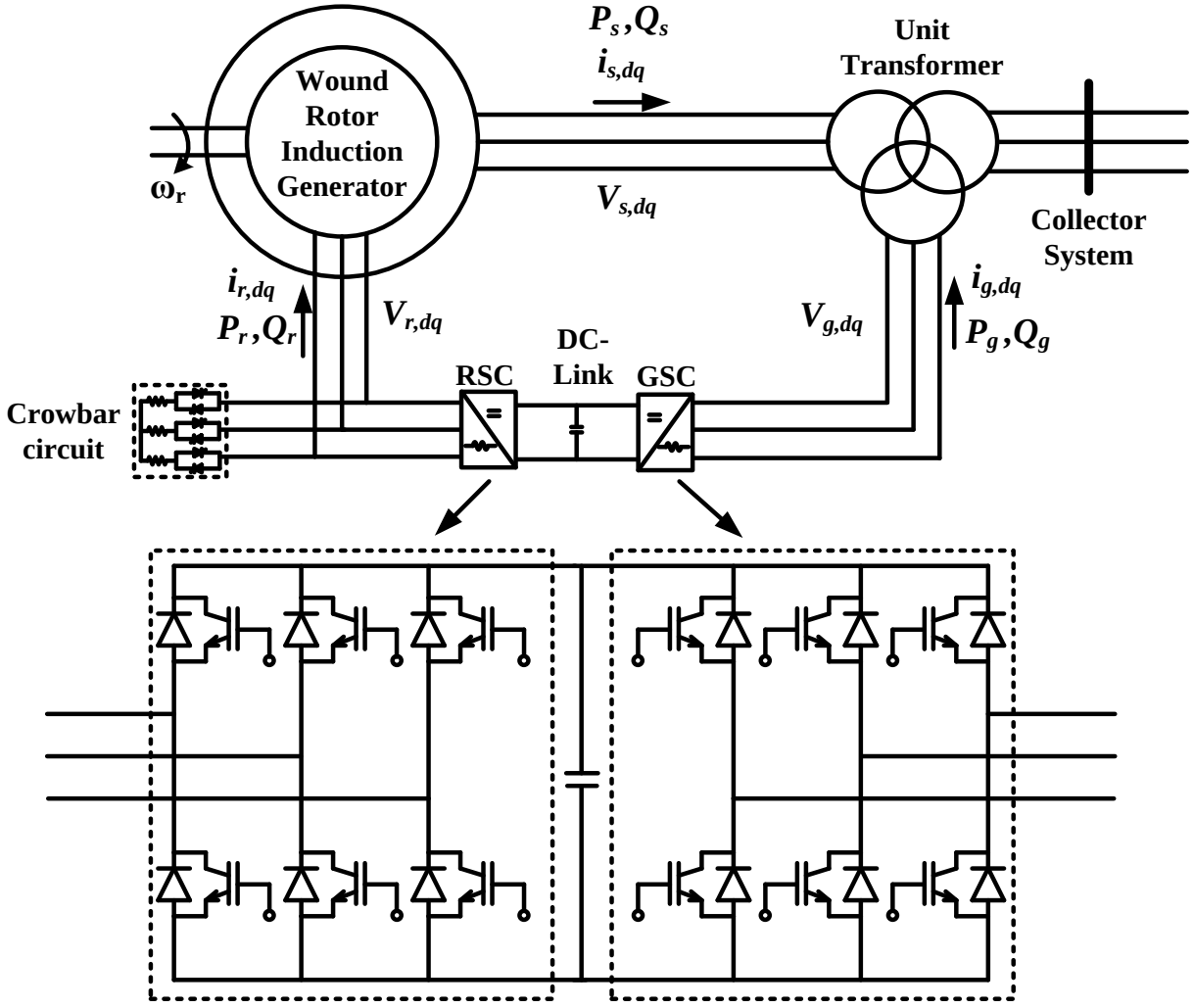

Figure 2.17: DFIG back-to-back converter with rotor and grid side controllers

The high frequency switching dynamics of the back to back converter can be neglected and the use of an average model of the converter is preferred as the phenomena under study in this thesis is not affected by these switching dynamics. The dynamics of the DC link

capacitor is represented by a first-order model [54]

$$C\frac{dV_{dc}}{dt} = \frac{P_r - P_g}{V_{dc}} = i_{dc} = m_{r,d}i_{r,d} + m_{r,q}i_{r,q} - m_{g,d}i_{g,d} - m_{g,q}i_{g,q} \tag{2.15}$$

where m_d and m_q represent the modulation indices of the PWM converter and V_{dc} is the voltage across the DC-link capacitor with a capacitance C. P_g and P_r represent the real power flow at the GSC and the RSC ends respectively. This average VSC model does not take into account the high frequency switching dynamics due to the IGBT based converters, but preserves the DC link dynamics.

Rotor Side and Grid Side Controllers:

The dynamics of the controllers are crucial for short circuit analysis, especially in cases with potential sub-synchronous control interactions, as explained in Chapter 4. The RSC and GSC control loops are shown in Figures 2.18 and 2.19, respectively.

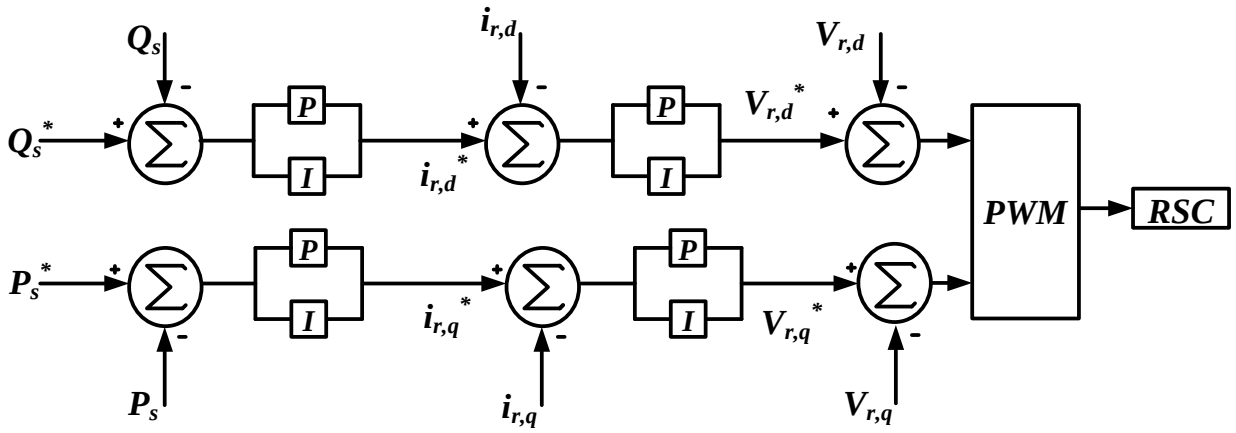

Figure 2.18: Rotor side converter controller

The RSC provides an independent control of the stator side active and reactive power by controlling the q-axis and d-axis rotor current (iq_r and id_r) components, respectively. It consists of two cascaded loops where the inner current control loop regulates the d-axis and q-axis rotor currents independently. The dq0 equations representing the RSC are

$$\frac{dx_{r,d}}{dt} = K_{I,P_s}(P_s^* - P_s), \tag{2.16}$$

$$m_{r,d} = x_{r,d} + K_{P,P_s}(P_s^* - P_s), \tag{2.17}$$

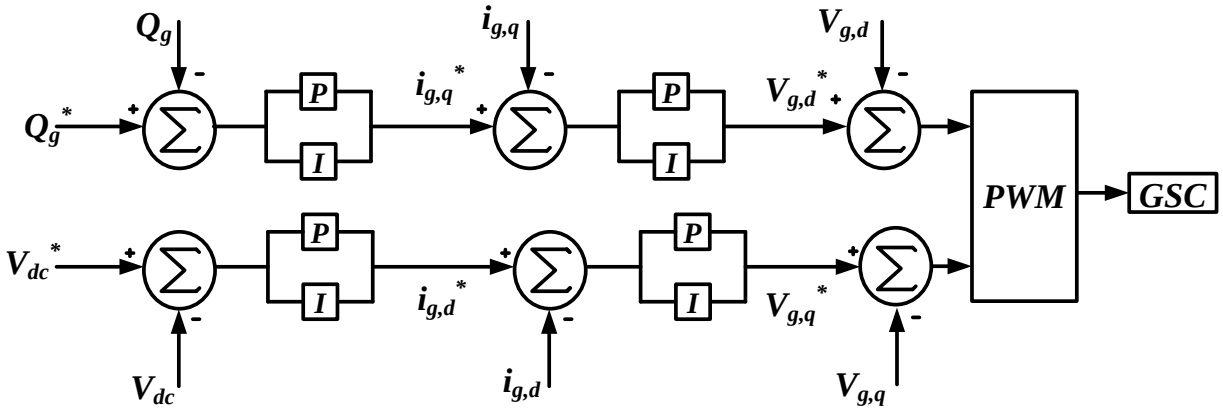

Figure 2.19: Grid side converter controller

$$\frac{dx_{r,q}}{dt} = K_{I,Q_s}(Q_s^* - Q_s) \tag{2.18}$$

and

$$m_{r,q} = x_{r,q} + K_{P,Q_s}(Q_s^* - Q_s) \tag{2.19}$$

where P_s^* and Q_s^* are the reference values for the stator active and reactive power, P_s and Q_s are the actual values for the stator active and reactive power, and K_I and K_P represent the gains of the integral and proportional controllers, respectively.

The objective of the GSC is to keep the DC link voltage at a constant value by controlling the q-axis current ($i_{g,q}$) and regulating the reactive power exchange between the GSC and the grid by controlling the d-axis current ($i_{g,d}$). The inner current control loop regulates the d-axis and q-axis grid side currents independently. The outer control loop regulates the DC-link voltage and the reactive power exchange between the GSC and the grid. The dq0 equations representing the GSC are

$$\frac{dx_{g,d}}{dt} = K_{I,V_{dc}}(V_{dc}^* - V_{dc}), \tag{2.20}$$

$$m_{g,d} = x_{g,d} + K_{P,V_{dc}}(V_{dc}^* - V_{dc}), \tag{2.21}$$

$$\frac{dx_{g,q}}{dt} = K_{I,i_{g,q}}(i_{g,q}^* - i_{g,q}) \tag{2.22}$$

and

$$m_{g,q} = x_{g,q} + K_{P,i_{g,q}}(i^*_{g,q} - i_{g,q}) \tag{2.23}$$

where V^*_{dc} and $i^*_{g,q}$ are the reference values for the DC-link voltage and the q axis component of the GSC current, and V_{dc} and $i_{g,q}$ are the actual values for the DC link voltage and the q axis component of the GSC current, respectively.

Transmission Network and Transformer:

The transmission network is modeled in order to include the effects of the series capacitor compensation as this is crucial to observe sub-synchronous interactions. Such sub-synchronous interactions in series compensated Type 3 wind farms are explained in detail in Section 4.2. The equations

$$L_{line}\frac{di_d}{dt} = v_{s,d} - R_{line}i_d + \omega_s L_{line}i_q - v_{c,d} - v_{b,d} \tag{2.24}$$

$$L_{line}\frac{di_q}{dt} = v_{s,q} - R_{line}i_q - \omega_s L_{line}i_d - v_{c,q} - v_{b,q} \tag{2.25}$$

$$C_{line}\frac{dv_{c,d}}{dt} = i_d + \omega_s C_{line}v_{c,q} \tag{2.26}$$

$$C_{line}\frac{dv_{c,q}}{dt} = i_q - \omega_s C_{line}v_{c,d} \tag{2.27}$$

represent the transmission network model, where R_{line}, L_{line}, and C_{line} represent the resistance, inductance, and capacitance of the transmission line, respectively.

A constant impedance RL model [44] is used for the transformer as shown in Equations 2.28 and 2.29 below.

$$L_t\frac{di_{t,d}}{dt} = v_{pri,d} - v_{sec,d} - R_t i_{t,d} + \omega_s L_t i_{t,q} \tag{2.28}$$

$$L_t \frac{di_{t,q}}{dt} = v_{pri,q} - v_{sec,q} - R_t i_{t,q} + \omega_s L_t i_{t,d} \tag{2.29}$$

2.3.3.3 LVRT based Protection Scheme and Crowbar Circuit

The increasing amount of wind integration constitutes a large share of the total power generation. Consequently, LVRT requirements make it necessary for wind farms to stay connected to the grid and provide reactive power support during and after voltage sags. This is required in order to maintain power availability and improve system voltage stability. These requirements are defined in grid codes issued by grid operators. For the wind generator to achieve this, the use of a crowbar circuit is required to protect the back-to-back converter during such an operation. This introduces two factors that must be considered for determining the short circuit behavior of the Type 3 wind generator, namely the crowbar resistance and the LVRT characteristics.

The protection strategy based on LVRT characteristics provides the following benefits:

- Capacity to stay connected to the grid during faults without tripping the unit breaker (based on LVRT curve).
- High rotor current during the fault is limited by crowbar action.
- Reactive power can be supplied to the grid during long dips for voltage restoration.

The LVRT curve is essentially a voltage versus time characteristic indicating the different voltage requirements after the occurrence of a voltage sag. The LVRT scheme incorporates grid codes that define that wind turbines must continue to operate if their after-fault voltage profile remains above the LVRT curve. The LVRT characteristic utilized in the test system simulation is shown in Figure 2.20 [55]. The test system built in this research work includes an LVRT based protection scheme and crowbar circuit, the scheme of which is shown in Figure 2.21. In a real power system, the required LVRT curve would be defined using the custom programming feature of numerical relays.

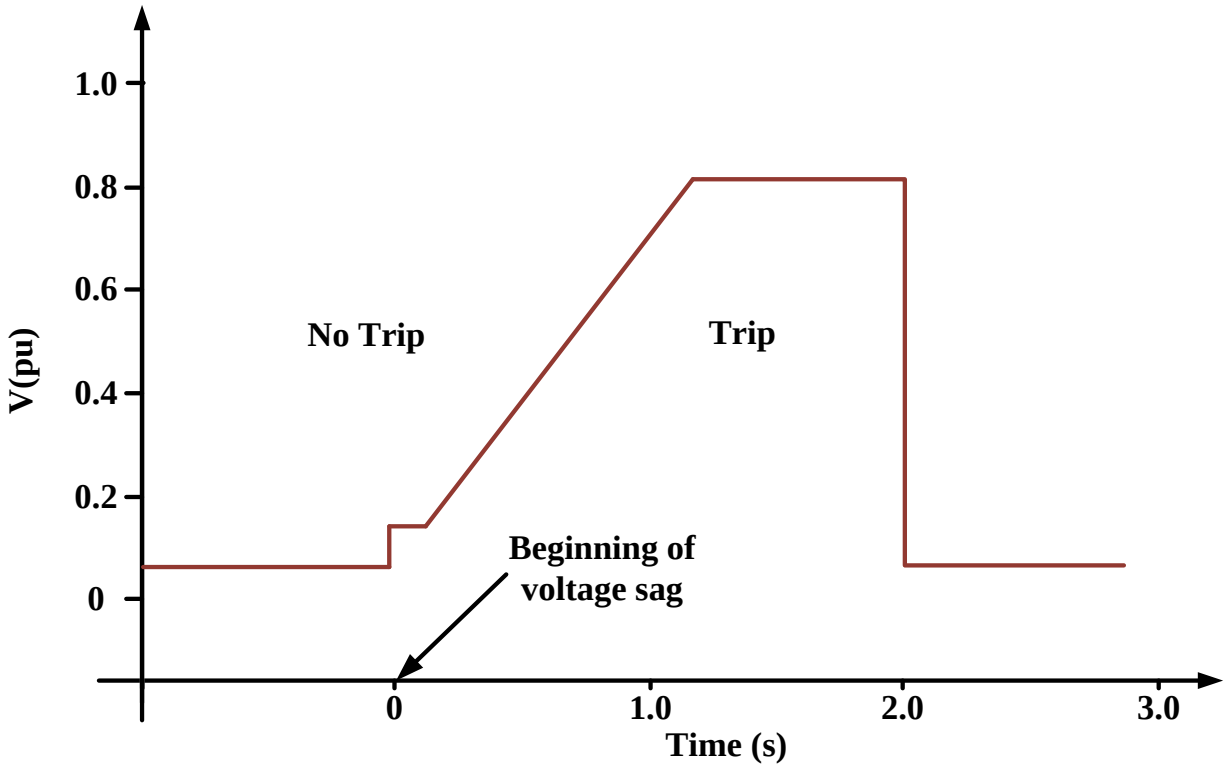

Figure 2.20: LVRT characteristics used in the test system

A fault far away from the wind farm can also lead to a voltage sag at the point of interconnection of the wind farm to the grid. Due to the occurrence of a fault or a voltage sag, the unit breaker trips if the voltage at the terminals of the generator goes lower than the LVRT curve. During this period, the crowbar circuit is activated if the per-unit DC-Link voltage goes higher than the threshold value by providing the appropriate gating signals to the crowbar trigger circuit. Meanwhile, the RSC is turned off to protect the back-to-back converter. During the crowbarred period, the crowbar resistance value used affects the magnitude of the short circuit current. The impedance of the bypass crowbar resistors is of importance but not critical. They should be sufficiently low to avoid too large a voltage on the converter terminals. On the other hand, they should be high enough to limit the current [56].

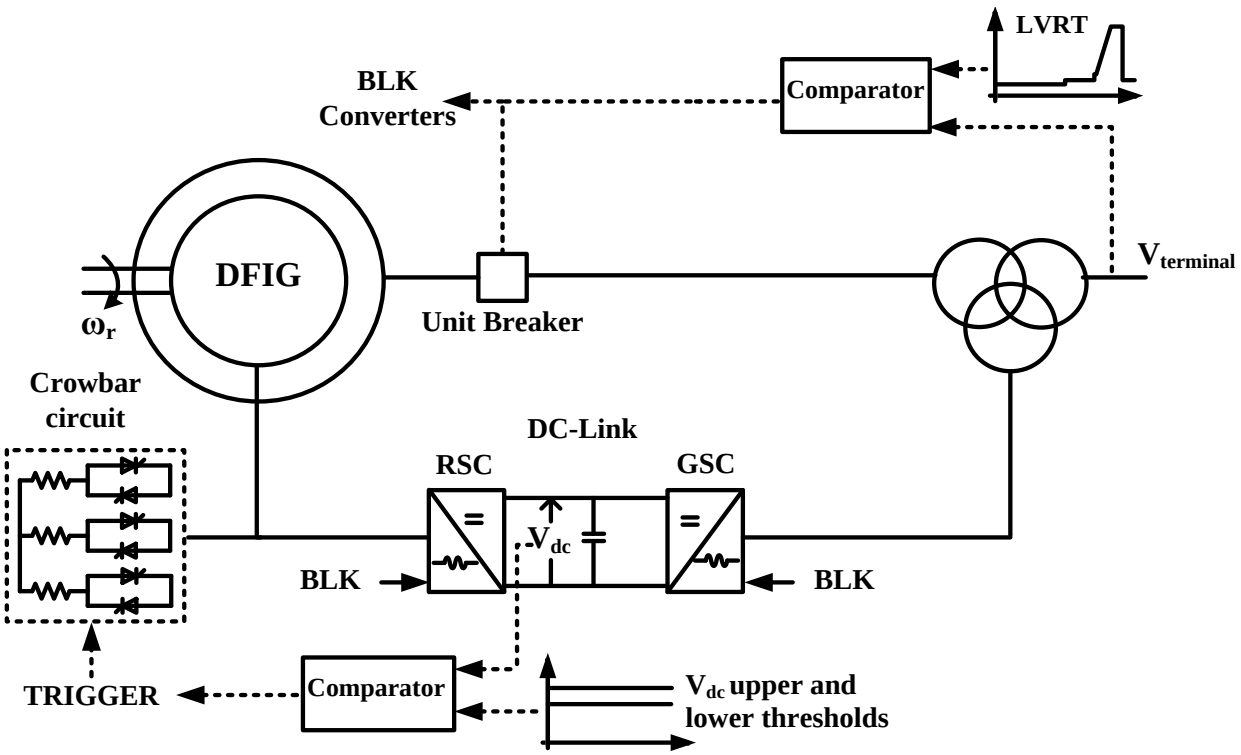

Figure 2.21: DFIG unit breaker protection based on LVRT Scheme, converter blocking and crowbar triggering

2.3.3.4 Validation of the Electromagnetic Transient Model

The validation of the EMT model is crucial as it is used as a benchmark model to verify the accuracy of the other modeling techniques that have been discussed. The wind farm consists of 150 Type 3 wind turbine generators each having a rated output of 3 MW. Thus, the entire wind farm is expected to produce 450 MW real power output at steady state operating conditions for a wind speed assumed to be constant. The EMT model of the Type 3 wind farm is validated by subjecting the system to changes and observing the corresponding response to see if it satisfies the performance requirements of the system.

Change in wind speed:

The wind farm is subjected to a change in wind speed from its operating wind speed of 15 m/s to 10 m/s and the response of the wind farm is studied. Figure 2.22 below shows the change in the wind speed and the corresponding reduction in the real power output of

the wind farm from its steady state output of 450 MW. The rotor side converter control responds by changing the $i_{r,q}{}^*$, thereby bringing the real power output back to its steady state value. This validates the steady state operation of the wind farm, i.e, whether it responds as expected for a change in wind speed.

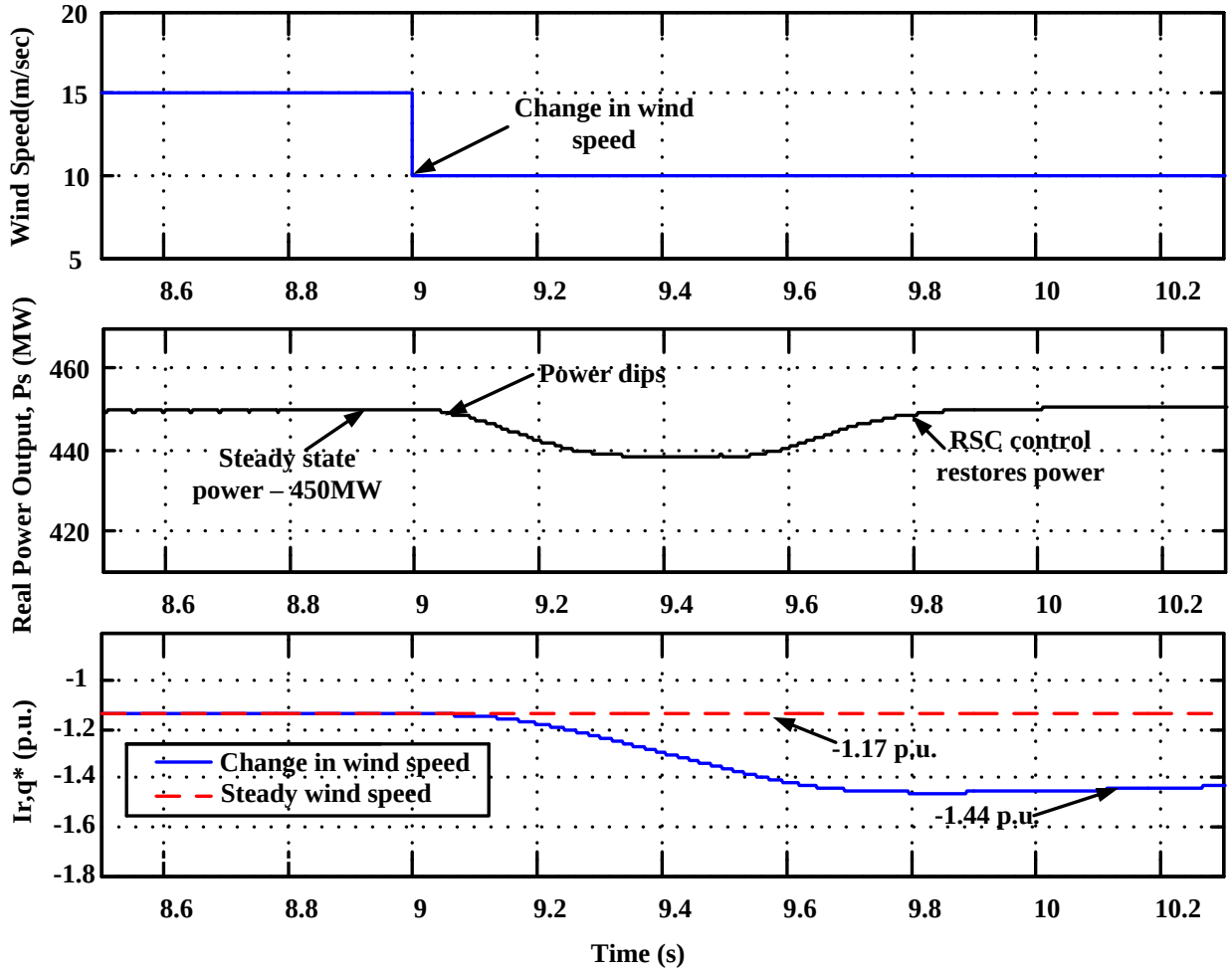

Figure 2.22: Response of a Type 3 wind farm to change in wind speed

Change in reactive power reference:

Following this, the value of the reactive power reference, $Q_s{}^*$, is changed to a higher value than the current operating value and the response of the wind farm in terms of its reactive power output is observed. The reference $Q_s{}^*$ value is determined either from the terminal voltage, the power factor, or the reactive power setting depending on the mode of control. In this case, the reactive power reference is manually changed and the rotor side converter control responds by changing the $i_{r,d}{}^*$ to a new corresponding value. This, in turn, changes the actual reactive power output of the wind farm as shown in Figure 2.23.

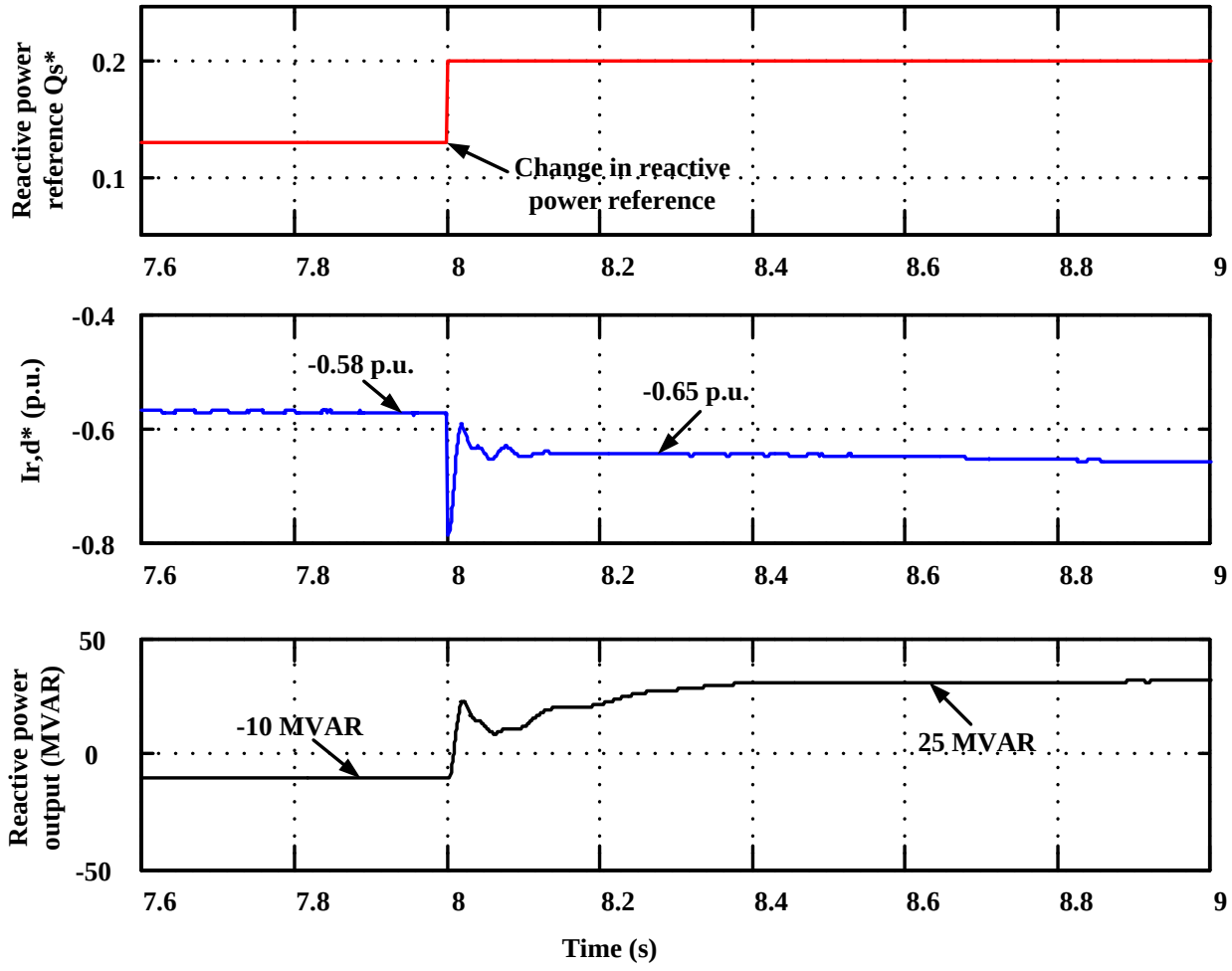

Figure 2.23: Response of a Type 3 wind farm to change in reactive power reference

Moreover, the functioning of the LVRT based protection, which is demonstrated in Sections 2.3.3.5 and 2.3.3.6, and the sub-synchronous interactions, which are shown in Chapter

3, are by themselves a validation of the proper functioning of the EMT model that has been built.

2.3.3.5 Application of Voltage Sag

A voltage dip or voltage sag is a sudden reduction (between 10 and 90 percent) of the voltage at a point in the electrical system that lasts for half a cycle to 1 min. There can be many causes for a voltage dip, namely short circuits somewhere in the grid, switching operations associated with the temporary disconnection of a supply, flow of heavy currents caused by the starting of large motor loads, arc furnaces, or transformer saturation.

Depending on the type of fault or disturbance causing them, voltage sags can be symmetrical or unsymmetrical in nature. Voltage sag characteristics are affected not only by the fault type causing them but also the distance to the fault, the system configuration, and the fault impedance [24]. An auto-transformer based voltage sag generator (VSG) component was developed in order to simulate a voltage sag condition and observe the wind generators response. The three phase VSG shown in Figure 2.24 is built using a three phase auto-transformer and thyristor based switches. It has the ability to control the type and duration of grid voltage sags. In the test system shown in Figure 2.16, the DFIG is now connected to the grid through the VSG.

Symmetrical Voltage Sag:

The following scenarios are implemented in the test system in order to observe the response of the DFIG for two different voltage sags:

Case 1 - 75 percent three phase voltage sag applied for 200 ms (at 7.0 s after start of simulation).

Case 2 - 75 percent three phase voltage sag applied for 500 ms (at 7.0 s after start of simulation).

The protection strategy is based on the criteria that if the RMS voltage at the terminals of the wind turbine goes lower than the LVRT curve, the unit breaker trips. The breaker

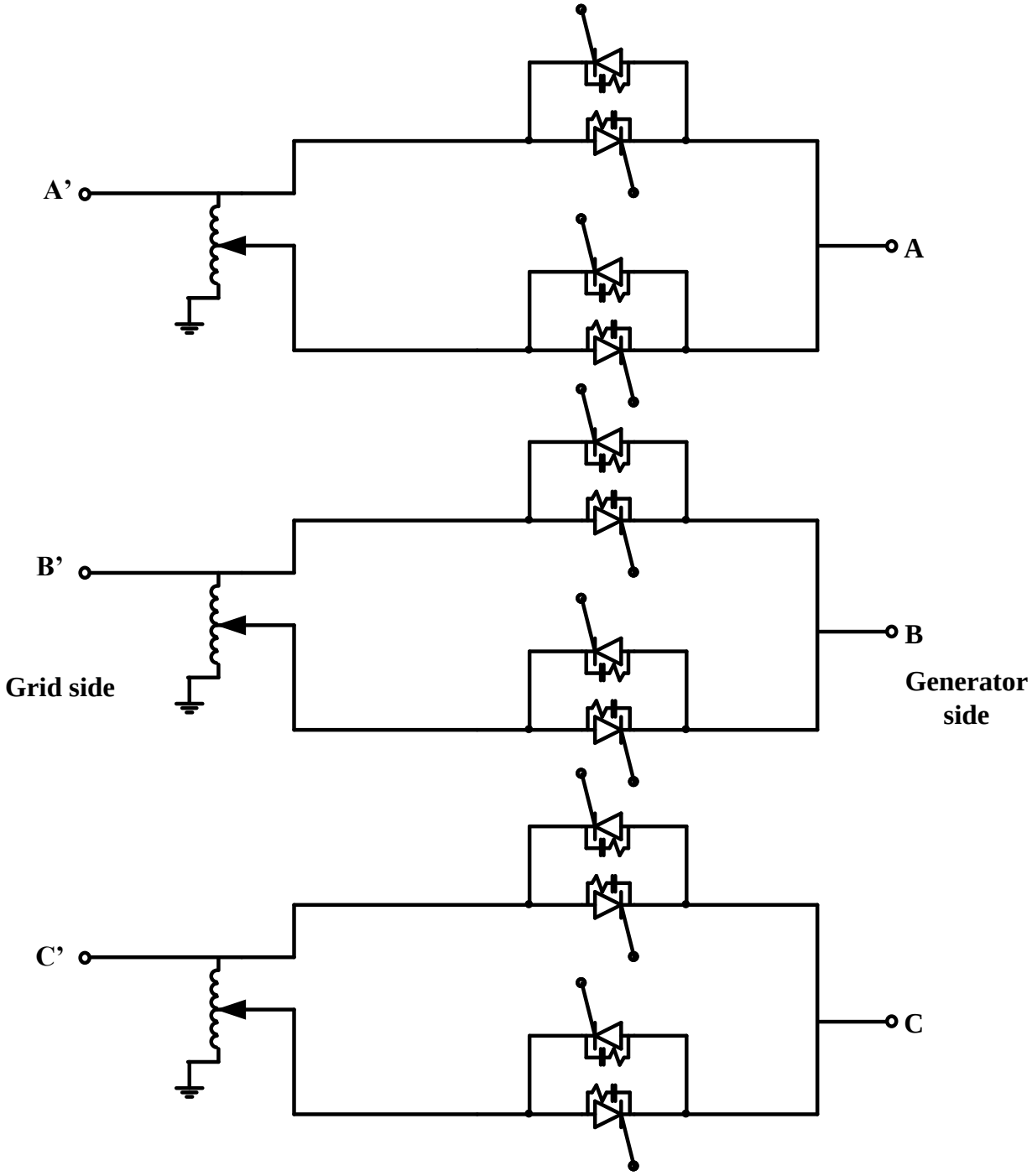

Figure 2.24: Voltage sag generator schematic diagram

does not trip for Case 1 (2.25) but trips for Case 2, as shown in Figure 2.26. During this period, if the per-unit DC-link voltage climbs higher than the threshold value (1.3 p.u in this case), then the crowbar circuit is activated. In our simulations, the crowbar is not activated

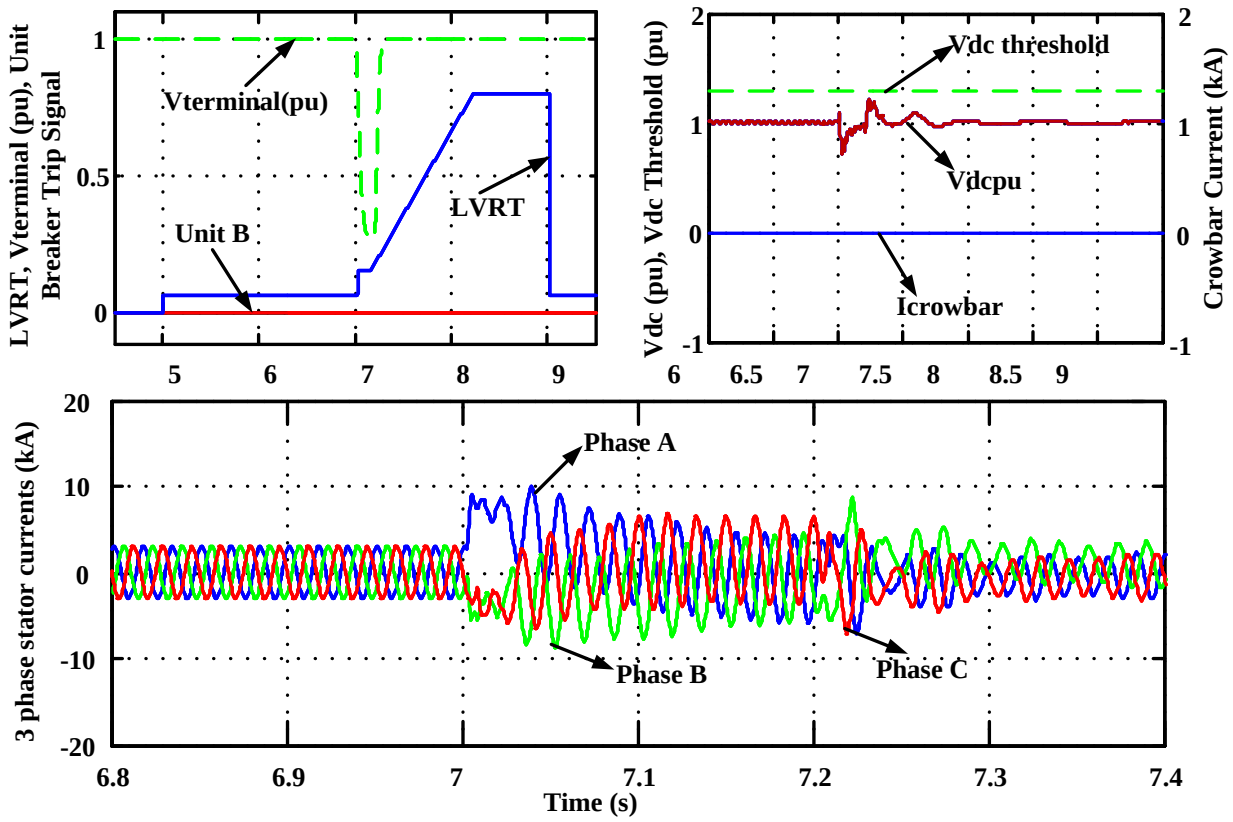

Figure 2.25: Response of DFIG to a 75 percent three phase voltage sag for 200 ms (Case 1)

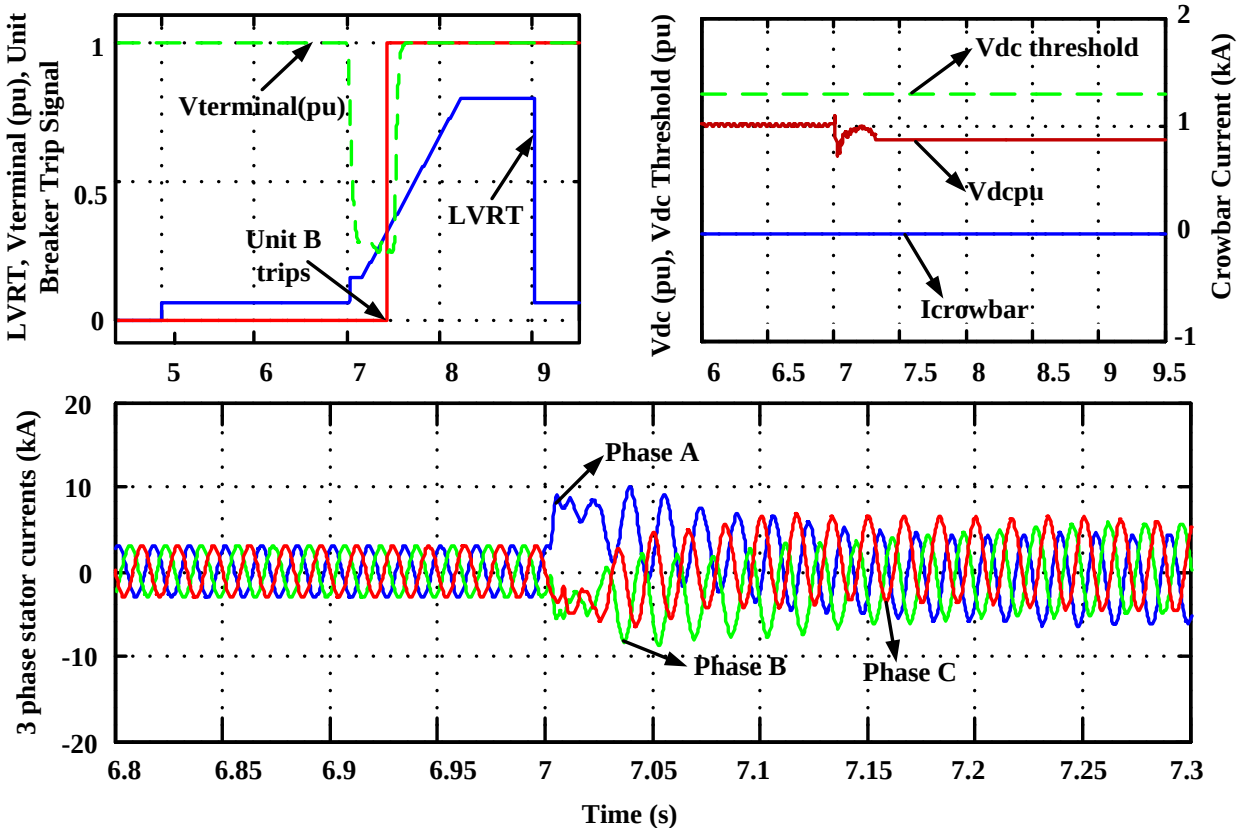

Figure 2.26: Response of DFIG to a 75 percent three phase voltage sag for 500 ms (Case 2)

for either case.

Unsymmetrical Voltage Sag:

Following this, a 75 percent phase A unsymmetrical voltage sag is applied (Case 3) and the behavior of the DFIG is observed. Either the three phase RMS terminal voltage or the phase A RMS voltage can be used to compare against the LVRT characteristic to determine the unit breaker tripping. Figure 2.27 shows the phase A RMS terminal voltage compared against the LVRT curve; the circuit breaker does not trip for this condition and the crowbar is not triggered.

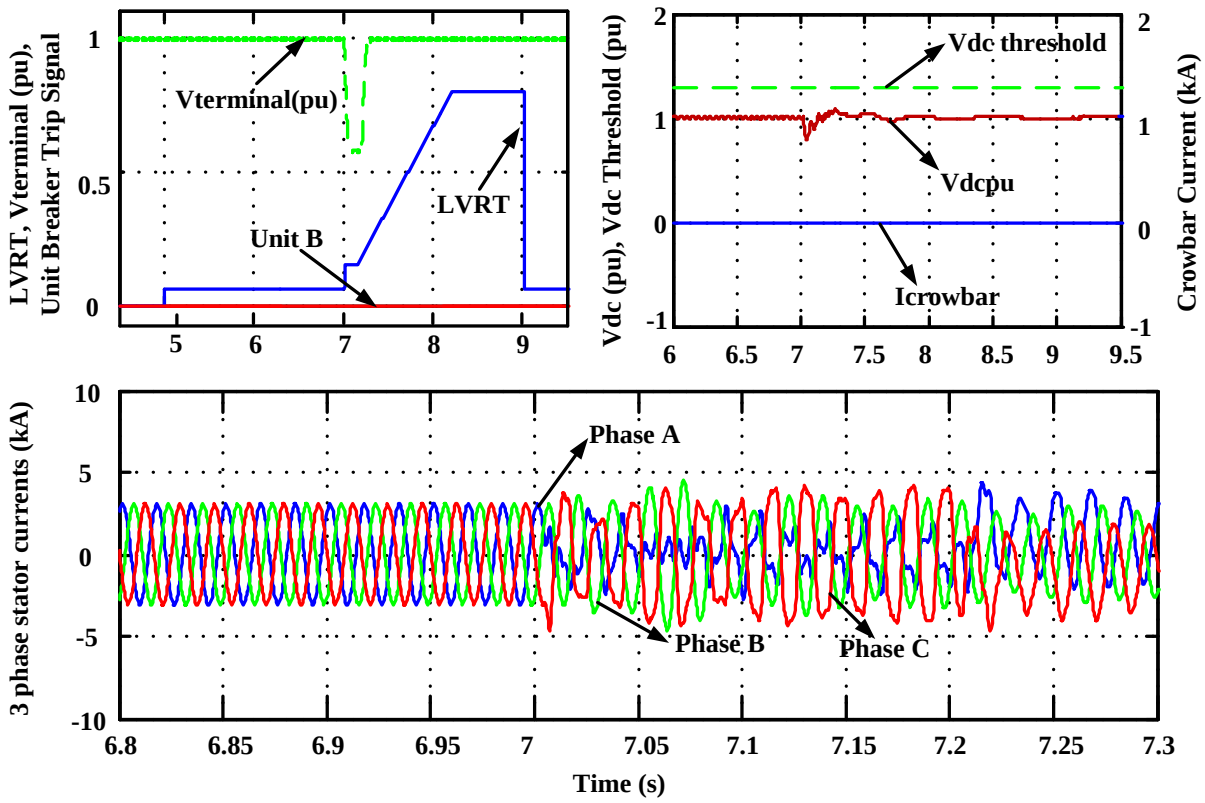

Figure 2.27: Response of DFIG to a 75 percent phase A voltage sag for 200 ms (Case 3)

2.3.3.6 Application of Faults

In this section, symmetrical (three phase) and unsymmetrical (single line to ground) faults are applied to the test system at the point of interconnection (POI) of the wind farm to the grid and the fault current behavior is studied for each case. POI is the node at which metering for the wind farm is installed and is on the high voltage side of the main transformer at the substation [10].

Symmetrical fault:

The response of the generator to a permanent three phase fault (Case 4) is shown in Figure 2.28. In such a scenario, the unit breaker trips and the crowbar is triggered. When the DC-link voltage exceeds the threshold, a spike in the crowbar current indicating crowbar activation is shown.

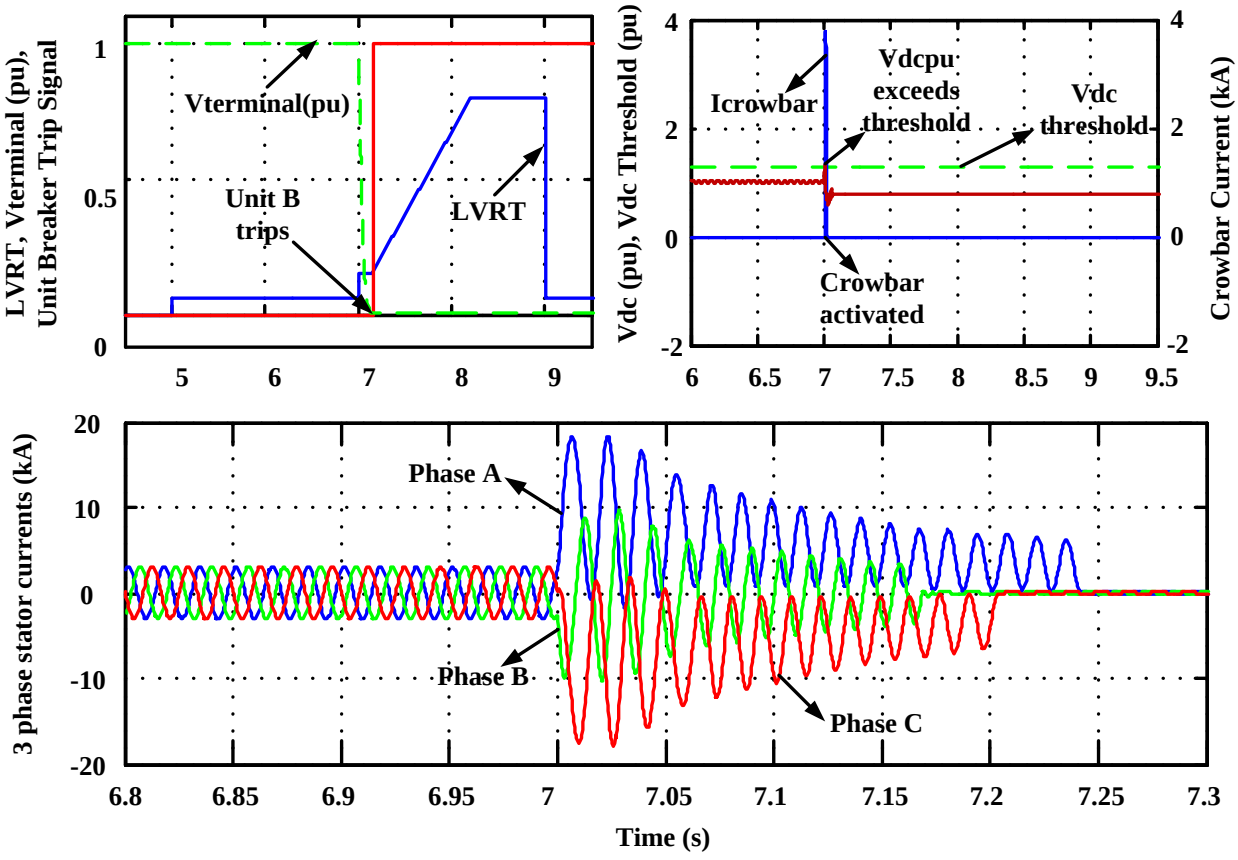

Figure 2.28: Response of DFIG to a permanent 3 phase fault (Case 4)

For a 3 phase permanent fault, Figure 2.29 shows the dominant frequency components present in the fault current obtained from fast Fourier transform (FFT) analysis. In order to obtain the magnitude of the fundamental frequency and the DC component during the first cycle after application of the fault, the FFT analysis was performed 0.016 s after the application of the fault, i.e., at 7.016 s. This is because the FFT computations are based on the sampled data window of the preceding input signal cycle. The 60 Hz frequency component is the most dominant compared to other components with a magnitude of 7.7495 kA. The FFT analysis is done at a base frequency of 60 Hz, so the fundamental 60 Hz frequency component is represented by the first harmonic. The magnitude of the DC component obtained using the FFT is 9.847 kA.

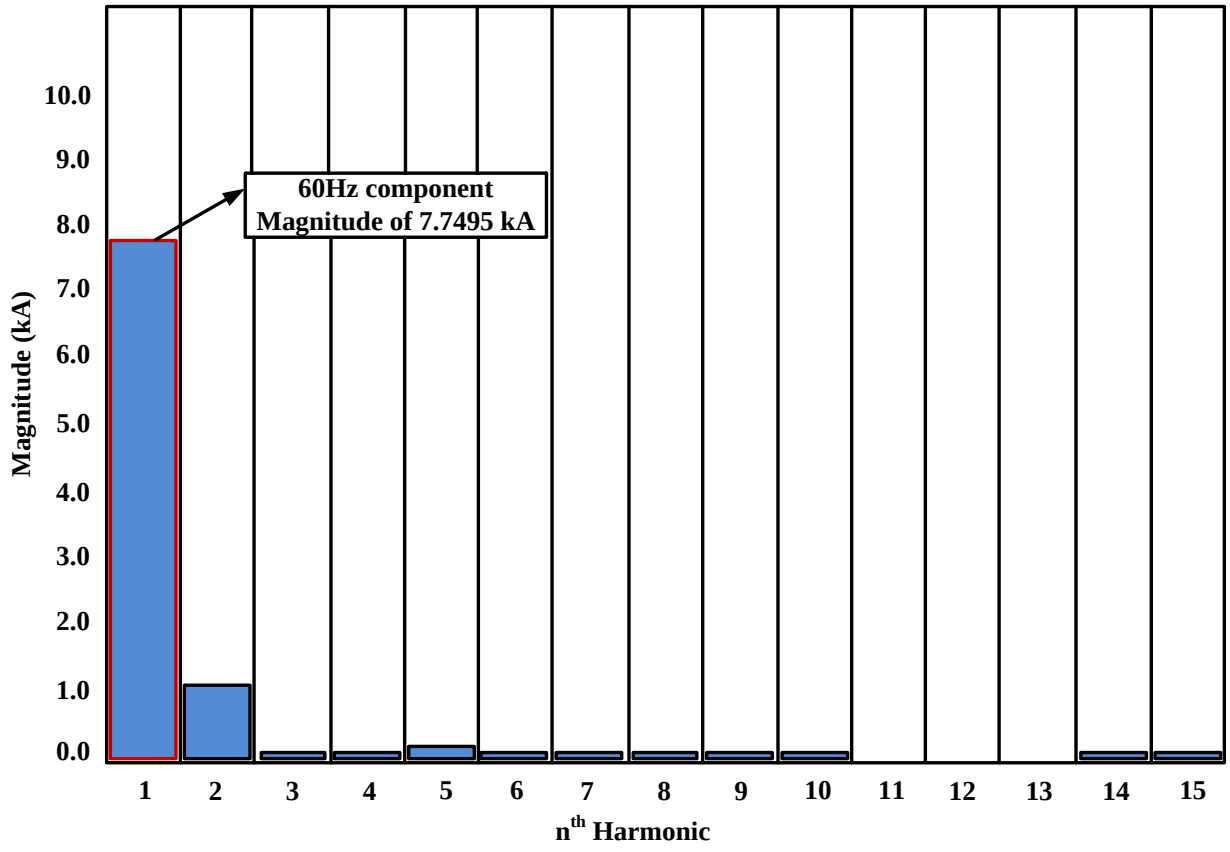

Figure 2.29: FFT output of phase A stator current after fault application

Following this, a Prony analysis of the phase A stator current is done in TSAT^{TM}[2]. Prony

[2]TSAT^{TM} is a leading-edge full time-domain simulation tool designed for comprehensive assessment of

analysis [57] samples the complex waveform and fits the record with a linear prediction estimate model (i.e. sum of complex damped sinusoid components) $y(t)$, which is given by

$$y(t) = \sum_{i=1}^{N} A_i e^{\sigma_i t} cos(2\pi f_i t + \phi_i), \tag{2.30}$$

where A_i is the amplitude, σ_i is the damping coefficient, f_i is the frequency and ϕ_i is the phase angle of the i^{th} frequency component. N is the total number of damped sinusoid components. Prony analysis of the phase A stator fault current reveals the 60 Hz frequency component and the DC component to be the most dominant components that constitute the waveform. Table 2.1 shows the parameters of the 60 Hz and DC components obtained from the analysis, where the percentage damping is calculated by $-\sigma/\sqrt{\sigma^2 + \omega^2}$ [58]. Consequently, the percentage damping of the DC component ($\omega = 0$) is obtained as 100 % irrespective of the sampling time window.

Table 2.1: Prony analysis of phase A stator current

Magnitude (kA)	Phase (deg)	Frequency (Hz)	Damping (%)
8.5698	0.000	0.000	100
7.3280	-114.970	60.225	1.294

The FFT results are obtained by sampling the first cycle of the waveform, whereas the Prony analysis had to be done over a period of time after the fault application. The Prony analysis also uses an approximate model to fit the waveform. This results in some difference between the results obtained from these two methods. From the FFT and the Prony analysis results, it is clear that the fault current is primarily composed of the 60 Hz fundamental frequency component and the decaying DC component for a symmetrical fault application. Figure 2.30 shows a fairly accurate reconstruction of the fault current using the 60 Hz frequency and DC components obtained from the results of Prony analysis compared against the actual fault current waveform.

dynamic behavior of complex power systems. Its a component of DSATools.

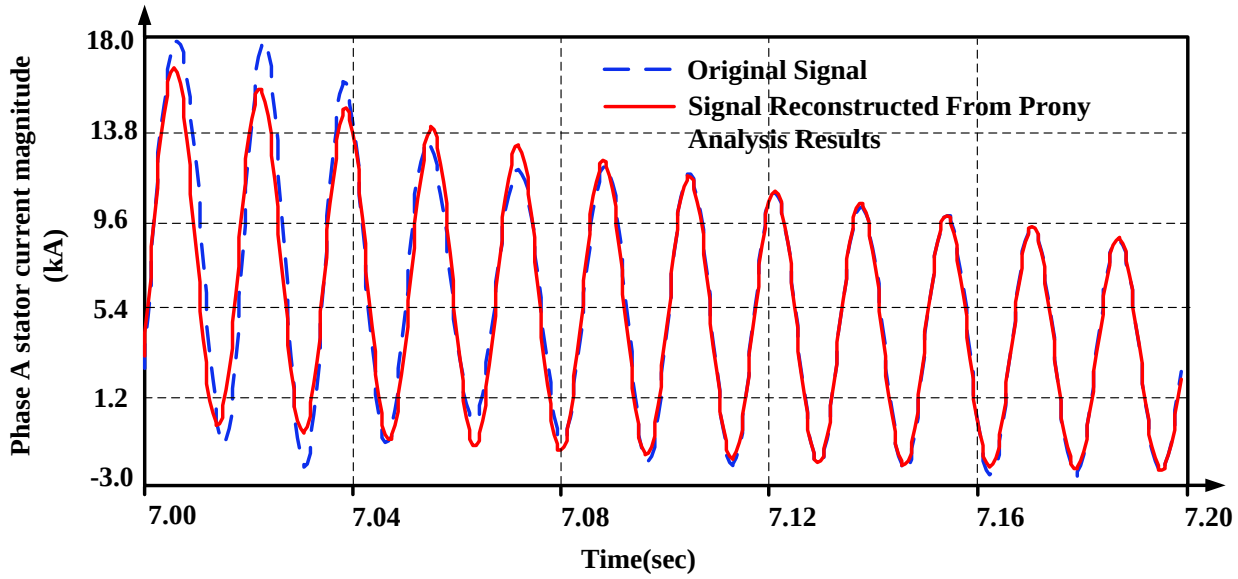

Figure 2.30: Prony analysis of phase A stator current after fault application

Unsymmetrical fault:

A single phase (Phase A) to ground fault of 200 ms is applied and the short circuit behavior is observed. Figures 2.31 and 2.32 show the short circuit behavior when three phase RMS voltage (Case 5) and phase A RMS voltage (Case 6) are compared against the LVRT curve, respectively, in order to decide the unit breaker tripping [59]. The unit breaker trips in the latter case. Similar FFT and Prony analyses of the phase A stator current waveform revealed that the fundamental frequency and the decaying DC components were the most dominant frequency components.

2.3.4 Type 4 Wind Turbine Generator

The Type 4 wind turbine generator's stator is connected to the grid through a full power AC-DC-AC converter. This means that the short circuit current is regulated and limited to the rating of the power converter. It is common practice to have the converter rated at 1.1 pu with an overload capacity of 10 percent [46]. Thus Type 4 wind turbines can be represented by a current source with upper and lower fault current limits for short circuit analysis [37].

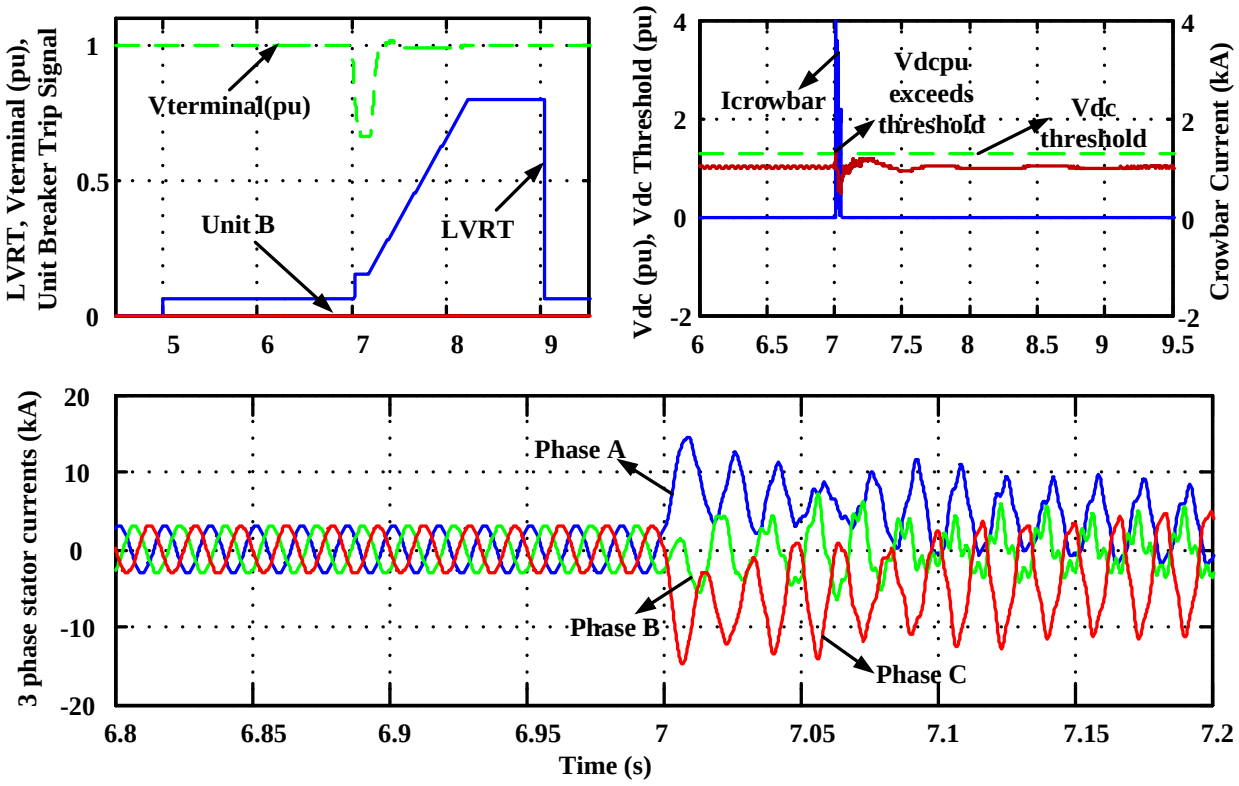

Figure 2.31: Phase A-G fault response (Case 5)

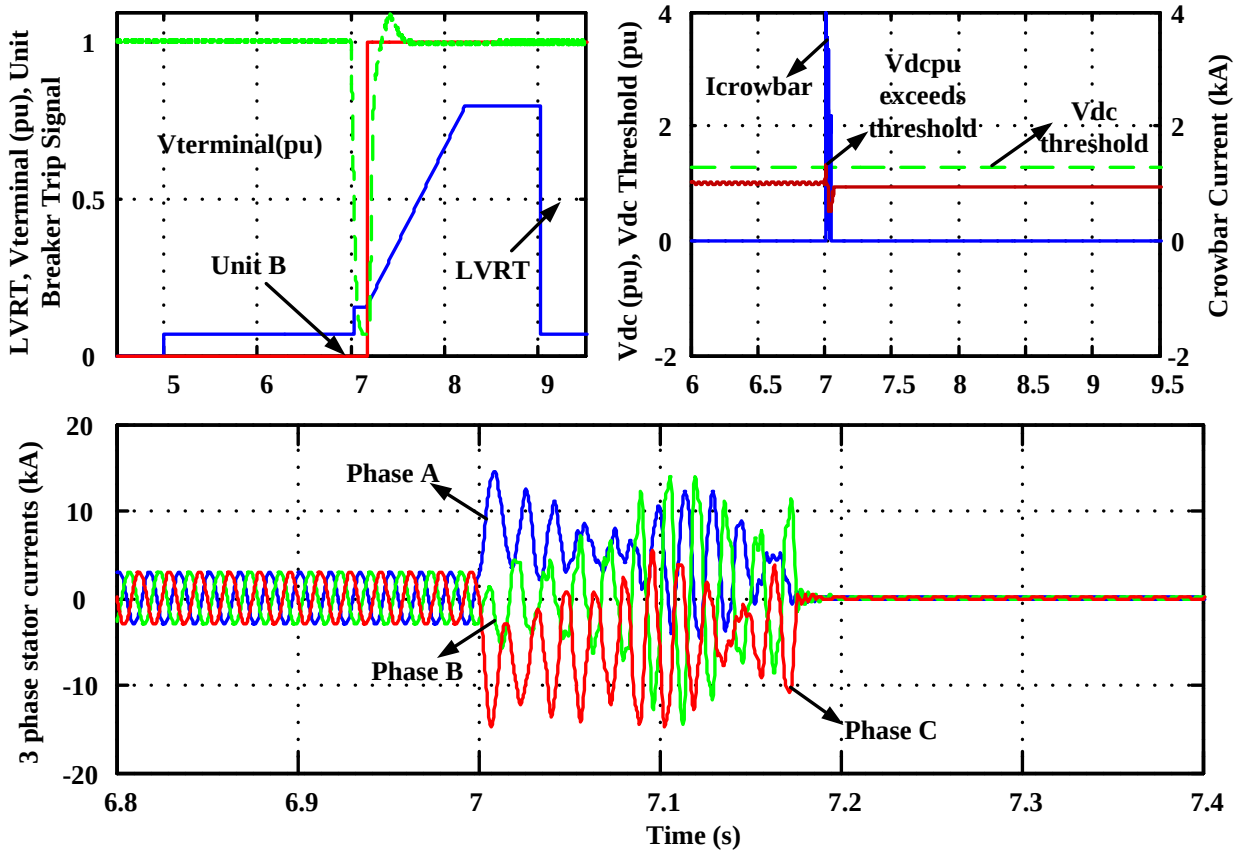

Figure 2.32: Phase A-G fault response (Case 6)

2.4 Summary

This chapter discusses not only the different types of wind turbine generators, but also the unique factors of each of these generators that influence their short circuit modeling accuracy. The typical short circuit behavior of each wind generator type was discussed, with the emphasis being on Type 3 wind generators as the main focus of this thesis. This characterization of the short circuit behavior will be used in Chapter 3 to determine which modeling techniques are well suited for each of the wind generators along with the advantages and disadvantages of each technique.

Chapter 3

Short Circuit Modeling of Wind Turbine Generators

3.1 Introduction

Short circuit modeling of wind turbine generators is crucial for finding the relay settings and equipment ratings and for protection coordination in a wind integrated power system. Various modeling techniques, from a simple electromechanical fundamental frequency model to a detailed EMT model, have been used to represent the short circuit behavior of wind turbine generators. The choice of the appropriate modeling technique depends on the degree of accuracy and level of sophistication needed for a particular study.

In Chapter 2, the typical short circuit behavior of the different types of wind turbine generators was characterized. This chapter presents a critical review of the commonly used techniques for modeling the short circuit behavior of wind turbine generators with their advantages and limitations. The short circuit studies done in Chapter 2 are used as the basis to select the appropriate modeling technique to accurately represent each type of wind generator.

The accuracy of these modeling techniques is validated against results from detailed EMT benchmark models. In order to do so, the envelope of the fault current must be obtained to find the RMS value of the fault current at the inception of the fault. For instance, the phase A fault current obtained from the detailed EMT simulation of a Type 1 wind generator for a three phase symmetrical fault at its terminals is considered. The upper and lower envelopes of the fault current waveform, as shown in Figure 3.1 below, are obtained and

extrapolated to the instant of fault application [17]. MATLAB^{TM} [1] curve fitting toolbox is used to obtain the fault current envelopes. Subtracting the value I_L from I_U gives the peak to peak fault current at fault inception from which the RMS value of fault current can be obtained. The RMS fault current at fault inception obtained from this method is $(11.123 - 0.06)kA/2\sqrt{2} = 3.91kA$.

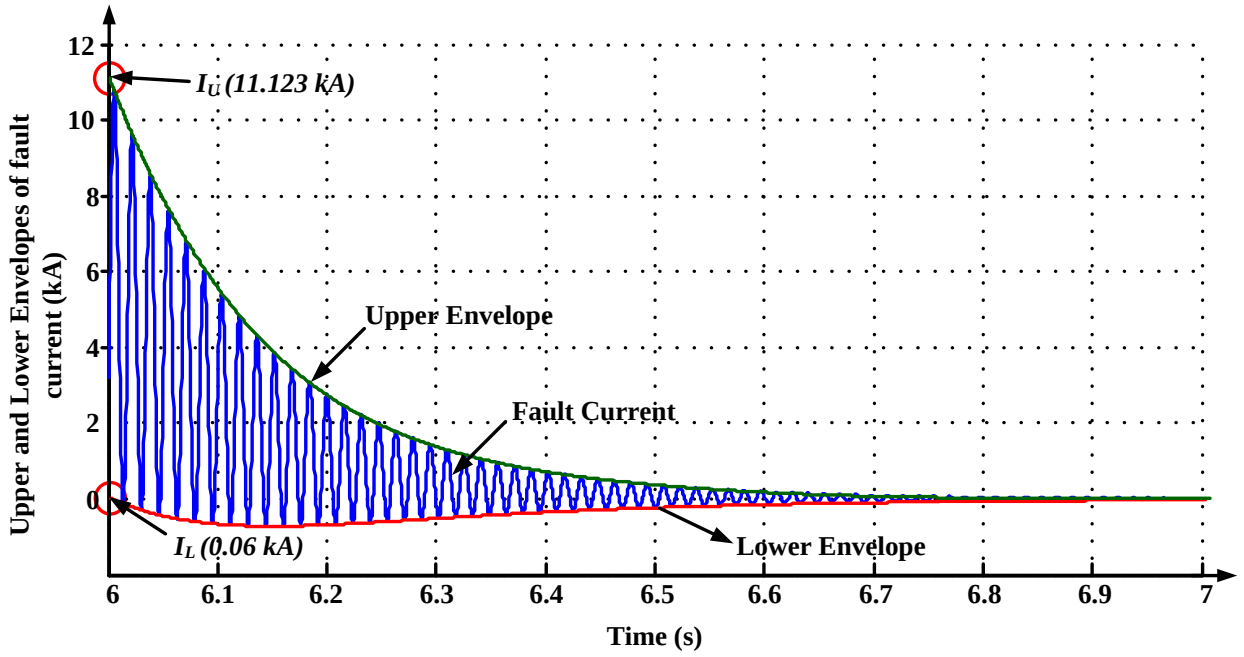

Figure 3.1: Upper and lower envelopes of the fault current waveform

As will be demonstrated in the forthcoming chapters, there are certain scenarios in which the fault current waveform does not exhibit the typical behavior of reaching the maximum value immediately after the fault application. In these cases, the fault current magnitude after the first few cycles tends to be higher than the magnitude immediately after the fault application.

[1] MATLAB^{TM} is a registered trademark of The MathWorks, Inc. MATLAB is a high-level language and interactive environment for numerical computation, visualization, and programming.

3.2 Voltage behind Transient Reactance Representation

This method is based on modeling the wind generator as a VBR circuit to represent its short circuit behavior. In this method, the sequence component networks are used as the basis for calculating the parameters of the VBR representation from which the short circuit current value at the inception of the fault can be calculated. The basis for this representation is that the generator's rotor flux remains relatively unchanged for a short duration immediately after a fault occurs, which allows the fault current to be calculated using basic circuit theory with the stator windings short-circuited [17].

3.2.1 Type 1 Wind Generator

For a symmetrical three phase fault applied at the terminals of the generator, it is studied whether the positive sequence network of the Type 1 wind generator test system (Figure 2.7) is sufficient to find the RMS value of the fault current at the inception of the fault. The equivalent circuit of the Type 1 wind generator test system is shown in Figure 3.2 below. It should be noted that, in all calculations, the rotor side parameters have been referred to the stator side. The positive sequence network is derived from this equivalent circuit.

The transient reactance of the machine (X') and the voltage behind the transient reactance (V') can be calculated from the equivalent circuit [17] and are expressed by the equations

$$jX' = jX_s + j(X_r \| X_m) \tag{3.1}$$

and

$$V' = V_\infty + jI_s(X' + X_{line} + X_{transformer}), \tag{3.2}$$

where X_s, X_r, and X_m are the stator, rotor, and mutual reactances respectively, V_∞ is the voltage at the infinite bus (grid), and I_s is the stator current. The winding resistances are not considered in the calculations as they have negligible values. However, this assumption

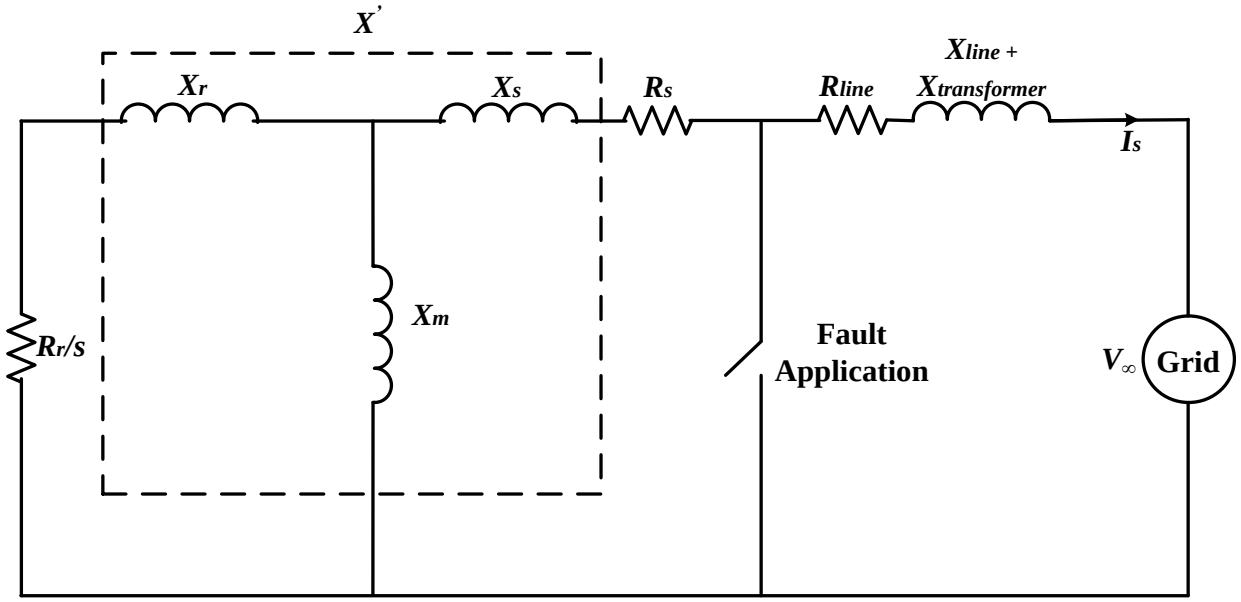

Figure 3.2: Equivalent circuit of the Type 1 wind generator test system

is not valid for Type 2 and 3 wind generators as they have external rotor resistance and crowbar resistance effects, respectively.

From the X'and V' values, the short circuit current at the inception of the fault can be found from the equation

$$I_{sc} = \frac{V'}{X'}. \tag{3.3}$$

The positive sequence network used for the voltage behind transient reactance representation of a Type 1 wind generator for a symmetrical fault is shown in Figure 3.3 below. All of the resistances have been neglected.

For an unsymmetrical Phase A to ground fault applied at the terminals of the generator, the methodology to find the fault current is very similar except that the sequence network of the test system would now also include the negative sequence component network. The negative sequence impedance is the same as the positive sequence impedance and all of the resistances are neglected. As the generator is wye-ungrounded and the unit transformer is delta on the secondary, there are no zero sequence components present. Hence the zero sequence network is not included. The positive and negative sequence networks are connected

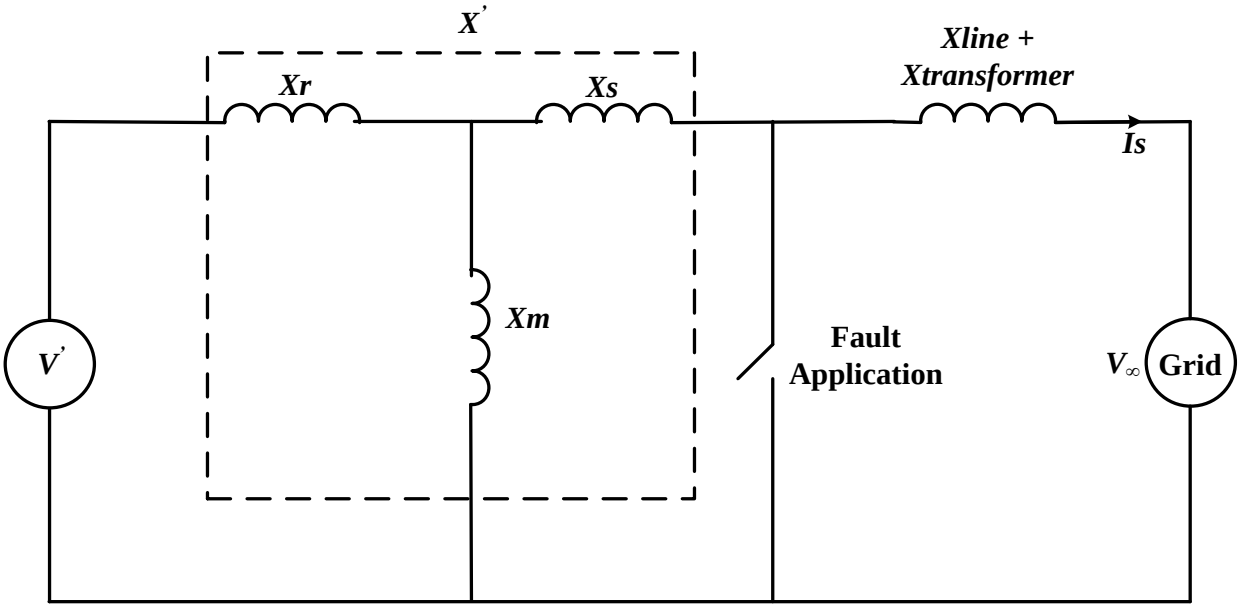

Figure 3.3: Voltage behind transient reactance model (positive sequence network) of Type 1 wind generator test system for symmetrical fault

in series for finding the fault current for a single line to ground fault.

Table 3.1 below shows the values of the Phase A RMS fault currents at the inception of the fault obtained from a detailed EMT model found using the upper and lower envelopes described before and from the VBR model for both symmetrical and unsymmetrical faults. The voltage behind transient reactance representation is fairly accurate with respect to representing the short circuit behavior of a Type 1 wind generator, even while neglecting the winding resistances and considering only the winding reactances.

Table 3.1: Comparison of results for Type 1 wind generator - ungrounded system

Modeling	3 phase fault current	Phase A-G fault current (ungrounded)
EMT	3.91 kA	2.51 kA
VBR	3.951 kA	2.632 kA

A test case with a wye-grounded generator and wye-wye grounded unit transformer was modeled to assess the impact of the zero sequence component on the fault current magnitude

and to find the accuracy of the VBR modeling. The zero sequence impedances for the generator, transformer, and transmission line respectively are half of, equal to, and 2.5 times of the positive sequence impedance. The result obtained as compared against the EMT result is shown in Table 3.2.

Table 3.2: Comparison of results for Type 1 wind generator - grounded system

Modeling	Phase A-G fault current (grounded)
EMT	5.424 kA
VBR	5.842 kA

3.2.2 Type 2 Wind Generator

This section discusses the modeling of a Type 2 wind generator test system with the sequence networks for the symmetrical and unsymmetrical faults to find the fault current values. In case of a Type 1 wind generator, using only the reactance values (neglecting the winding resistances) to calculate the transient reactance gave sufficiently accurate results. However, it was shown in Section 2.3.2 (Refer Figure 2.14) that the external rotor resistance value for a Type 2 wind generator plays an important role in determining the magnitude of the fault current.

This means that the external rotor resistance $R_{r_{ext}}$ should be included in the calculation of the transient impedance Z' (transient reactance was used for Type 1 wind generator) which is shown in Equation 3.4 below. Figure 3.4 shows the voltage behind transient reactance representation (positive sequence network) of the Type 2 wind turbine generator for a symmetrical three phase fault application where the winding resistances and the external rotor resistance have been included for the fault current calculation.

$$Z' = (R_s + jX_s) + (((R_r + R_{r_{ext}})/s + jX_r) \| jX_m) \tag{3.4}$$

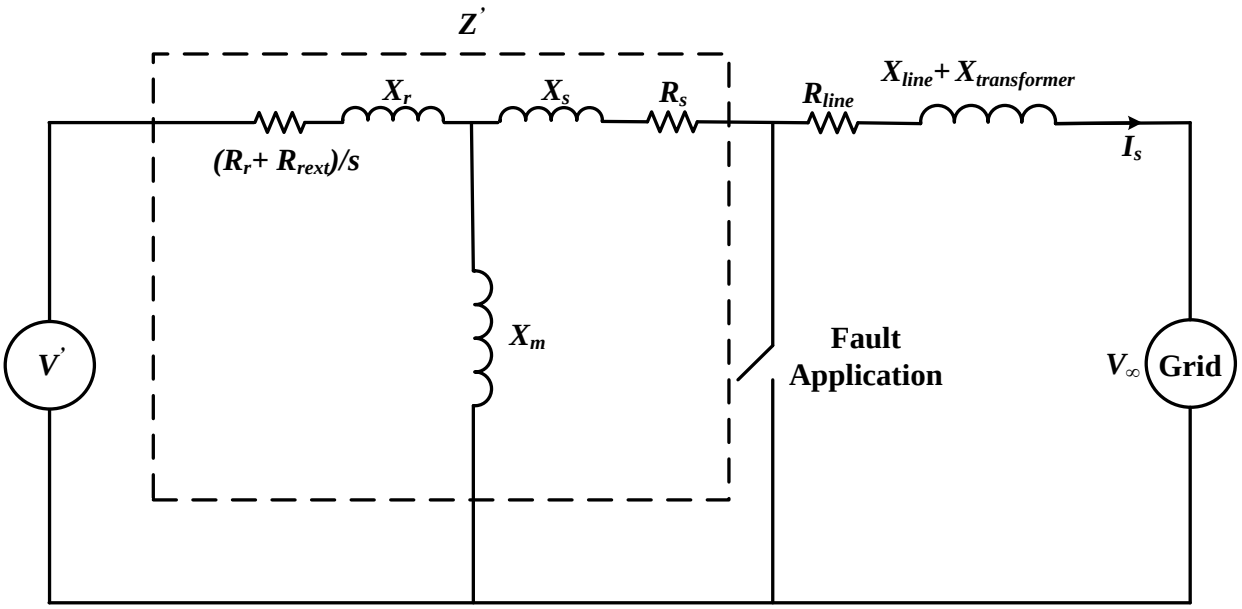

Figure 3.4: Positive sequence network of Type 2 wind generator test system

Further, the voltage behind the transient impedance and the short circuit current are calculated from the equations

$$V' = V_\infty + I_s(Z' + R_{line} + jX_{line} + jX_{transformer}) \tag{3.5}$$

and

$$I_{sc} = \frac{V'}{Z'}. \tag{3.6}$$

Similarly, for an unsymmetrical phase A to ground fault at the terminals of the Type 2 wind generator, the fault current at the inception of the fault is calculated from the positive and negative sequence symmetrical component circuits connected in series. However, the negative sequence impedance is calculated as

$$Z'_{-} = (R_s + jX_s) + (((R_r + R_{r_{ext}})/(2 - s) + jX_r) \| jX_m) \tag{3.7}$$

Table 3.3 shows the values of short circuit currents calculated for symmetrical and unsymmetrical fault conditions with and without considering the rotor external resistance. These are compared against the results from the detailed EMT simulation model. VBR1 represents

the model results neglecting the effect of rotor external resistance and VBR2 represents the model results including the effect of rotor external resistance. Including the rotor external resistance value for the three phase fault current calculation reduces the accuracy error for both symmetrical and unsymmetrical fault representations.

Table 3.3: Comparison of results for Type 2 wind generator

Modeling	Three phase fault current (kA)	Phase A-G fault current (kA)
EMT	3.025	1.944
$VBR1$	3.9602	2.759
$VBR2$	3.1668	2.074

The VBR method of modeling can be used to calculate fairly accurately, the symmetrical and unsymmetrical fault current contributions of Type 1 and Type 2 wind generators at the inception of the fault.

3.2.3 Type 3 Wind Generator

This section discusses the accuracy of the VBR model for a Type 3 wind generator. The short circuit behavior of a Type 3 wind generator is much more complex compared to the Type 1 and Type 2 wind generators. Some of these complexities have been discussed previously in Section 2.3.3 and others will be discussed in the forthcoming chapters.

To find the accuracy of the voltage behind transient reactance model, the short circuit current behavior obtained from the detailed EMT model shown in Section 2.3.3.6 is used as a benchmark. Envelopes are used to find the fault current at the inception of the fault from the EMT simulation results.

Figure 3.5 shows the positive sequence network of the Type 3 wind generator [15] where the rotor crowbar resistance is included in the circuit to protect the back-to-back converter in case of a fault scenario. It was shown in Section 2.3.3.6 that the crowbar is not triggered throughout the duration of the fault application in the detailed EMT model. However, this

is not the case in VBR modeling where the crowbar is assumed to be triggered during the entire duration of the fault, which reduces the modeling accuracy.

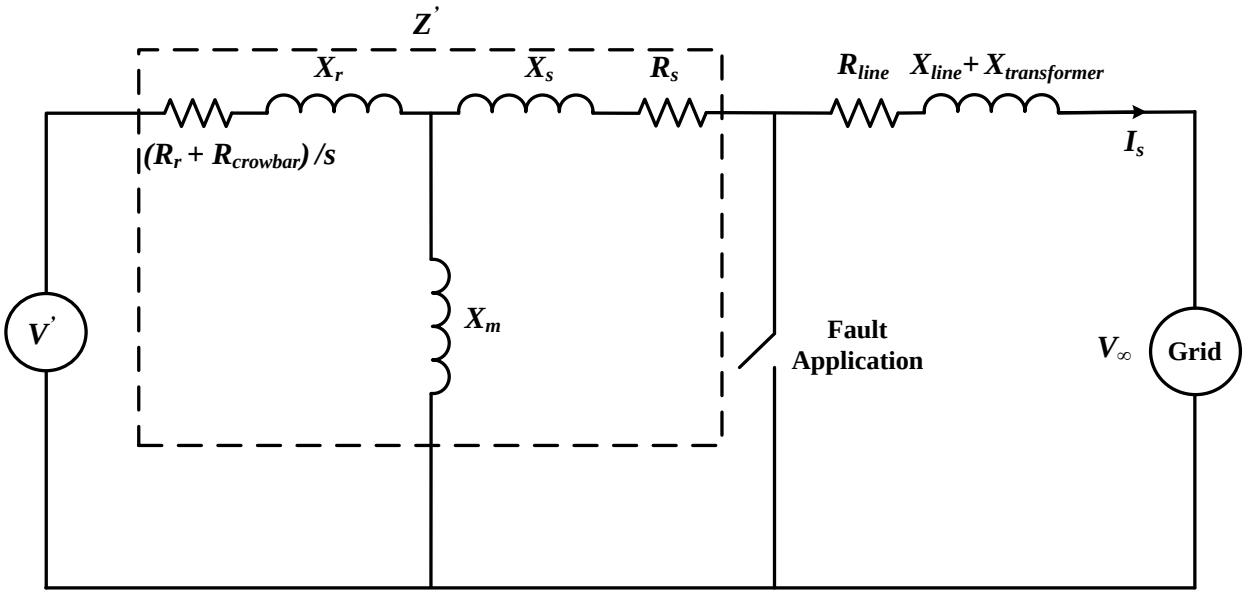

Figure 3.5: Voltage behind transient reactance model (positive sequence network) of Type 3 wind generator test system for a symmetrical fault

The fault current for a symmetrical three phase fault applied at the terminals of the generator is found using the positive sequence network where the net rotor resistance is calculated as $(R_r+R_{crowbar})/s$. All of the winding resistances and the rotor crowbar resistance are included in the short circuit current calculations. In the case of an unsymmetrical fault at the terminals of the generator, both the positive and negative sequence networks are included in the calculations. The net rotor resistance for the negative sequence network is calculated as $(R_r + R_{crowbar})/(2 - s)$. Table 3.4 below shows the accuracy of the voltage behind transient reactance model for representing the Type 3 wind generator's symmetrical and unsymmetrical fault behavior compared to the benchmark EMT model. It is not as accurate as demonstrated for the Type 1 and 2 wind generators.

Table 3.4: Accuracy of voltage behind transient reactance modeling for Type 3 wind generator

Modeling	Three phase fault current (kA)	Phase A-G fault current (kA)
EMT	6.31	4.80
VBR	6.618	3.8808

3.2.4 Section Summary

In the VBR modeling method, the positive sequence network equivalent was used for symmetrical three phase fault calculations. The sequence network consisting of the positive and negative sequence components was used for unsymmetrical phase A to ground fault calculations. This modeling technique was determined to be accurate enough for representing Type 1 and 2 wind generators. The inclusion of the external rotor resistance for short circuit calculations improved the modeling accuracy for Type 2 wind generators. However this method is not as accurate for a Type 3 wind generator. This modeling technique yields the fault current at the moment the fault occurs but not during the entire fault duration.

3.3 Representation by Analytical Expression

This method is based on representing the short circuit current behavior of wind generators by means of an analytical expression obtained for the stator fault current from the per phase equations used to represent an induction machine for transient studies. These equations in a synchronously rotating reference frame are given by

$$\psi_s = L_s i_s + L_m i_r, \tag{3.8}$$

$$\psi_r = L_r i_r + L_m i_s, \tag{3.9}$$

$$V_s = R_s i_s + \omega_s \psi_s + \frac{d\psi_s}{dt}, \tag{3.10}$$

and

$$V_r = R_r i_r + \sigma \omega_s \psi_r + \frac{d\psi_r}{dt}. \tag{3.11}$$

As discussed in reference [14], the expression for the phase A stator fault current is

$$Is_a = \sqrt{2}\frac{V_s}{Z'}[e^{-t/T_s}\cos\alpha - (1-l)e^{j\omega_s t}e^{-t/T_r}\cos(\omega_s t + \alpha)]. \tag{3.12}$$

L_{s-eqv} is the equivalent inductance looking from the stator into the short circuited rotor given by $L_s + (L_r \| L_m)$ and L_{r-eqv} is the equivalent inductance looking from the rotor into the short circuited stator given by given by $L_r + (L_s \| L_m)$ where L_m is the mutual inductance. T_s and T_r are the damping time constants of the stator and rotor, respectively. They are computed using $T_s = L_{s-eqv}/R_s$ and $T_r = L_{r-eqv}/R_{r-eff}$. R_s is the stator winding resistance. R_{r-eff} is the effective rotor resistance and varies with the wind generator type under study. L_s and L_r are the stator and rotor winding self inductances. l is the leakage factor, which is calculated as $1 - (L_m^2/L_s L_r)$. All rotor parameters are referred to the stator side. Z' is the transient impedance and α is the voltage phase angle. The stator fault current for all of the wind generator types is obtained using the above Equation 3.12; however, the calculation of T_r, and Z' are dependent on the type of wind generator under study.

3.3.1 Type 1 Wind Generator

As discussed previously, the stator fault current of a Type 1 wind generator can be resolved into two components, namely an AC and a DC component [46] that are shown in Figures 3.6 and 3.7, respectively. The DC component shown in Figure 3.7 and in the first term of Equation 3.12 is damped with a time constant of T_s. Similarly the AC component shown in Figure 3.6 and in the second term of Equation 3.12 is damped with a time constant of T_r. This behavior is expressed mathematically by the above Equation 3.12 where, for a Type 1 wind generator, it is sufficient to use the value of the transient reactance X' (Refer Equation 3.1) for Z' and L_{r-eqv}/R_r for T_r.

The phase A stator fault current for a symmetrical three phase fault obtained from this analytical expression is compared against that obtained from the EMT model as shown in

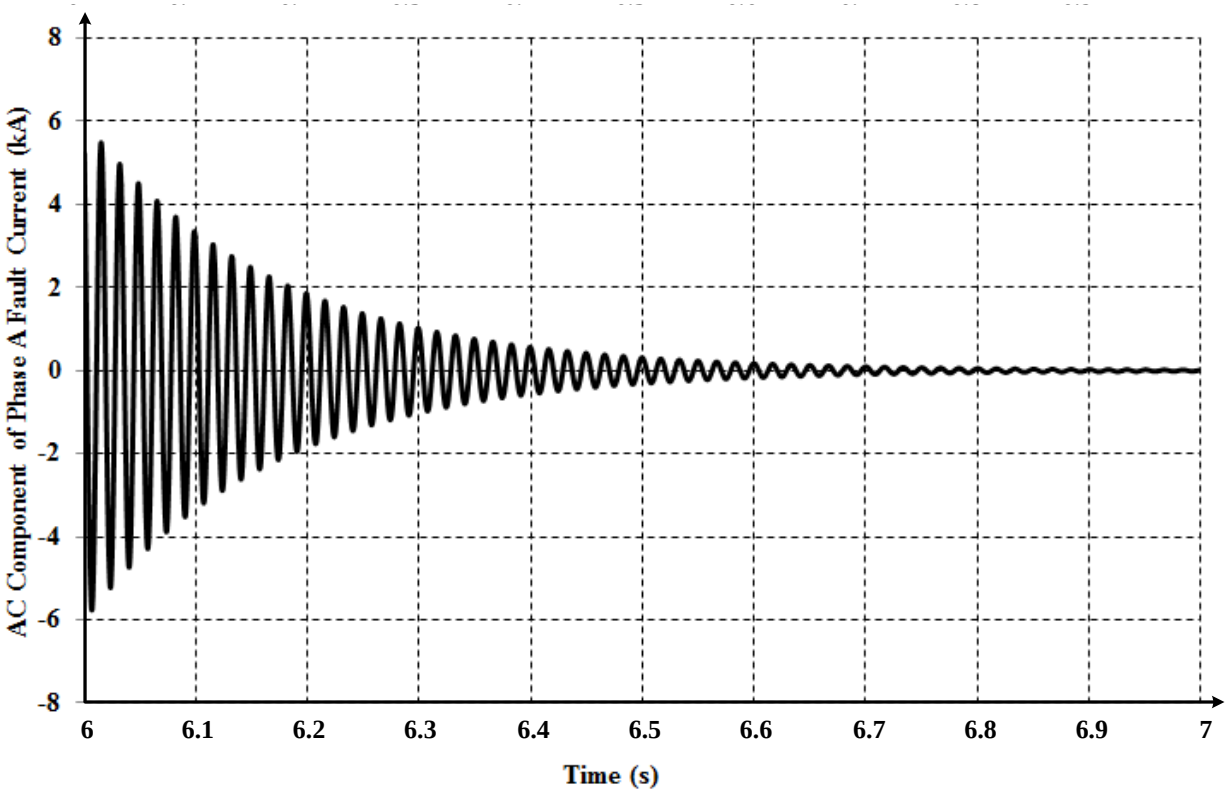

Figure 3.6: AC Component of Phase A fault current

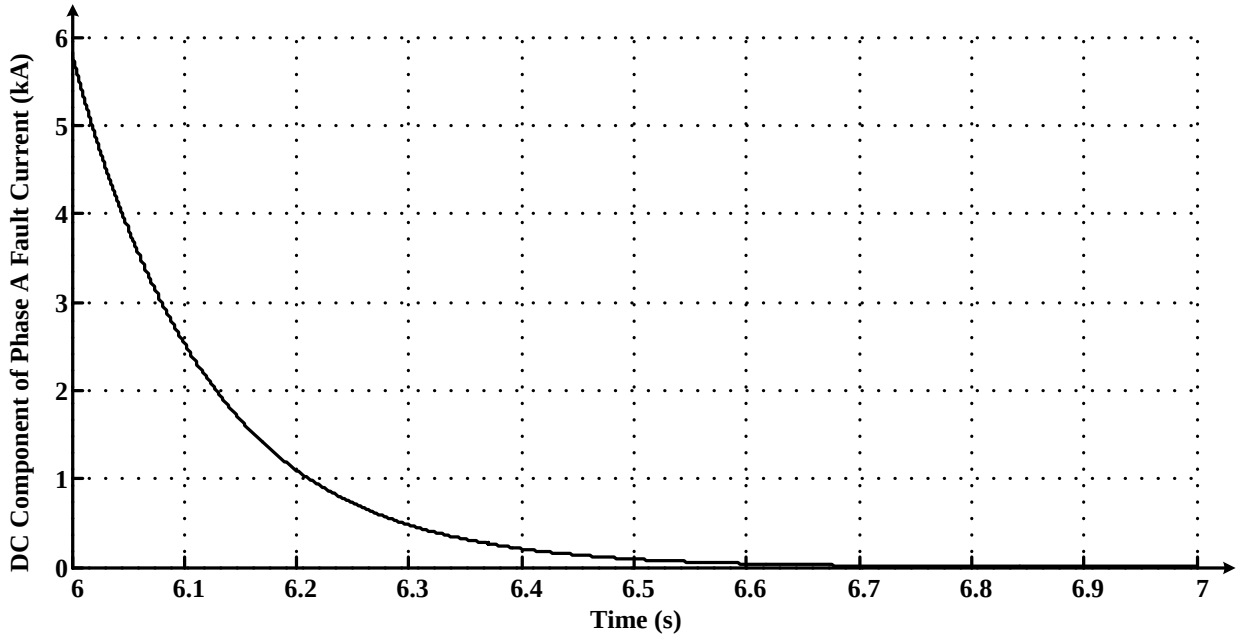

Figure 3.7: DC Component of Phase A fault current

Figure 3.8. This representation by the analytical expression gives highly accurate results for a Type 1 wind turbine generator.

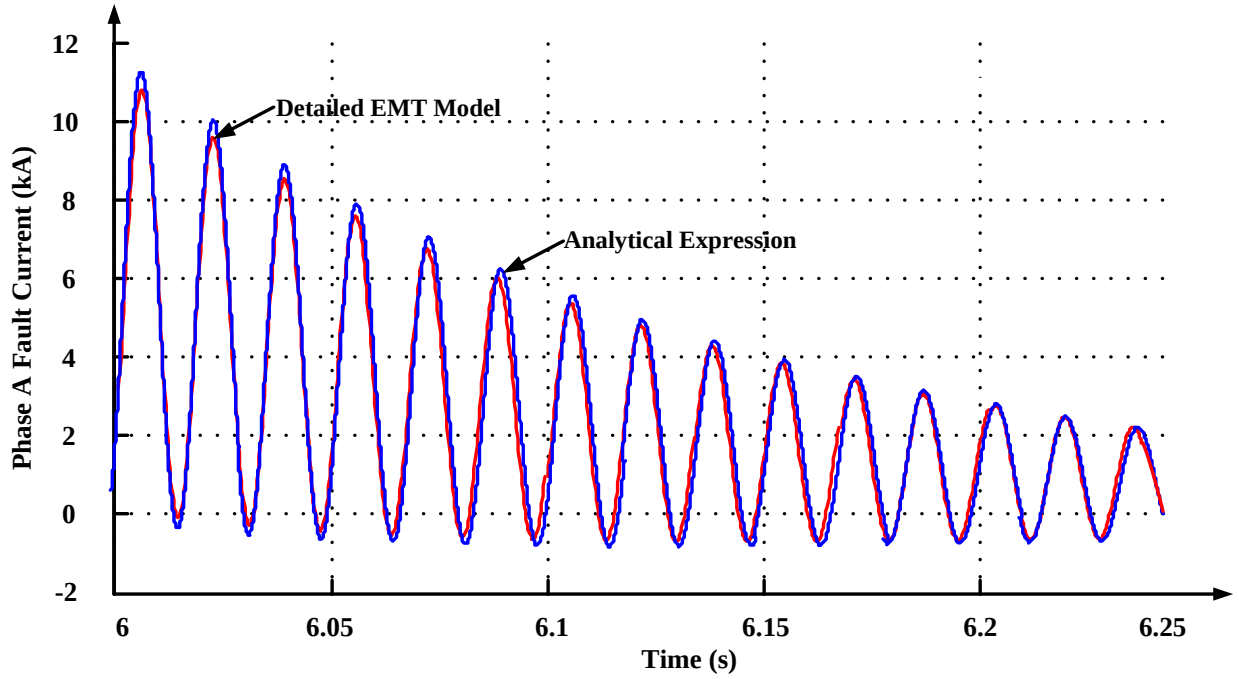

Figure 3.8: Three phase fault - Phase A stator currents - Type 1 wind generator - EMT model versus analytical expression

3.3.2 Type 2 Wind Generator

Similar to a Type 1 wind generator, the short circuit current of a Type 2 wind generator is found from the mathematical expression in Equation 3.12. The effect of the external rotor resistance on the short circuit behavior was explained in Section 2.3.2 according to which, the model accuracy improves significantly by including the rotor external resistance value in the calculations.

This aspect is achieved by using a value of $\sqrt{X'^2 + R_{r_{ext}}^2}$ for Z' in the denominator term ignoring the stator and rotor winding resistances [14]. The rotor decay time constant is calculated as $T_r = L_{r-eqv}/(R_r + R_{r_{ext}})$ for a Type 2 wind turbine generator. Figure 3.9 shows the short circuit current waveforms obtained from the above mathematical expression with and without considering the external rotor resistance and compared against the EMT

model results. The short circuit current obtained considering the external rotor resistance is more accurate and closer to the results from the EMT model.

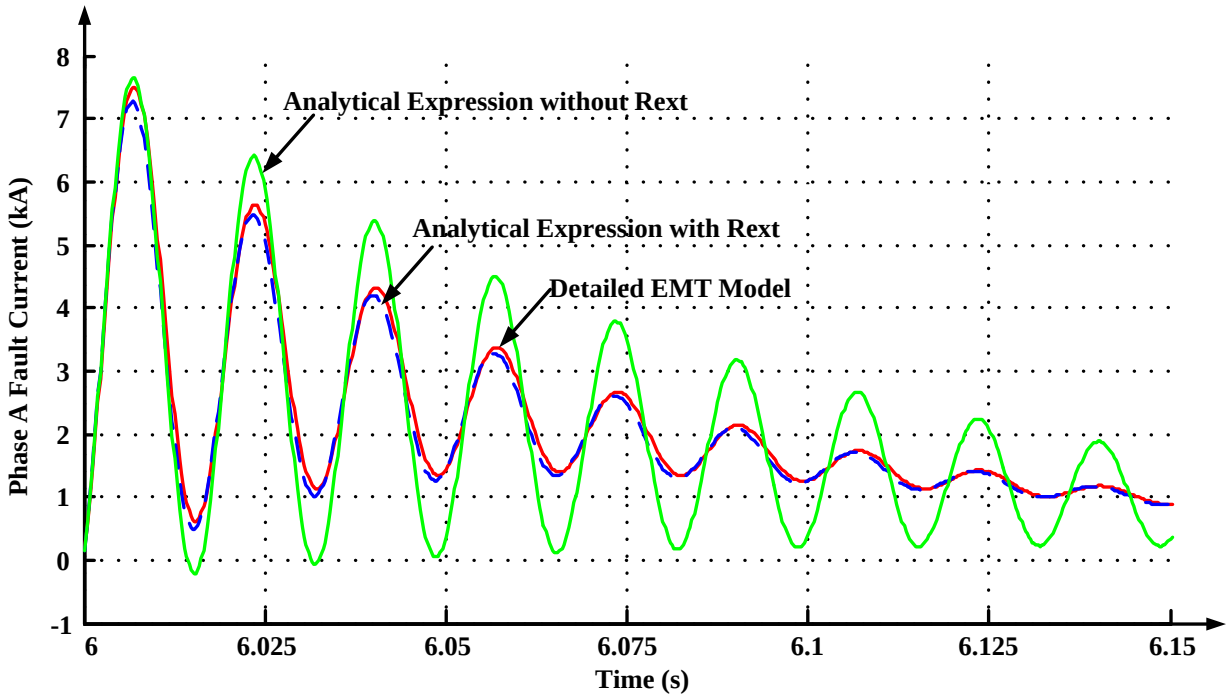

Figure 3.9: Phase A Stator Currents - Type 2 wind generator - EMT model versus analytical expression

3.3.3 Type 3 Wind Generator

Because different complexities influence how a Type 3 wind generator behaves for a short circuit, it is a challenging task to accurately represent it using simple modeling techniques. Some of these complexities, such as the unit breaker protection logic based on a LVRT scheme with crowbar circuit, were discussed previously.

In order to include the effect of the rotor crowbar resistance, the transient impedance calculated as $Z' = \sqrt{X'^2 + R_{crowbar}^2}$ ignoring the stator and rotor winding resistances and the rotor decay time constant calculated as $T_r = L_{r-eqv}/(R_r + R_{crowbar})$ are used in the Equation 3.12. The accuracy of this mathematical model as compared to the EMT model is shown in Figure 3.10. This model is not as accurate for Type 3 wind generators as for Type

1 and 2 wind generators. Though the effect of the crowbar resistance is taken into account, it is still not accurate because this method considers the crowbar resistance to be included in the rotor circuit for the entire duration of the fault. In reality, the duration of application of the crowbar for a Type 3 wind generator is determined by the variation of the DC-link voltage during the fault, as explained in Section 2.3.3.3.

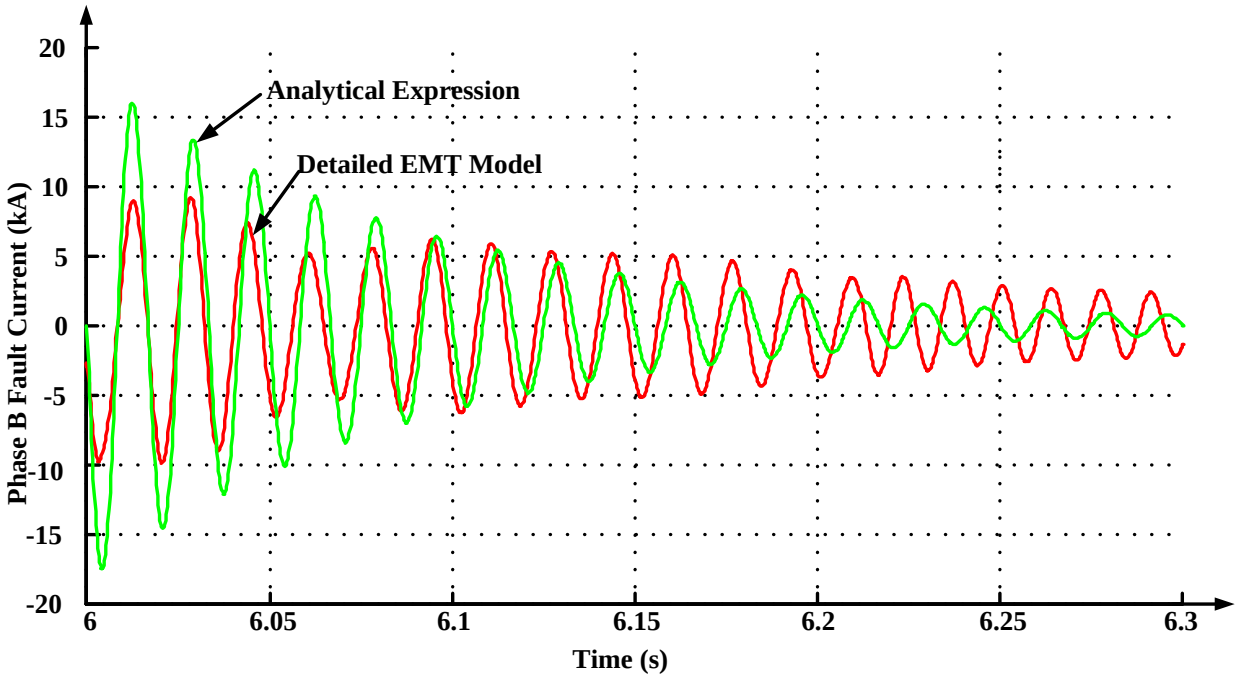

Figure 3.10: Phase B stator currents - Type 3 wind generator - EMT model versus analytical expression

3.3.4 Section Summary

The mathematical method of short circuit modeling discussed in this section is capable of producing the fault current waveform as a function of time for the entire fault duration. This is not possible by using the previously discussed VBR representation, which only gives the fault current at the inception of the fault. This method is fairly accurate for short circuit representation of Type 1 and Type 2 wind generators. Though the effect of the crowbar resistance is taken into account for a Type 3 wind generator modeling, the duration of application of the crowbar is assumed to be for the entire fault duration. This leads to

inaccuracy in representing the exact behavior.

3.4 Voltage Dependent Current Source Modeling

3.4.1 Introduction

The short circuit behavior of Type 1 and Type 2 wind generators can be sufficiently represented using the previously discussed simple modeling techniques. Type 4 wind generators, with their fault current limited by their full power converter, can be accurately represented by a current source with upper and lower limits based on the converter rating for short circuit analysis [37]. Inaccuracies were present in the modeling methods for Type 3 wind generators discussed so far. The voltage dependent current source modeling discussed in this section and the discussions in the forthcoming sections focus specifically on modeling short circuits in Type 3 wind turbine generators.

3.4.2 Type 3 Wind Generator Modeling

The method of modeling discussed in this section is based on representing the short circuit behavior of wind generators by voltage dependent current source models defined by look up tables. These look up tables contain data in the form of maximum and minimum short circuit current values as a function of the point of interconnection voltage.

The short circuit data that form the look up table can be obtained by measuring the maximum and minimum short circuit current of the wind generator when the point of interconnection voltage is varied by applying voltage sags in the range of 20 to 90 percent [37]. The application of voltage sags and the voltage sag generator topology were discussed in detail in Section 2.3.3.5. The short circuit behavior in terms of the phase A stator current as observed for the different voltage sags are shown in Figure 3.11. A detailed EMT model of the Type 3 wind generator was used in these cases to obtain the short circuit currents.

In some cases in Figure 3.11, the stator current does not reach its maximum value im-

mediately after application of the sag. Rather, it tends to be higher immediately after the sag period when the voltage recovers. In such cases, using envelopes to find the fault current magnitude gives the fault current at the inception of the fault but not necessarily the maximum value, which is essential to determine relay settings.

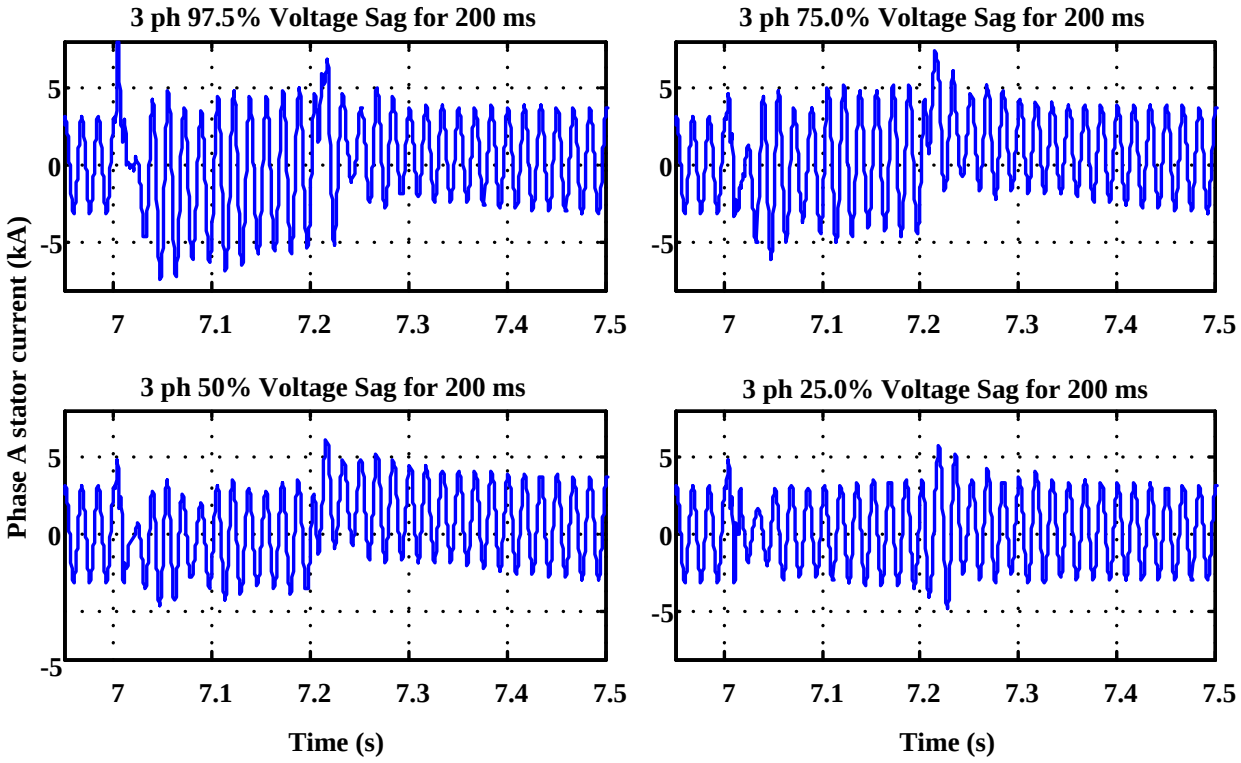

Figure 3.11: Short circuit currents for different percentages of 3-phase voltage sags for a Type 3 wind generator

The loci of the maximum and minimum fault currents obtained for different percentage sags form the upper and lower fault current envelopes, respectively, as shown in Figure 3.12. The data from these envelopes in the form of a look up table were used to model the voltage dependent current source model as shown in Figure 3.13 below.

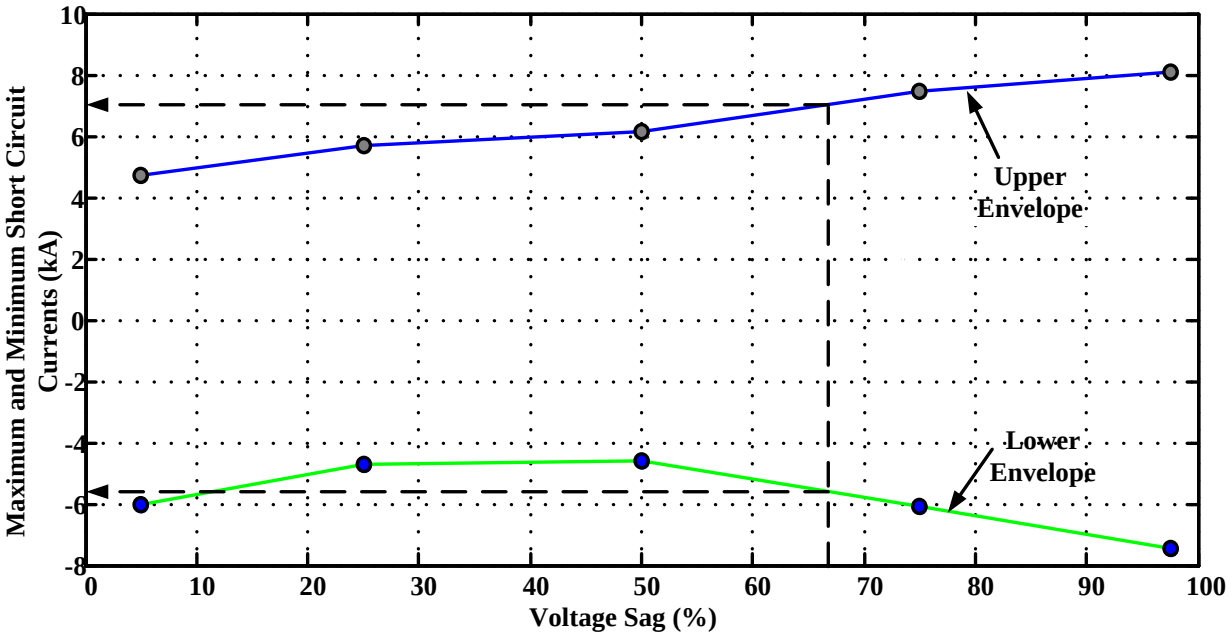

Figure 3.12: Maximum and minimum short circuit current envelopes as a function of the applied voltage sag

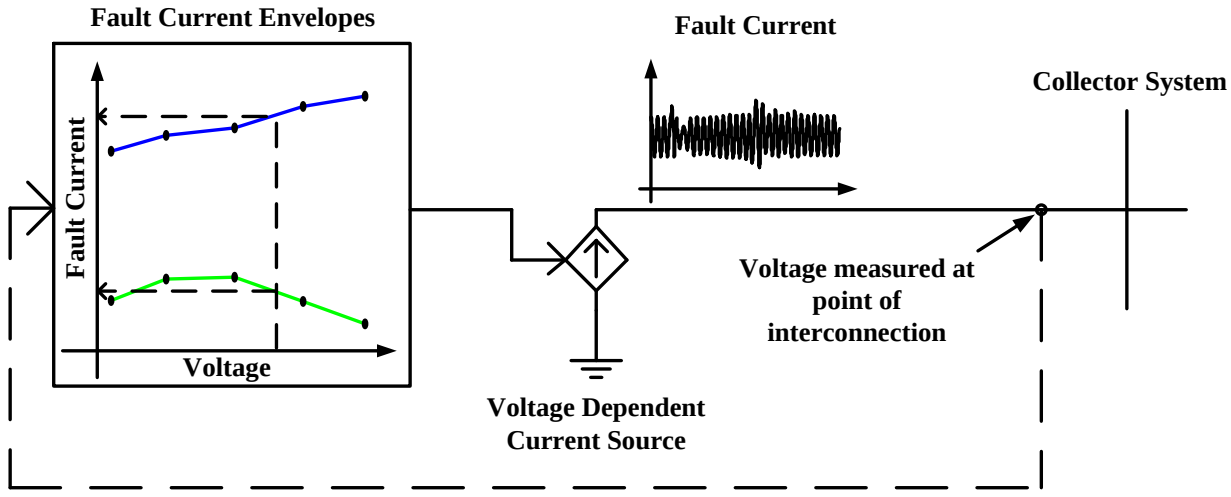

Figure 3.13: Voltage dependent current source model of Type 3 wind generator

3.4.3 Section Summary

The voltage dependent current source model is capable of generating the short circuit current characteristics of the Type 3 wind generator using a black-box like approach. The

accuracy of this model, i.e., the accuracy of the short circuit current envelopes, depends on the level of sophistication of the actual model used to obtain the maximum and minimum fault currents. In this case, a detailed EMT model was used for that purpose. It is clear that the voltage dependent current source model is not a stand-alone model, as it requires the short circuit current values to be obtained from detailed EMT models or from the wind generator manufacturer.

3.5 Summary

Voltage behind transient reactance modeling is a fairly accurate method for Type 1 and 2 wind generators; however, it is not as accurate for Type 3 wind generators. The accuracy of this approach improves with the inclusion of the rotor external resistance and the crowbar resistance for modeling Type 2 and Type 3 wind generators, respectively.

Representation using the analytical expression is highly accurate for short circuit modeling of symmetrical fault behavior in both Type 1 and Type 2 wind generators. The same level of accuracy is not achieved for Type 3 wind generator representation as this model does not consider complexities such as crowbar activation based on LVRT characteristics.

The voltage dependent current source model is capable of representing the Type 3 wind generator short circuit behavior through a black-box like approach, and its accuracy depends on the sophistication of the model that is actually used to obtain the fault current envelopes. Thus, it is not a standalone model to represent the short circuit behavior of a Type 3 wind generator.

Chapter 4 introduces scenarios under which the fault current contribution of the Type 3 wind generator could be more complex in terms of containing sub-synchronous frequency components. This illustrates the requirement for models to be able to not only model the fundamental frequency behavior but also the non-fundamental frequency components.

Chapter 4

Sub-synchronous Frequencies in Type 3 Wind Generator Fault Current Behavior

4.1 Introduction

As far as Type 3 wind farms are concerned, there could be fault conditions where the fault current may contain sub-synchronous frequency components that influence the fault current magnitude. One such event of sub-synchronous interactions in a Type 3 wind farm was reported in Texas in October 2009 [32]. The normal clearing of a fault on a 345 kV transmission line led to a network configuration where two Type 3 wind farms got radially connected to a series compensated transmission line. This configuration led to the development of sub-synchronous control interactions between the series compensated transmission line and the wind farms, which resulted in current distortion, damage to the control circuits in the wind farms, and severe over-voltages.

In this chapter, a scenario is created where sub-synchronous control interactions occur in a Type 3 wind farm connected to a series compensated transmission. This is done using a detailed EMT model built for both symmetrical and unsymmetrical fault conditions. This is followed by frequency analysis of the fault current with the sub-synchronous component present, giving valuable insights for the proposed modeling in Chapter 5.

4.2 Sub-synchronous Frequency Components in the Fault Current

Wind farms are located in wind-rich areas that are usually far away from load centers. This implies that these wind farms must be connected to load centers through long transmission lines. These transmission lines are series compensated in order to improve their power transfer capability, with the compensation providing a virtual reduction of the line reactance. Figure 4.1 shows the test system in which a Type 3 wind farm is connected to a series compensated transmission system, where R_L and X_L represent the transmission line resistance and inductive reactance, respectively. X_C represents reactance of the series capacitor compensation. The series capacitor has a bypass switch that can be opened in order to include the series compensation in the line. The wind farm is represented by a single equivalent machine.

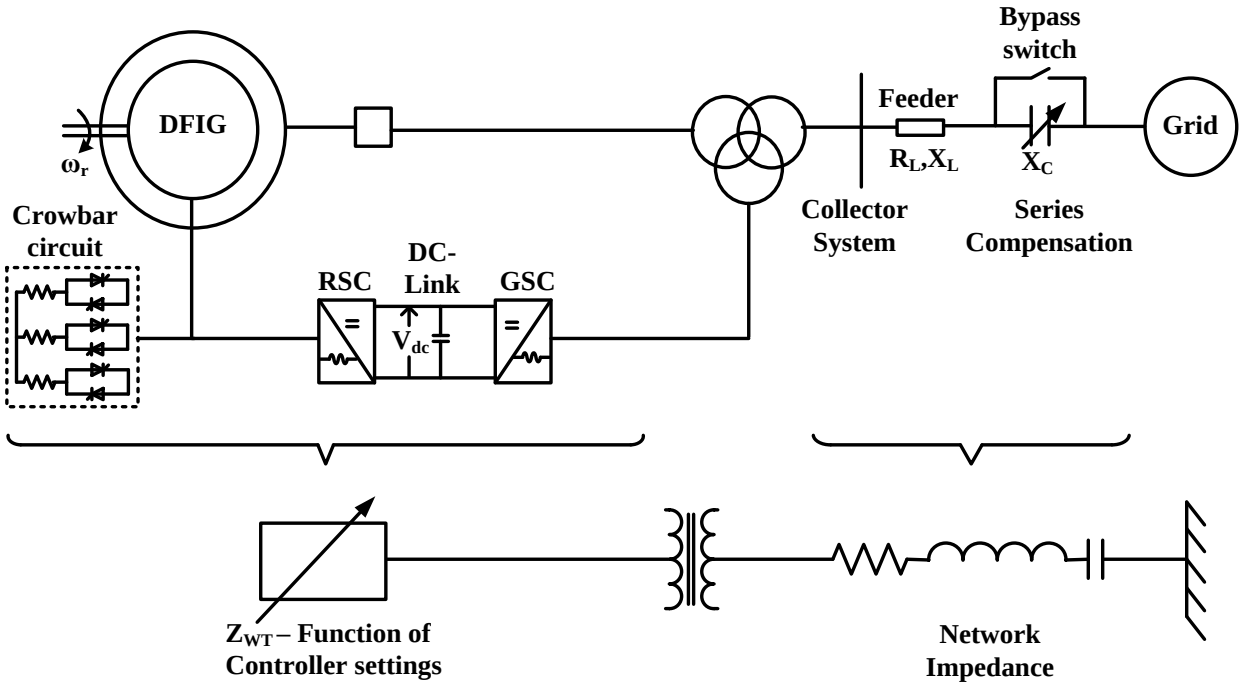

Figure 4.1: Type 3 wind generator test system with series compensation

The use of series compensation introduces the risk of sub-synchronous resonance (SSR) [60] and sub-synchronous control interactions (SSCI) [6,54] in power systems. Sub-synchronous

resonance is the power system condition in which the series compensated electrical network exchanges energy with the turbine generator shaft system at sub-synchronous frequencies of the system. SSR occurs when there is a correlation between the natural mechanical torsional modes of oscillation of the generator turbine system and the electrical network resonant frequency. This is known as the torsional interaction effect. This leads to a high level of energy exchange between the network and the turbine generator, resulting in sustained or growing oscillations that can eventually lead to turbine shaft damage. The other cause for the occurrence of SSR is the induction generator effect. The induction generator effect occurs due to self-excitation, when the total resistance of the series resonant circuit (generator and series compensated transmission line) is negative at sub-synchronous frequencies creating negative damping.

SSCI is a relatively new phenomenon in which the wind turbine controls have been observed to interact with the series compensated transmission line. Specifically, it is the control interaction between the power electronic control system and the series compensated transmission line. SSCI has no fixed frequency of concern, as the frequency of oscillations is based on the configuration of the controls and electrical system. The SSCI phenomenon is mainly observed in Type 3 wind generators connected to series compensated transmission lines due to the controllers of the back-to-back converter being connected between the rotor of the generator and the grid.

Such an interaction phenomena for a Type 3 wind farm has been studied in [6] which also identifies the control loops in the RSC that are responsible for the sub-synchronous interactions. This indicates how the SSCI phenomena can be attributed to the interaction between the series compensated network and the power electronic converter of the Type 3 wind generator. In order to study such a phenomena, the test system shown in Figure 4.1 is modeled. The wind turbine generator can be seen as a controllable impedance, the impedance of which depends upon settings of the controller. The test system parameters are given in Appendix A.3.

4.3 Test Simulation and Analysis

4.3.1 Wind Farm Aggregation

It is important that the fault contribution is found not only from a single wind generator but from an entire wind farm. A wind farm consists of several wind generator-transformer units that are connected to the main sub-station transformer through cables running from each unit. These cables form the collector circuit of the wind farm. This means that the fault calculations now must take into account the collector circuit impedances as well.

However, the fault contribution from a wind farm can be accurately calculated without taking the collector impedances into account and the equivalencing of a wind farm can be made simple yet accurate by ignoring all cable impedances [18, 48]. The difference in the total impedance of the wind farm with and without the cable was found to be less than 3 percent [48].

The research work in this thesis uses an aggregate model of the Type 3 wind farm to study its short circuit behavior. The collective behavior of a group of wind turbines is represented by an equivalent lumped machine. This assumption is supported by several recent studies that suggest that wind farm aggregation provides a reasonable approximation for system interconnection studies [54].

4.3.2 Application of Symmetrical Fault

The bypass switch of the series capacitor (53.4 F) shown in Figure 4.1 is opened 5 s after the start of simulation, thereby introducing a series compensation of 50 percent on the transmission line. Following this, a 200 ms three phase fault is applied 8.0 s after the start of the simulation at the point of interconnection of the wind farm to the grid. The Phase A stator fault current measured is shown in Figure 4.2. A buildup of sub-synchronous oscillations can be observed in the fault current waveform.

Figure 4.3 compares the phase A stator currents obtained from a straightforward three

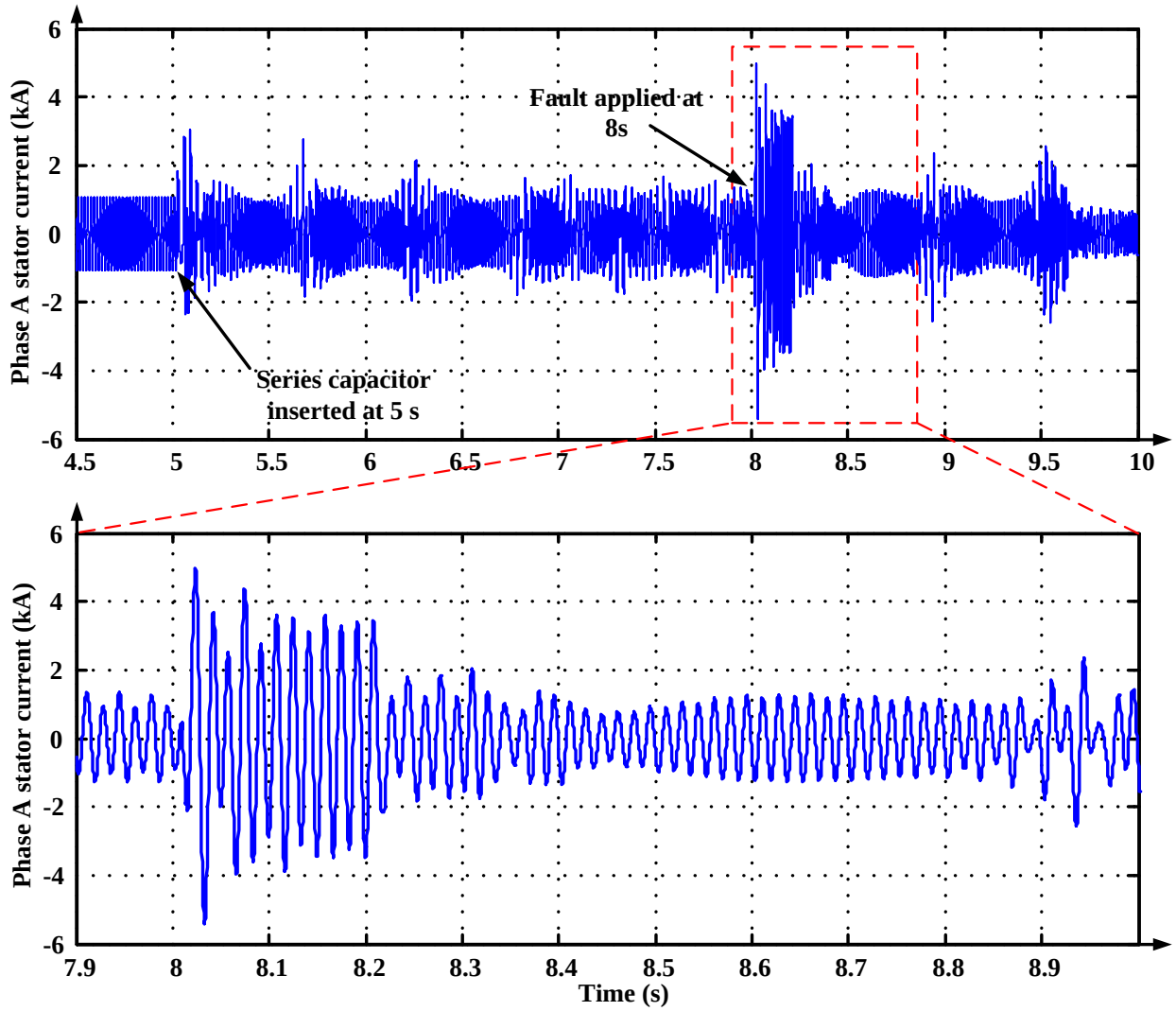

Figure 4.2: Type 3 wind farm symmetrical fault current with sub-synchronous frequency components

phase fault and a three phase fault with the SSCI component present. The magnitude of the fault current is significantly affected by the SSCI occurrence. This again confirms that models that are only able to represent the fundamental frequency components will be inaccurate for determining such complex fault behavior.

Now the stator current waveform is scanned using FFT to determine the relative magnitude of the sub-synchronous frequency component as compared to the fundamental frequency component. Figure 4.4 shows the relative magnitudes of the harmonic components

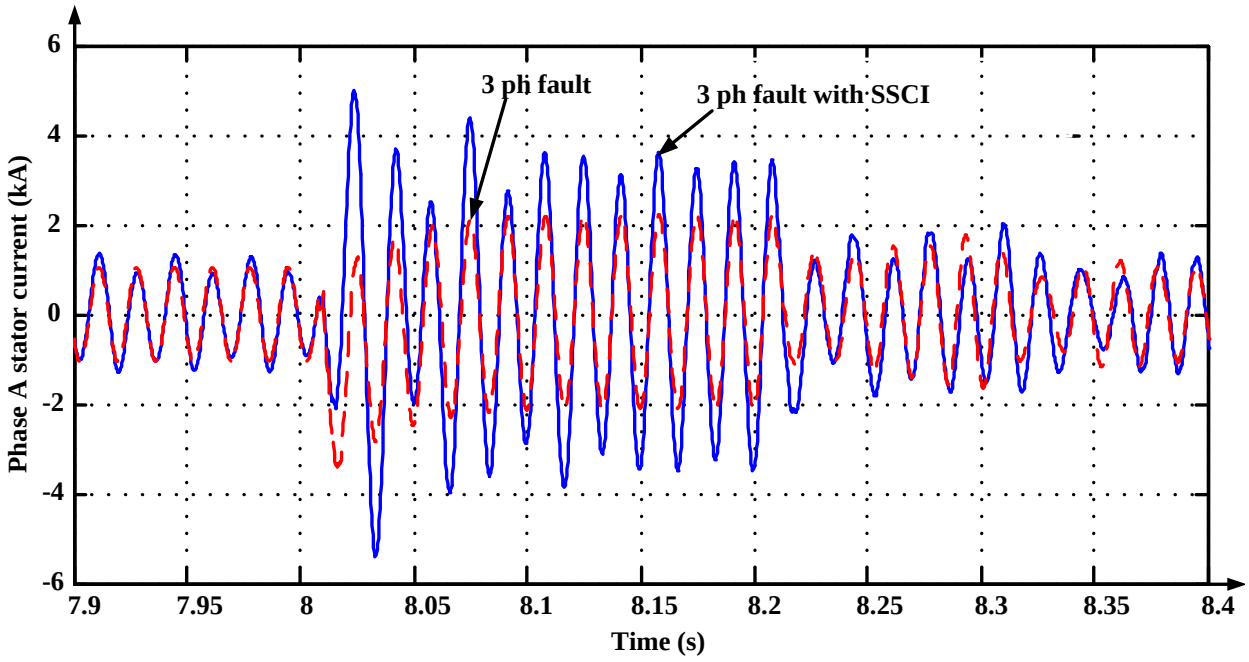

Figure 4.3: Comparison of stator fault current without and with SSCI for a three phase fault

of the phase A stator fault current waveform (base frequency of 6 Hz is used for FFT). The dominant frequency components are the fundamental frequency component ($60Hz$) and the sub-harmonic frequency component ($\approx 36Hz$).

Following this, a Prony analysis of the stator current waveform is done. The results of the Prony analysis in Figure 4.5 show that, apart from the fundamental frequency component, a sub-synchronous component of approximately 36.5 Hz is also present in the current waveform. Table 4.1 shows the relative magnitudes of the most dominant frequency components. These results correspond with the FFT analysis done before.

Table 4.1: Prony analysis of phase A symmetrical fault current with SSCI

Magnitude (kA)	Phase (deg)	Frequency (Hz)	Damping (%)
3.3879	8.627	60.030	-0.002
0.5571	74.781	36.485	7.638

Unsymmetrical fault (phase A to ground fault) behavior was studied in a manner similar to symmetrical fault behavior as discussed in the previous section. Following the

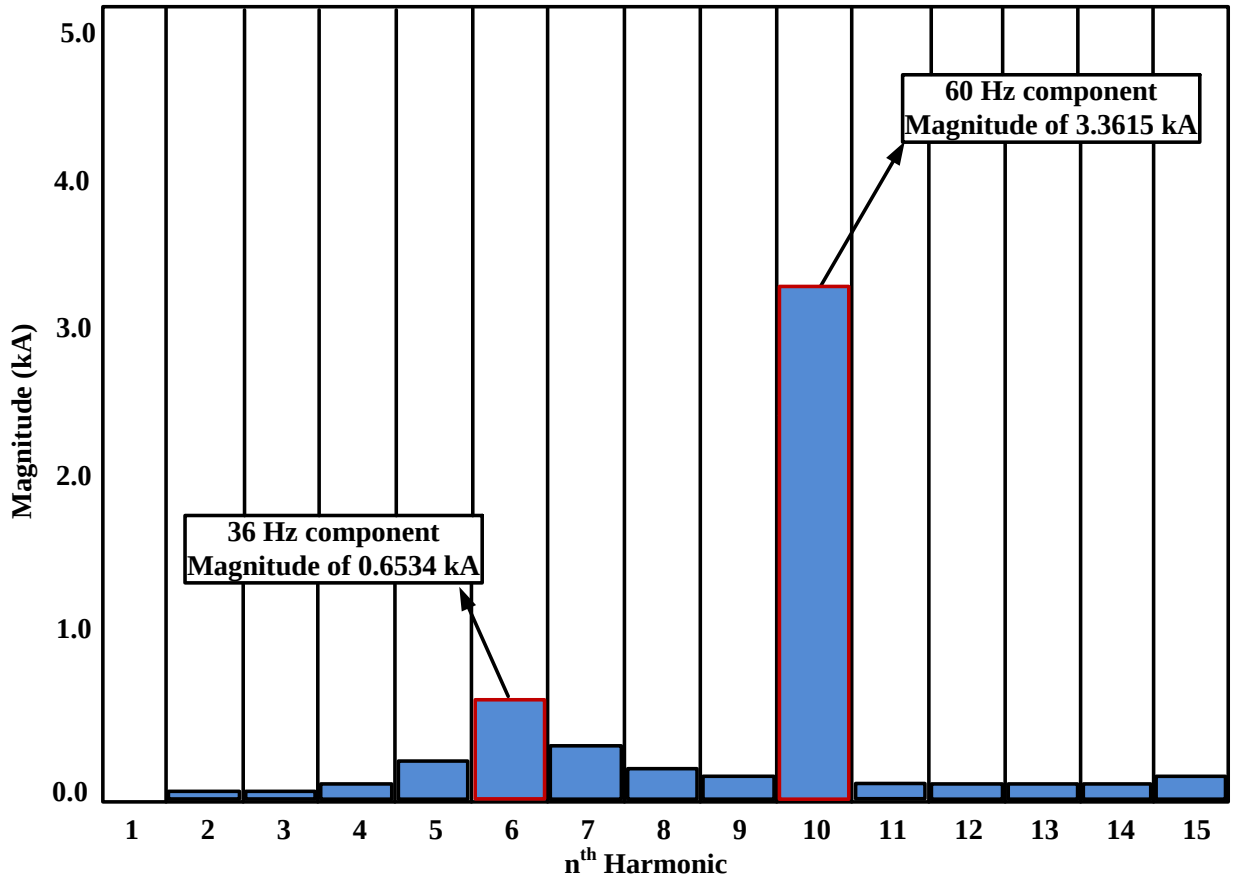

Figure 4.4: FFT analysis of phase A symmetrical fault current with SSCI

insertion of the series compensation of 53.4 μF (50 percent compensation), a 200 ms phase A to ground fault was applied and the fault current behavior was analyzed. Figure 4.6 shows the comparison of phase A fault currents for a phase A to ground fault applied with and without the insertion of the series compensation. The figure shows that SSCI has a significant impact on the magnitude of the fault current.

For the unsymmetrical fault scenario, the fault current waveform was again analyzed with FFT and Prony analysis. The fault current's dominant frequency components were the fundamental frequency and the 36.5 Hz sub-synchronous frequency components due to the occurrence of SSCI.

Symmetrical and unsymmetrical fault application and analysis for a 30 percent and a 70 percent compensated transmission line show that SSCI phenomena occur introducing their

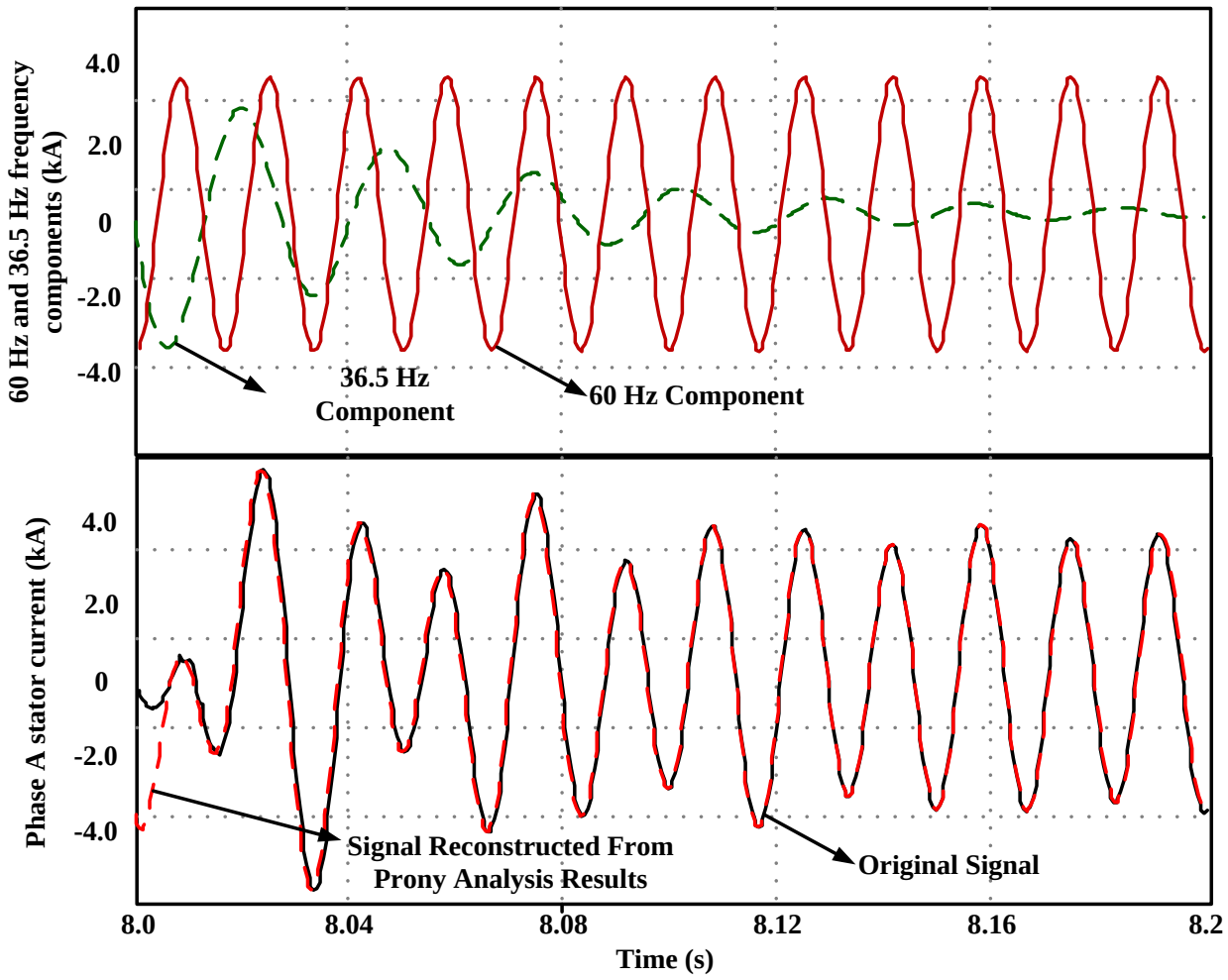

Figure 4.5: Prony analysis of phase A symmetrical fault current with SSCI

characteristic sub-synchronous frequency components ($\approx 28Hz$ and $\approx 42Hz$ respectively). The FFT analysis of the phase A stator fault current for these scenarios is shown in Figure 4.7 indicating the dominant frequency components.

4.4 Frequency Scanning

The resonant frequency at which possible sub-synchronous oscillations could occur is found using the frequency scanning technique. This involves determining the magnitude and phase angle of the driving point impedance when looking into the system from the generator terminals for all scanning frequencies. The magnitude and the phase angle values obtained

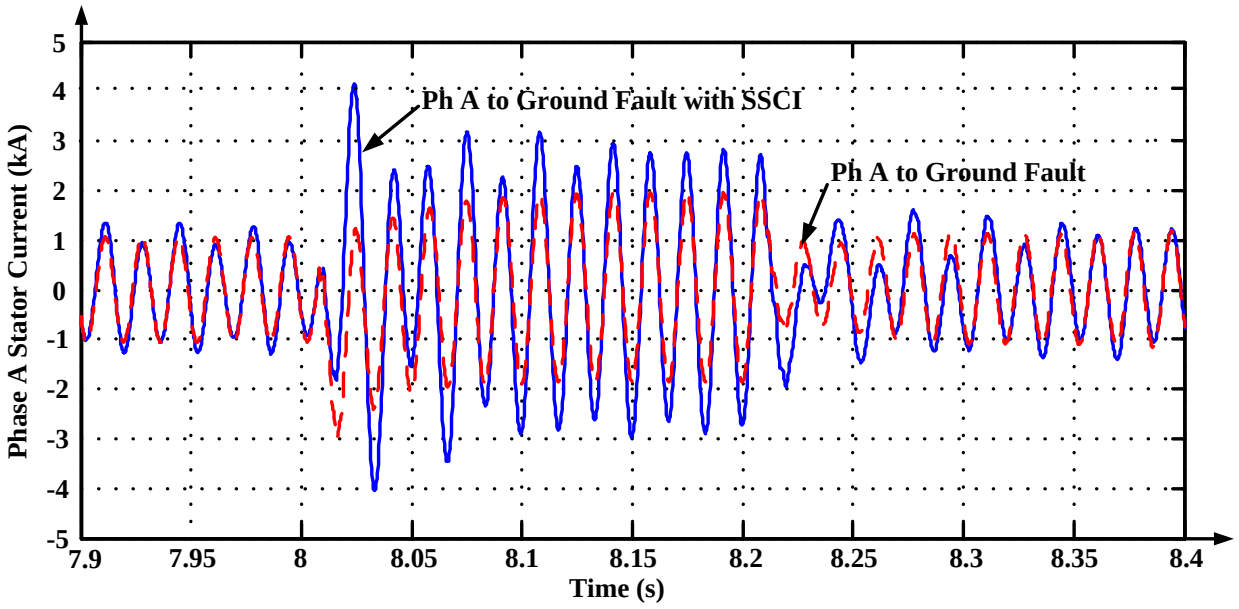

Figure 4.6: Comparison of phase A stator fault current without and with SSCI for a phase A to ground fault

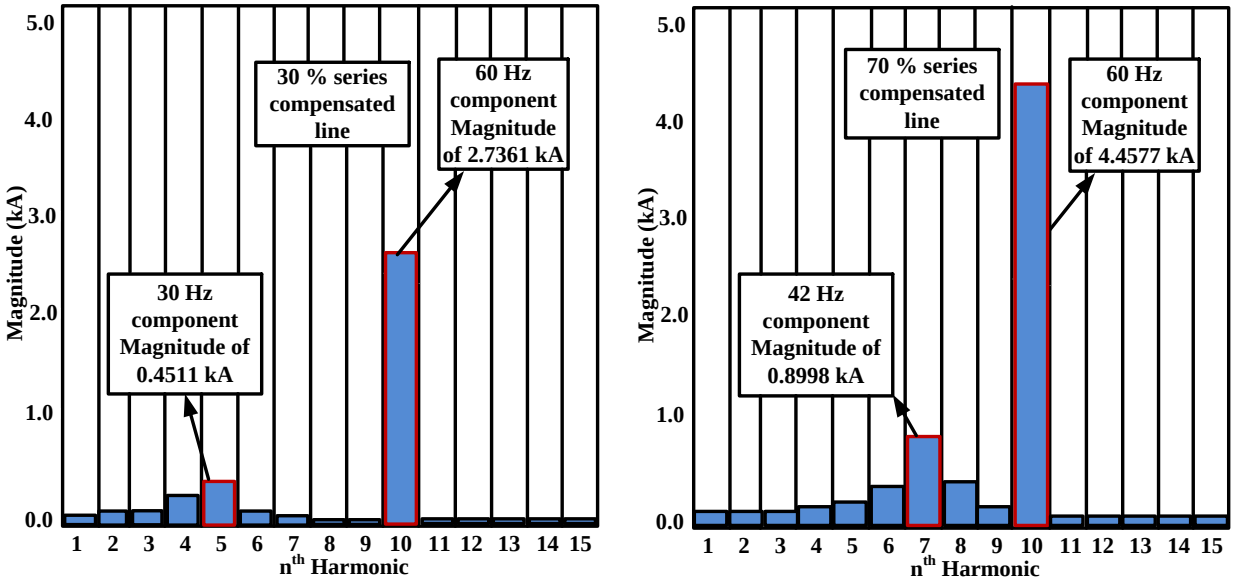

Figure 4.7: FFT analysis of phase A stator current for 30 and 70 percent compensation for a symmetrical fault

from the frequency scan are plotted as a function of the scanning frequency. From this plot, the network resonant frequency at which sub-synchronous interactions could occur can be found. This is the frequency at which there is a change in sign of the phase and a dip in

the impedance magnitude. This corresponds to a series network resonance seen by the wind farm under study [27].

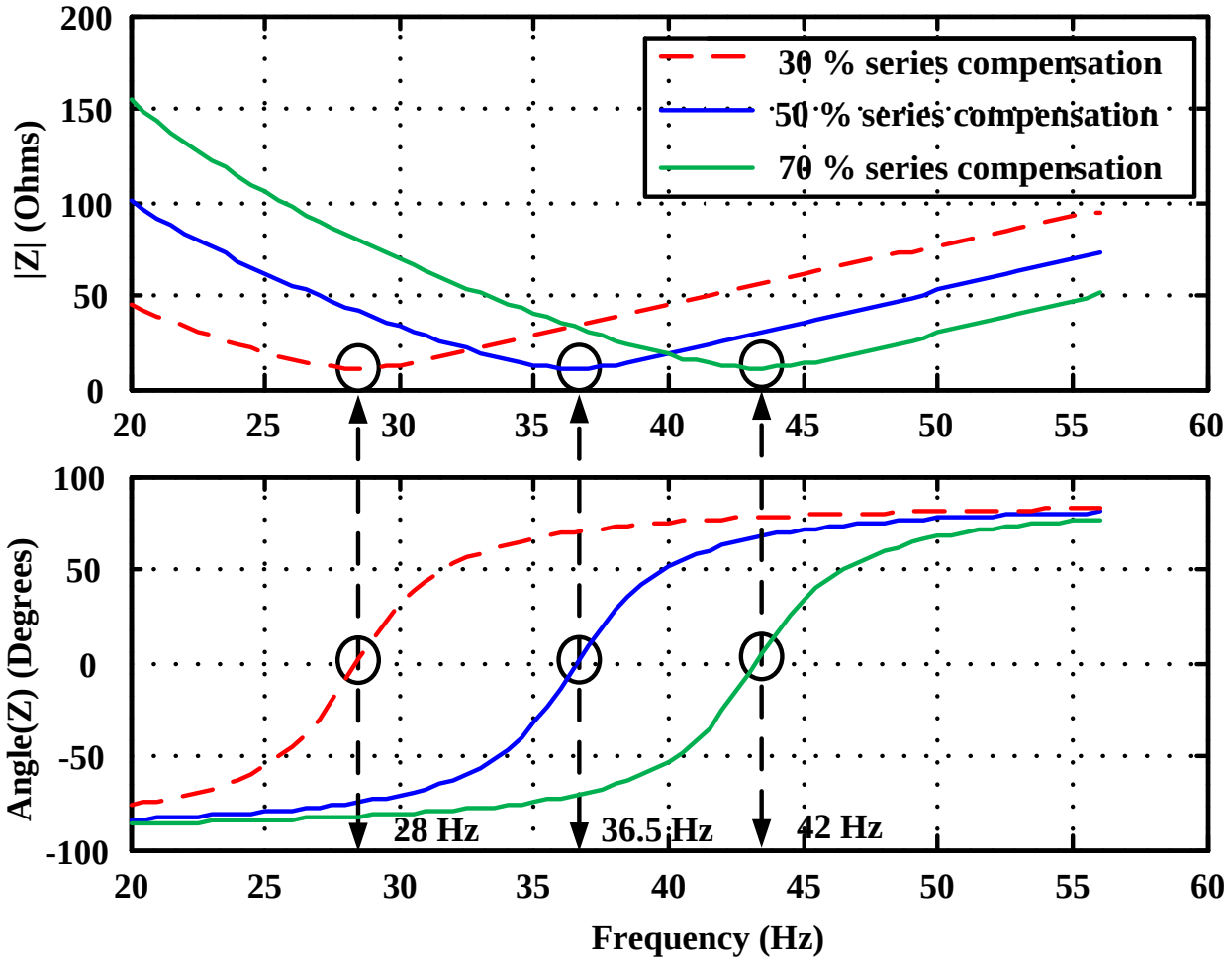

Figure 4.8: Frequency Scanning - magnitude and phase angle plot of network driving point impedance

From the Prony analysis in the previous section, the most dominant frequency component observed following the fundamental frequency component was the sub-synchronous component of 36.5 Hz for a 50 percent series compensated line. Figure 4.8 shows the results of the frequency scanning for three different percentages of series capacitor compensation. For 50 percent compensation, there is a dip in the impedance magnitude and a corresponding change of sign of the phase angle at a frequency of 36.5 Hz. This frequency corresponds to the frequency of the sub-synchronous component present in the stator current. This re-establishes the insertion of the series compensation as the reason behind the occurrence of

the sub-synchronous component in the current waveform. Similarly, the impedance magnitude and phase angle variation with frequency for the other series capacitor compensation levels can be observed to have their respective values of resonant frequency.

4.5 Representation by Modeling Methods

The accuracy of models representing sub-synchronous interactions is determined not only by the ability to represent fundamental frequency characteristics but also sub-synchronous frequency components. As discussed previously, the voltage behind transient reactance and the representation using analytical expression are fundamental frequency models. This means they are not capable of representing the sub-synchronous interaction behavior of Type 3 wind generators. This is a major factor that reduces the accuracy of these models to represent such behavior of Type 3 wind generators.

The voltage dependent current source model discussed in Section 3.4 is capable of representing the complex short circuit behavior of Type 3 wind generators. However, the following issues reduce the suitability of this method:

- This model is not a stand alone model as it is dependent on another modeling method (electromagnetic transient model in this case) or the manufacturer to obtain the fault current envelopes.
- As the fault current does not reach its maximum immediately after the application of the fault, using envelopes to find the fault current at the inception of the fault does not necessarily give the maximum fault current.

4.6 Summary

The fundamental frequency electro-mechanical modeling methods are not capable of accurately representing the short circuit behavior of Type 3 wind generators as they are not capable of including the effect of sub-synchronous interactions. A voltage dependent current

source, though accurate, is not a standalone model. Due to these factors, development of a model that is accurate and simplified compared to the EMT model and with the ability to represent sub-synchronous frequency interactions is required. Chapter 5 discusses the proposed modeling approach of the Type 3 wind generator and its application.

Chapter 5

Dynamic Phasor Modeling of Type 3 Wind Generators

5.1 Introduction

The various short circuit modeling complexities of the Type 3 wind generator and their degree of influence on short circuit behavior were explained in the previous chapters. In order for the short circuit behavior to be accurately represented, the model developed must be capable of taking into account these complexities. Power utilities worldwide use either fundamental frequency representations or detailed EMT models in their transient programs to model the short circuit behavior of wind generators.

The fundamental frequency model provides a simplified method of modeling, but is incapable of incorporating some critical aspects of Type 3 wind farm behavior, such as non-fundamental frequencies, making it inaccurate. EMT simulation is a widely accepted method for accurately modeling the behavior of complex power system components. It is capable of modeling every component of the test system in detail and including all of the associated frequency components. Even though EMT modeling is highly accurate and capable of detailed modeling, it is a cumbersome task when it comes to modeling a system of considerable size and complexity, such as a Type 3 wind farm consisting of hundreds of wind generators. The highly accurate nature of the EMT model lends itself to be used as a benchmark model to validate the proposed modeling technique.

In this chapter, an accurate model that is neither based on fundamental frequency simplifications nor as cumbersome as a detailed EMT model is proposed and implemented for

representing Type 3 wind farm short circuit behavior. A middle ground between the fundamental frequency and EMT models is achieved using this proposed modeling method. This method is based on the generalized averaging scheme discussed in reference [38], in which the variables of the power system under study are represented as dynamic phasors or time varying Fourier coefficients. This method of modeling, also known as dynamic phasor modeling can be used to select only the required frequency components to accurately represent the desired fault behavior of a Type 3 wind farm.

This chapter introduces the dynamic phasor modeling approach in general, followed by the derivation of modeling equations for the Type 3 wind farm in particular. The advantages of this technique over conventional modeling methods are discussed. Following this, the ability of this technique to represent different fault behaviors of the Type 3 wind farm is put to test and the accuracy of the results obtained are discussed and validated against benchmark EMT models.

5.2 Dynamic Phasor Approach

The Fourier series representation of a complex time domain periodic signal $x(\tau)$ with a period T is given by

$$x(\tau) = \sum_{k=-\infty}^{\infty} X_k.e^{jk\omega\tau} \tag{5.1}$$

where $\omega = 2\pi/T$ and X_k is the k^{th} complex Fourier coefficient. When power system transients occur, the time domain signal is no longer purely periodic. In order to represent complex transient waveforms such as these, use of a modified form of the above shown Fourier series representation is required. This modified representation is known as dynamic phasors representation and is based on generalized averaging theory [38]. This model approximates the time domain waveform $x(\tau)$ in the interval $\tau\epsilon(t-T,t]$ by a Fourier series representation as

$$x(\tau) = \sum_{-\infty}^{\infty} X_k(t).e^{jk\omega\tau}. \tag{5.2}$$

In this representation, the Fourier coefficients X_k are time varying [45]. $\langle x\rangle_k(t)$ is the k^{th} time varying Fourier coefficient, which is defined as

$$X_k(t) = \frac{1}{T}\int_{t-T}^{t} x(\tau).e^{-jk\omega\tau}d\tau = \langle x\rangle_k(t). \tag{5.3}$$

This is represented as $\langle x\rangle_k$ in the upcoming sections for the sake of simplicity. The appropriate dynamic phasors (Fourier coefficients) to accurately represent the short circuit behavior of the Type 3 wind generator must be determined. If K is the set of selected Fourier coefficients, the equation

$$x(t) \approx \sum_{k\epsilon K} X_k(t).e^{jk\omega\tau} \tag{5.4}$$

is the Fourier series approximation of the original signal.

The above definition of dynamic phasor modeling can be extended for a three phase system with the equations

$$\begin{bmatrix} x_a(\tau) \\ x_b(\tau) \\ x_c(\tau) \end{bmatrix} = \sum_{-\infty}^{\infty} \begin{bmatrix} X_{a,k}(t) \\ X_{b,k}(t) \\ X_{c,k}(t) \end{bmatrix} .e^{jk\omega\tau} \tag{5.5}$$

and

$$\begin{bmatrix} X_{a,k}(t) \\ X_{b,k}(t) \\ X_{c,k}(t) \end{bmatrix} = \frac{1}{T}\int_{t-T}^{t} \begin{bmatrix} x_a(\tau) \\ x_b(\tau) \\ x_c(\tau) \end{bmatrix} .e^{-jk\omega\tau}d\tau = \begin{bmatrix} \langle x_a\rangle_k(t) \\ \langle x_b\rangle_k(t) \\ \langle x_c\rangle_k(t) \end{bmatrix} . \tag{5.6}$$

The following properties of dynamic phasors are important in developing the model:

1. The relation between the derivative of $x(\tau)$ and the derivative of $X_k(t)$ is given by

$$\left\langle \frac{dx(t)}{dt} \right\rangle_k = \frac{dX_k(t)}{dt} + jk\omega X_k(t). \tag{5.7}$$

2. The product of two time-domain variables equals a discrete time convolution of the two dynamic phasor sets of variables given by

$$\langle xy\rangle_k = \sum_{l=-\infty}^{\infty} (X_{k-l}Y_l). \tag{5.8}$$

Dynamic phasor modeling based on the generalized averaging theory has great potential and offers a number of advantages over conventional modeling methods. First, it makes the modeling computationally efficient compared to EMT modeling as only appropriate dynamic phasors are selected. Second, the selection of set K permits consideration of a wider bandwidth of frequencies, such as non-fundamental frequencies, making the method more accurate than traditional fundamental frequency approximations. References [34, 40, 41, 44] describe the dynamic phasor modeling approach for accurately modeling complex power system components and its advantages. A dynamic phasor model of a Type 3 wind farm is developed in this thesis to accurately model its short circuit behavior for balanced and unbalanced faults as well as when significant sub-synchronous frequencies are present in the system.

As the dynamic phasor model of the Type 3 wind farm system is capable of accurately modeling not only fault current behavior such as balanced and unbalanced faults, but also sub-synchronous control interactions, it provides the necessary information to design both protection and control settings for wind farms. The model is also generic in nature, i.e., it does not require manufacturer proprietary information, such as control algorithms, which are difficult to obtain. The model developed in this research work will serve as a powerful tool for a power utility engineer to design relay settings as well as control settings for damping SSCI oscillations for a Type 3 wind farm connected to a series compensated transmission line.

5.3 Dynamic Phasor Modeling

Modeling the various components of the Type 3 wind generator test system was described in Section 2.3.3.2 in terms of dq0 time domain differential equations. The parameters of the test system are given in Appendix A.3. By substituting the differential equations for different components of the test system in Equation 5.7 above, the dynamic phasor model equations are obtained and described in this section.

The selection of the set (K) of dynamic phasors for each of these components is based on

the required short circuit behavior to be studied, namely a symmetrical or unsymmetrical fault with or without the influence of sub-synchronous interactions. In a dq0 reference frame rotating at synchronous speed, the positive sequence component will appear on the d and q axes as DC, i.e., with frequency 0 (k=0 for positive sequence components), and the negative sequence component will appear with a frequency of $2\omega_s$ (k=2 for negative sequence components). The zero sequence component will appear on the 0 axis with a frequency of ω_s (k=1 for zero sequence components). Hence, the designation $\langle x \rangle_0$ is used to represent the positive sequence, $\langle x \rangle_2$ the negative sequence, and $\langle x \rangle_1$ the zero sequence dynamic phasors, respectively. The Δ-Y transformer is the most commonly used transformer configuration and it does not allow the zero sequence current to flow through. Zero sequence dynamic phasors are ignored for studies with Δ-Y transformer. Also, a test system utilizing a Y-Y grounded transformer for which zero sequence quantities cannot be neglected is studied for achieving completeness of results.

As explained previously, the dynamic phasor modeling technique proposed in this research work is capable of modeling sub-synchronous frequency components to accurately represent SSCI phenomena. In Section 4.3.2, the frequency of the sub-synchronous component for SSCI occurrence in the Type 3 wind farm test system in which the wind farm was connected to a 50 percent compensated transmission line was determined to be 36.5 Hz, which is approximately 0.6 times the system fundamental frequency of 60Hz. Hence, such a sub-synchronous frequency component would appear on the d and q axes at a frequency approximately $0.6\omega_s$ (k=0.6). Table 5.1 gives the appropriate choice of dynamic phasors to represent the different fault scenarios discussed in Section 5.4.

For a 50 percent compensated system, the sub-synchronous frequency dynamic phasor will be represented by $\langle x \rangle_{0.6}$. Further, based on the degree of compensation, the frequency of this sub-synchronous component would change as described in Chapter 4. Accordingly, the correct value of k can be selected to represent the appropriate sub-synchronous component accurately. For a 30 and 70 percent compensated system, the sub-synchronous frequency dynamic phasor will be represented by $\langle x \rangle_{0.5}$ and $\langle x \rangle_{0.7}$ respectively based on their characteristic frequency of $\approx 28Hz$ and $\approx 42Hz$.

Table 5.1: Selection of appropriate dynamic phasors for 50 percent compensated system

Fault Condition	**Dynamic phasors**
Symmetrical Fault	$\langle x_{dq} \rangle_0$
Unsymmetrical Fault	$\langle x_{dq} \rangle_0$, $\langle x_{dq} \rangle_1{}^*$, $\langle x_{dq} \rangle_2$
Symmetrical Fault with SSCI	$\langle x_{dq} \rangle_0$, $\langle x_{dq} \rangle_{0.6}$
Unsymmetrical Fault with SSCI	$\langle x_{dq} \rangle_0$, $\langle x_{dq} \rangle_1{}^*$, $\langle x_{dq} \rangle_2$, $\langle x_{dq} \rangle_{0.6}$

* $\langle x_{dq} \rangle_1$ is included only for Y-Y grounded transformer

Drive Train:

The dq dynamic phasor model for the drive train, consisting of the turbine, shaft, and gear box, is represented by a single equivalent mass and is obtained by substituting Equation 2.2 in 5.7. It is given by

$$\frac{d\langle \omega_r \rangle_k}{dt} = \frac{\langle T_m \rangle_k - \langle T_e \rangle_k}{2H} - jk\omega_s \langle \omega_r \rangle_k \tag{5.9}$$

where the electrical torque is

$$\langle T_e \rangle_k = \langle \psi_{r,q}.i_{r,d} \rangle_k - \langle \psi_{r,d}.i_{r,q} \rangle_k. \tag{5.10}$$

The dynamic phasors for ω_r and T_e are chosen based on the type of fault, as shown in Table 5.1. For the mechanical torque T_m, only the positive sequence dynamic phasor is chosen.

Stator Voltages:

The dynamic phasor model for the stator flux linkage obtained by substituting Equation 2.5 in 5.7 is given by

$$\langle \psi_{s,dq} \rangle_k = L_{ss} \langle i_{s,dq} \rangle_k + L_{sr} \langle i_{r,dq} \rangle_k \tag{5.11}$$

and the dynamic phasor model of the stator voltage is similarly obtained as

$$\langle V_{s,dq} \rangle_k = R_{ss} \langle i_{s,dq} \rangle_k + J\omega_s \langle \psi_{s,dq} \rangle_k + \frac{d\langle \psi_{s,dq} \rangle_k}{dt} - jk\omega_s \langle \psi_{s,dq} \rangle_k. \tag{5.12}$$

The appropriate choice of the dynamic phasors for the stator flux linkages $\psi_{s,dq}$, currents $i_{s,dq}$, $i_{r,dq}$ and voltages $V_{s,dq}$ are based on Table 5.1. The definition of the resistance and the J matrices remain the same as before.

Rotor Voltages:

The dynamic phasor model for the rotor flux linkage obtained by substituting Equation 2.10 in 5.7 is given by

$$\langle \psi_{r,dq} \rangle_k = L_{rs} \langle i_{s,dq} \rangle_k + L_{rr} \langle i_{r,dq} \rangle_k \tag{5.13}$$

and the dynamic phasor model of the rotor voltage is similarly obtained as

$$\langle V_{r,dq} \rangle_k = R_{rr} \langle i_{r,dq} \rangle_k + J \langle \sigma \rangle_k \omega_s \langle \psi_{r,dq} \rangle_k + \frac{d\langle \psi_{r,dq} \rangle_k}{dt} - jk\omega_s \langle \psi_{r,dq} \rangle_k. \tag{5.14}$$

The appropriate choice of the dynamic phasors for the rotor flux linkages $\psi_{r,dq}$, currents $i_{s,dq}$, $i_{r,dq}$ and voltages $V_{r,dq}$ are based on Table 5.1. The definition of the resistance matrix remains the same as before. The dynamic phasor dq equation of the slip, obtained by substituting Equation 2.14 in 5.7, is given as

$$\langle \sigma \rangle_k = \frac{\omega_s - \langle \omega_r \rangle_k}{\omega_s} \tag{5.15}$$

where k is selected as shown in Table 5.1.

Back-to-Back Converter:

The dynamic phasor model of the back-to-back converter average model obtained by substituting Equation 2.15 in 5.7 is

$$C \frac{d\langle V_{dc} \rangle_k}{dt} = \langle m_{r,d}.i_{r,d} \rangle_k + \langle m_{r,q}.i_{r,q} \rangle_k - \langle m_{g,d}.i_{g,d} \rangle_k - \langle m_{g,q}.i_{g,q} \rangle_k - jk \langle V_{dc} \rangle_k. \tag{5.16}$$

The set of appropriate dynamic phasors is selected based on Table 5.1.

The dynamic phasor model equations for the PI controllers in the RSC are obtained from Equations 2.16 to 2.19 and in the GSC are obtained from Equations 2.20 to 2.23 by using the properties of the dynamic phasors as shown below.

Rotor Side Controller:

$$\frac{d\langle x_{r,d} \rangle_k}{dt} = K_{I,P_s} (\langle P_s \rangle_k^* - \langle P_s \rangle_k) - jk\omega_s \langle x_{r,d} \rangle_k \tag{5.17}$$

$$\langle m_{r,d}\rangle_k = \langle x_{r,d}\rangle_k + K_{P,P_s}(\langle P_s^*\rangle_k - \langle P_s\rangle_k) \tag{5.18}$$

$$\frac{d\langle x_{r,q}\rangle_k}{dt} = K_{I,Q_s}(\langle Q_s^*\rangle_k - \langle Q_s\rangle_k) - jk\omega_s\langle x_{r,q}\rangle_k \tag{5.19}$$

$$\langle m_{r,q}\rangle_k = \langle x_{r,q}\rangle_k + K_{P,Q_s}(\langle Q_s^*\rangle_k - \langle Q_s\rangle_k) \tag{5.20}$$

Grid Side Controller:

$$\frac{d\langle x_{g,d}\rangle_k}{dt} = K_{I,V_{dc}}(\langle {V_{dc}}^*\rangle_k - \langle V_{dc}\rangle_k) - jk\omega_s\langle x_{g,d}\rangle_k \tag{5.21}$$

$$\langle m_{g,d}\rangle_k = \langle x_{g,d}\rangle_k + K_{P,V_{dc}}(\langle V_{dc}^*\rangle_k - \langle V_{dc}\rangle_k) \tag{5.22}$$

$$\frac{d\langle x_{g,q}\rangle_k}{dt} = K_{I,i_{g,q}}(\langle i_{g,q}^*\rangle_k - \langle i_{g,q}\rangle_k) - jk\omega_s\langle x_{g,q}\rangle_k \tag{5.23}$$

$$\langle m_{g,q}\rangle_k = \langle x_{g,q}\rangle_k + K_{P,i_{g,q}}(\langle i_{g,q}^*\rangle_k - \langle i_{g,q}\rangle_k) \tag{5.24}$$

The appropriate choice of the set K of dynamic phasors (refer to Table 5.1) for modeling the controllers in the RSC and GSC is very important for accurate representation of the specific fault behavior under study. This is important, especially for the model to accurately represent the SSCI behavior, as the controllers play an important role in the occurrence of this phenomena.

Transmission Network and Transformer:

Apart from the controllers and converters, the series compensated transmission network must also be accurately represented using the appropriate dynamic phasors to accurately obtain the SSCI behavior of a Type 3 wind farm. This is due to the fact that SSCI behavior is primarily dependent on the RSC and GSC controller settings and the series compensation in the transmission line. The dynamic phasor model equations, as shown below, are obtained from Equations 2.24 to 2.27 using the properties of dynamic phasors that have been defined previously.

$$L_{line}\frac{\langle di_d\rangle_k}{dt} = \langle v_{s,d}\rangle_k - R_{line}\langle i_d\rangle_k + \omega_s L_{line}\langle i_q\rangle_k - \langle v_{c,d}\rangle_k - v_{b,d} \tag{5.25}$$

$$L_{line}\frac{\langle di_q\rangle_k}{dt} = \langle v_{s,q}\rangle_k - R_{line}\langle i_q\rangle_k - \omega_s L_{line}\langle i_d\rangle_k - \langle v_{c,q}\rangle_k - v_{b,q} \tag{5.26}$$

$$C_{line}\frac{\langle dv_{c,d}\rangle_k}{dt} = \langle i_d\rangle_k + \omega_s C_{line}\langle v_{c,q}\rangle_k \tag{5.27}$$

$$C_{line}\frac{\langle dv_{c,q}\rangle_k}{dt} = \langle i_q\rangle_k - \omega_s C_{line}\langle v_{c,d}\rangle_k \tag{5.28}$$

The dynamic phasor model equations of the constant impedance RL model of the transformer obtained from Equations 2.28 and 2.29 are

$$L_t\frac{d\langle i_{t,d}\rangle_k}{dt} = \langle v_{pri,d}\rangle_k - \langle v_{sec,d}\rangle_k - R_t\langle i_{t,d}\rangle_k + \omega_s L_t\langle i_{t,q}\rangle_k - jk\omega_s L_t\langle i_{t,d}\rangle_k \tag{5.29}$$

and

$$L_t\frac{d\langle i_{t,q}\rangle_k}{dt} = \langle v_{pri,q}\rangle_k - \langle v_{sec,q}\rangle_k - R_t\langle i_{t,q}\rangle_k + \omega_s L_t\langle i_{t,d}\rangle_k - jk\omega_s L_t\langle i_{t,q}\rangle_k. \tag{5.30}$$

5.4 Discussion of Results

This section discusses the modeling accuracy of the proposed dynamic phasor modeling to represent the following short circuit behavior of the Type 3 wind farm test system:

- Symmetrical fault behavior.
- Unsymmetrical fault behavior for test system with Δ-Y and Y-Y grounded transformer configurations.
- Symmetrical fault behavior with a series compensated transmission line for different percentage compensation.
- Unsymmetrical fault behavior for test system with Δ-Y and Y-Y grounded transformer configurations with series compensated transmission line.

The choice of the set of dynamic phasors (set K) is based on the type of fault application and the frequencies of interest required to accurately represent the fault current behavior.

5.4.1 Symmetrical Fault Behavior

For the test system comprised of an aggregate model of 150 Type 3 wind turbine generators, the fault behavior for a symmetrical three phase fault of 200 ms applied at 8.0 s at the point of interconnection with the grid obtained from the detailed EMT model is shown in Figure 5.1. For this scenario the series compensation was not applied in the transmission line.

The above fault current for the symmetrical fault scenario mainly consists of the 60 Hz fundamental frequency component as demonstrated in the previous chapters. The test system was modeled with the proposed dynamic phasor model discussed in Section 5.3. The appropriate dynamic phasors must be chosen for accurate modeling. The variation of the positive sequence dynamic phasor is shown in Figure 5.2. The positive sequence component of the current is the most dominant frequency component for the symmetrical fault condition.

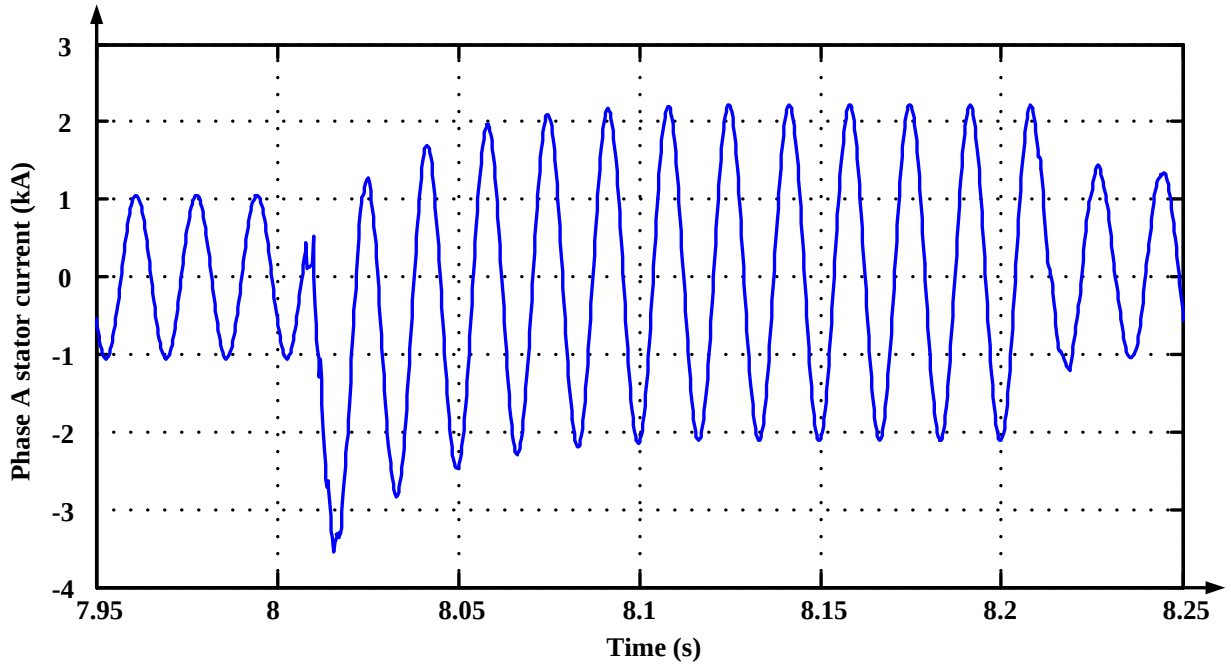

Figure 5.1: Fault current for Type 3 wind farm symmetrical fault application - EMT model

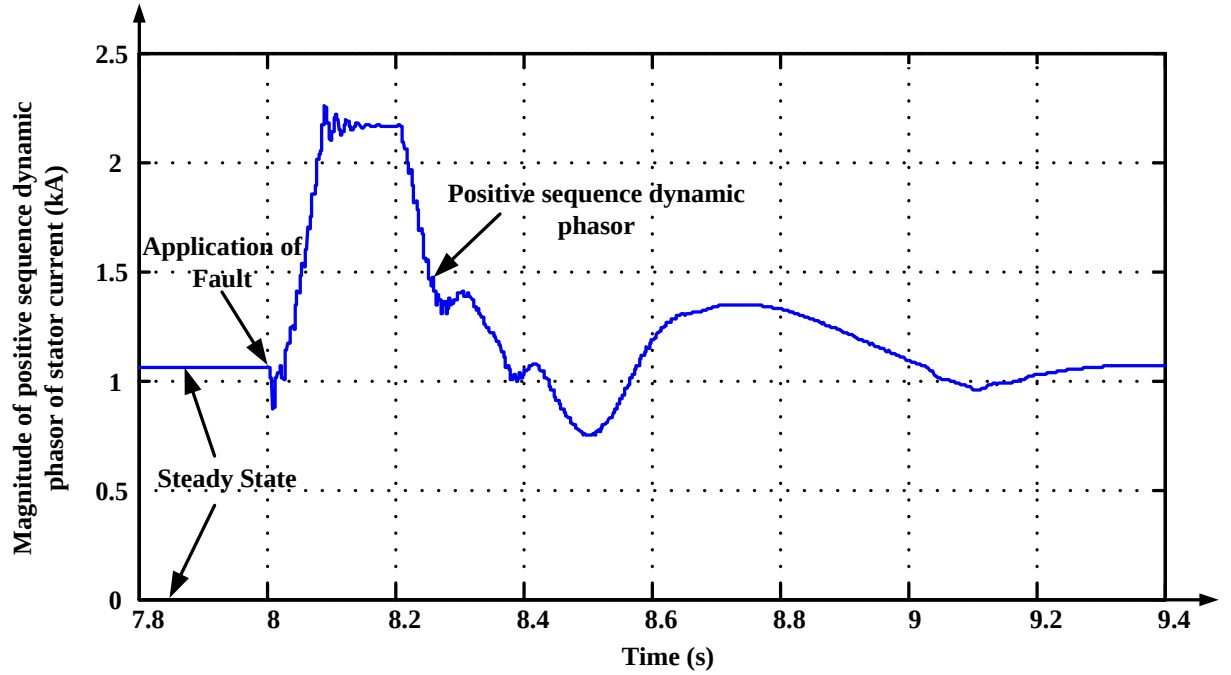

Figure 5.2: Variation of positive sequence dynamic phasor for a symmetrical fault

The appropriate choice of the required dynamic phasors (Fourier coefficients) to accurately represent the symmetrical short circuit behavior would be the 60 Hz fundamental

frequency coefficients (positive sequence dynamic phasor). Negative sequence dynamic phasors are not included as this is a symmetrical fault and zero sequence dynamic phasors are not included as the transformer is ungrounded. The selection of appropriate dynamic phasors was discussed previously in Table 5.1.

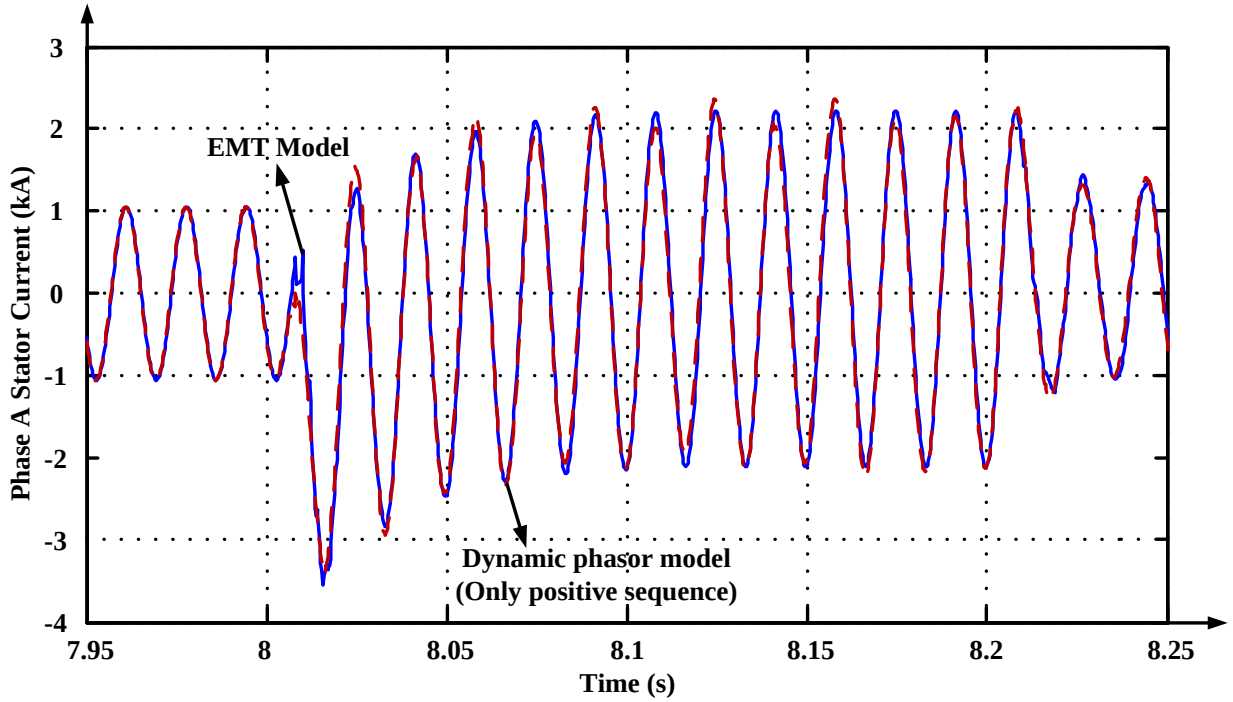

Figure 5.3: Comparison of EMT and dynamic phasor modeling for symmetrical fault

The fault current output (phase A stator current) for the symmetrical three phase fault is shown in Figure 5.3, which compares the EMT and dynamic phasor model results. The fault current waveforms show that the positive sequence dynamic phasor is capable of accurately representing the symmetrical fault behavior of the Type 3 wind generator. However, the upcoming sections show that just using the positive sequence (fundamental frequency) dynamic phasor is not sufficient to obtain accurate short circuit behavior.

5.4.2 Unsymmetrical Fault Behavior

For the test system with a Δ-Y transformer, a 200 ms unsymmetrical phase A to ground fault was applied at the point of interconnection to the grid and the response of the wind

farm in terms of the phase A stator fault current is shown in Figure 5.4 below.

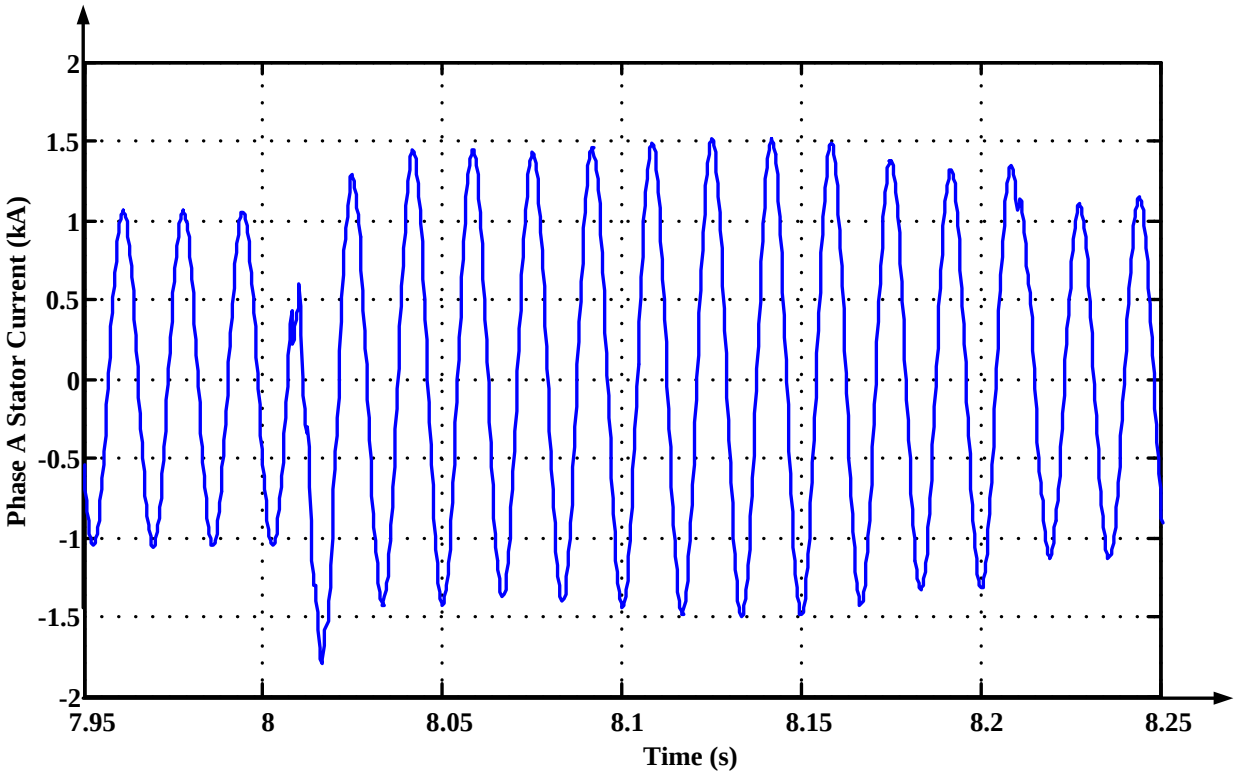

Figure 5.4: Fault current for Type 3 wind farm unsymmetrical fault application - EMT model with Δ-Y transformer

An unsymmetrical fault current contains both positive and negative sequence components. No zero sequence components are present due to the transformer configuration. Hence, the positive and negative sequence dynamic phasors were chosen in order to accurately model the unsymmetrical fault behavior. Figure 5.5 below shows the relative magnitudes of the positive and negative sequence dynamic phasors.

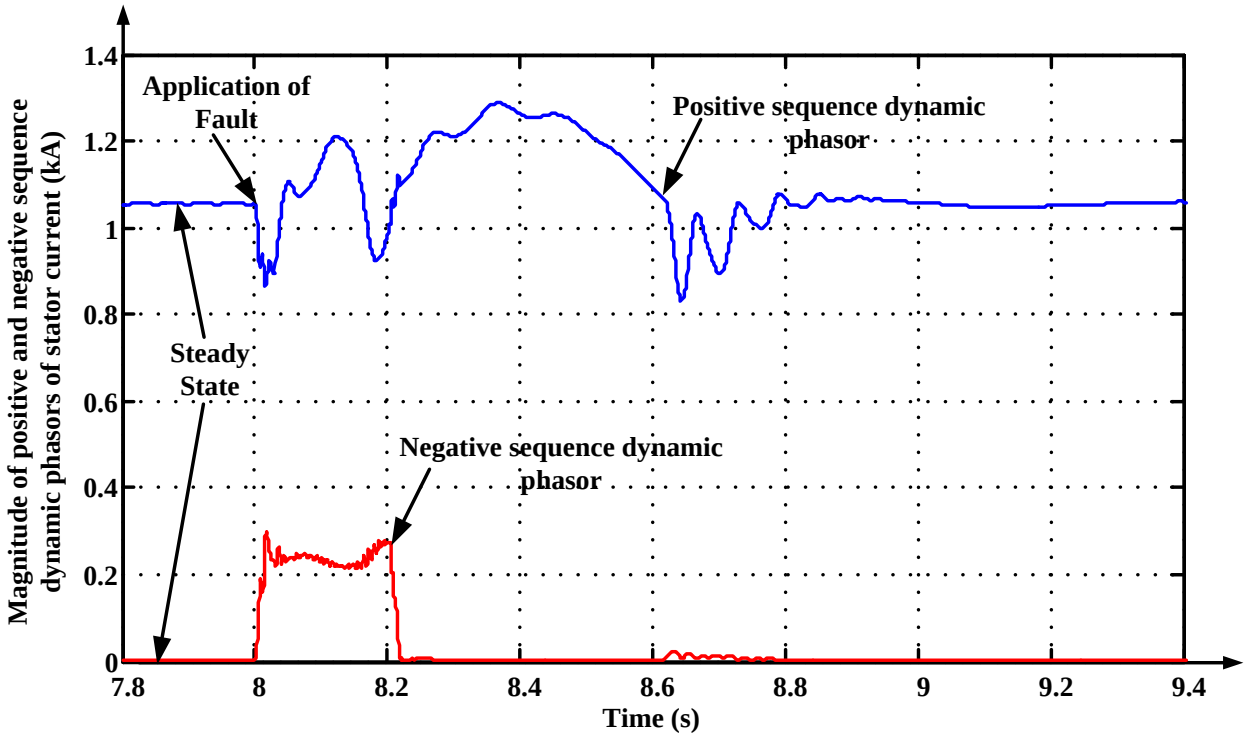

Figure 5.5: Relative magnitude of positive and negative sequence dynamic phasors for an unsymmetrical fault with Δ-Y transformer

The accuracy of the dynamic phasor model was assessed by comparison with the EMT model results. The phase A stator fault current obtained from the dynamic phasor model is compared with the EMT simulation results as shown in Figure 5.6. A high degree of accuracy was achieved with the dynamic phasor representation for unsymmetrical fault behavior while using a Δ-Y transformer configuration in the test system.

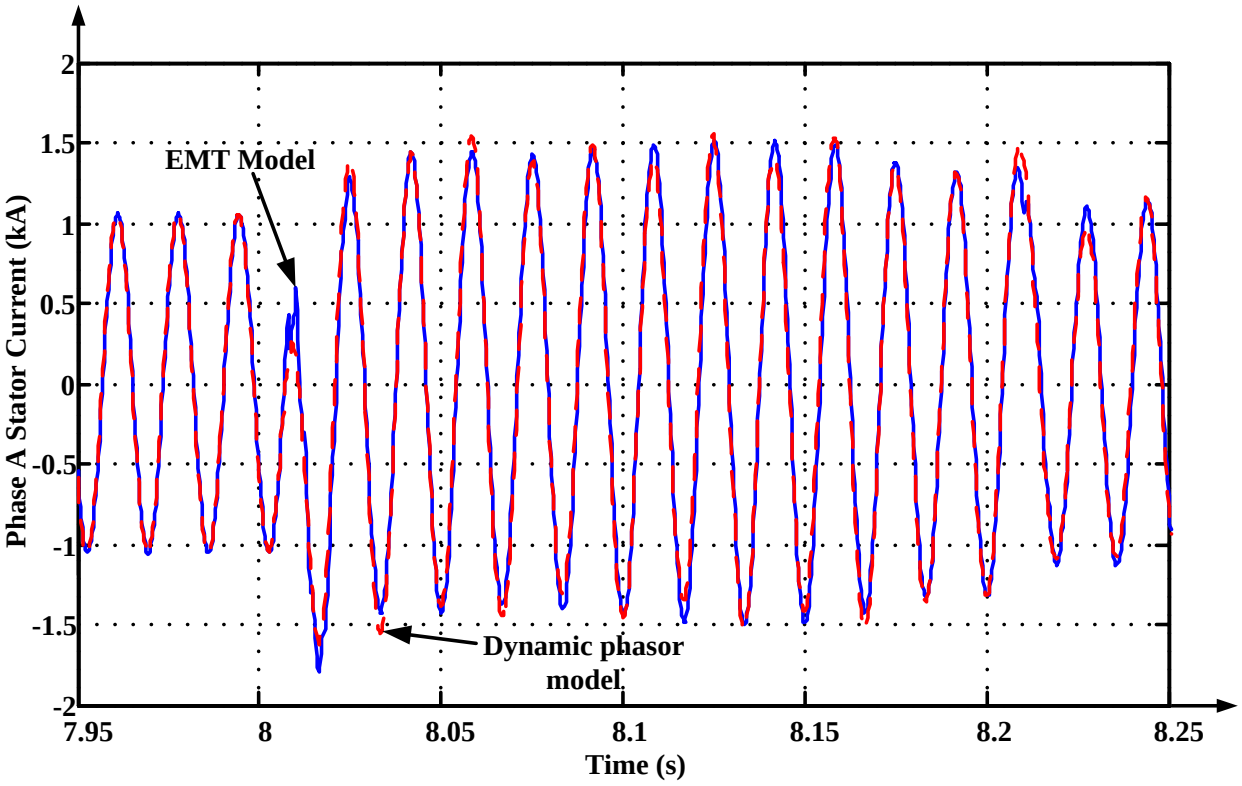

Figure 5.6: Comparison of EMT and dynamic phasor modeling for Type 3 wind farm unsymmetrical fault application with Δ-Y transformer

The same fault was applied in a test system with a Y-Y grounded transformer configuration. This would allow zero sequence currents to flow for an unsymmetrical fault. The phase A stator fault current is shown in the Figure 5.7.

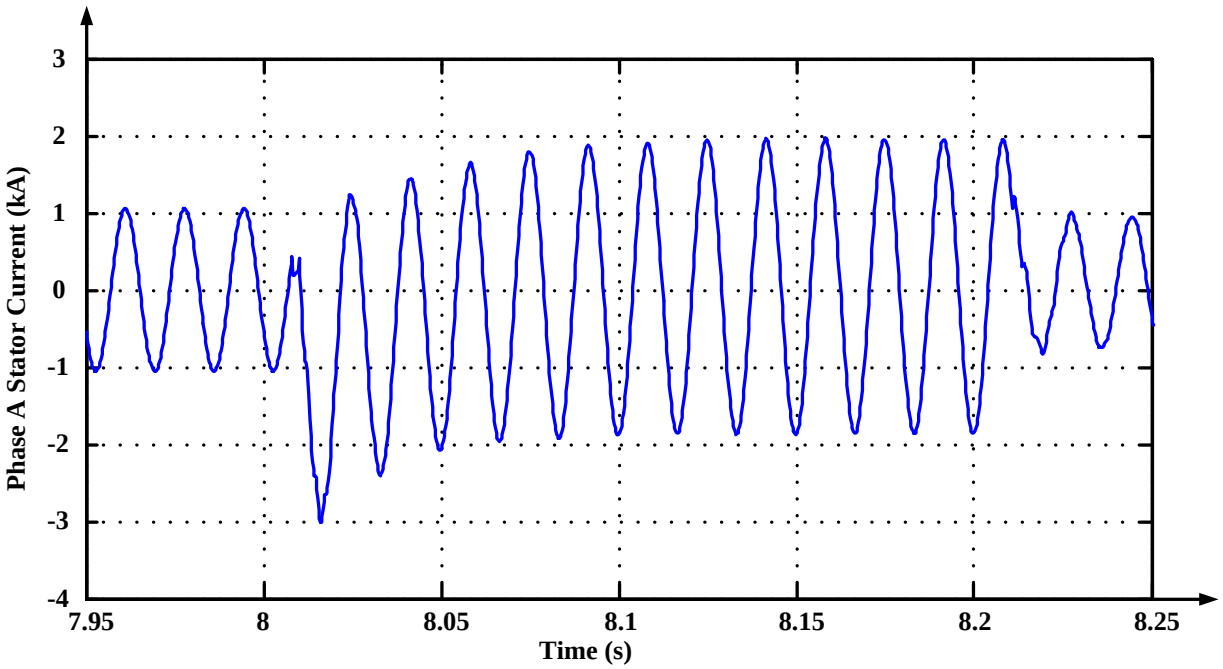

Figure 5.7: Fault current for Type 3 wind farm unsymmetrical fault application - EMT model with Y-Y grounded transformer

Hence the positive, negative and zero sequence dynamic phasors were included to accurately model this behavior. Figure 5.8 shows the variation of the chosen dynamic phasors during the fault application period.

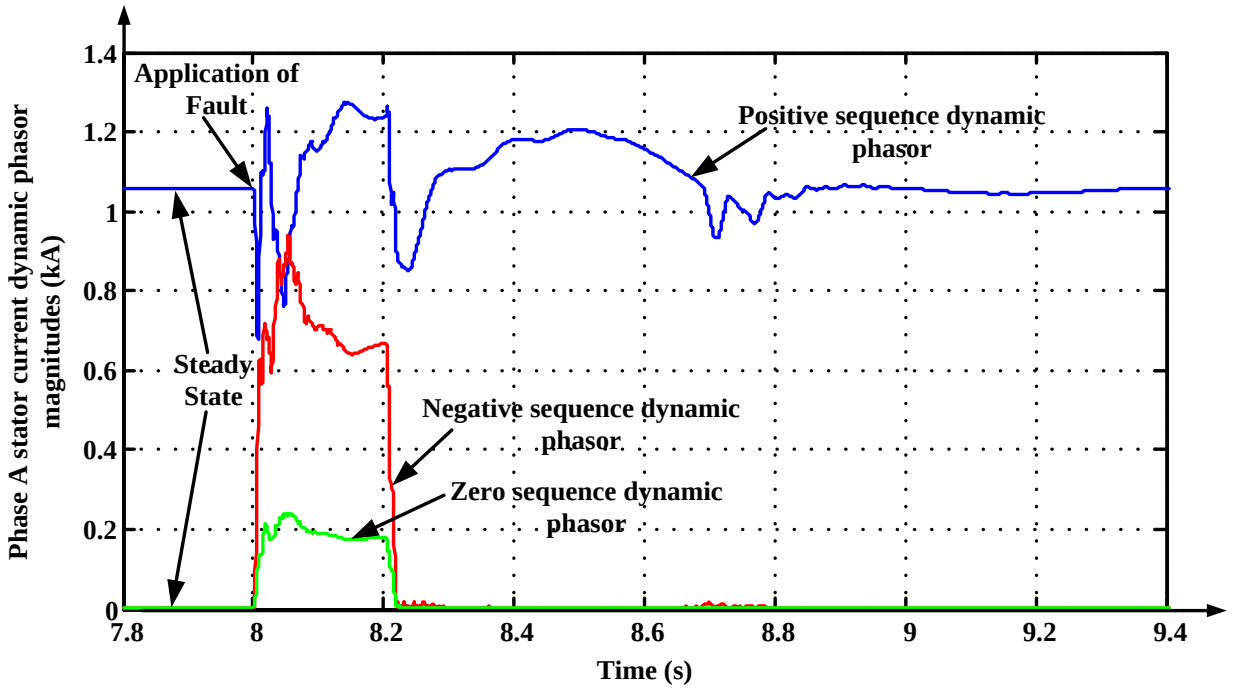

Figure 5.8: Relative magnitude of positive and negative sequence dynamic phasors for an unsymmetrical fault with Y-Y grounded transformer

Figure 5.9 shows the comparison between the phase A stator fault current obtained from the dynamic phasor model and the EMT simulation. With the appropriate choice of the dynamic phasors, a high degree of accuracy was achieved for test systems using both Δ-Y and Y-Y grounded transformer configurations.

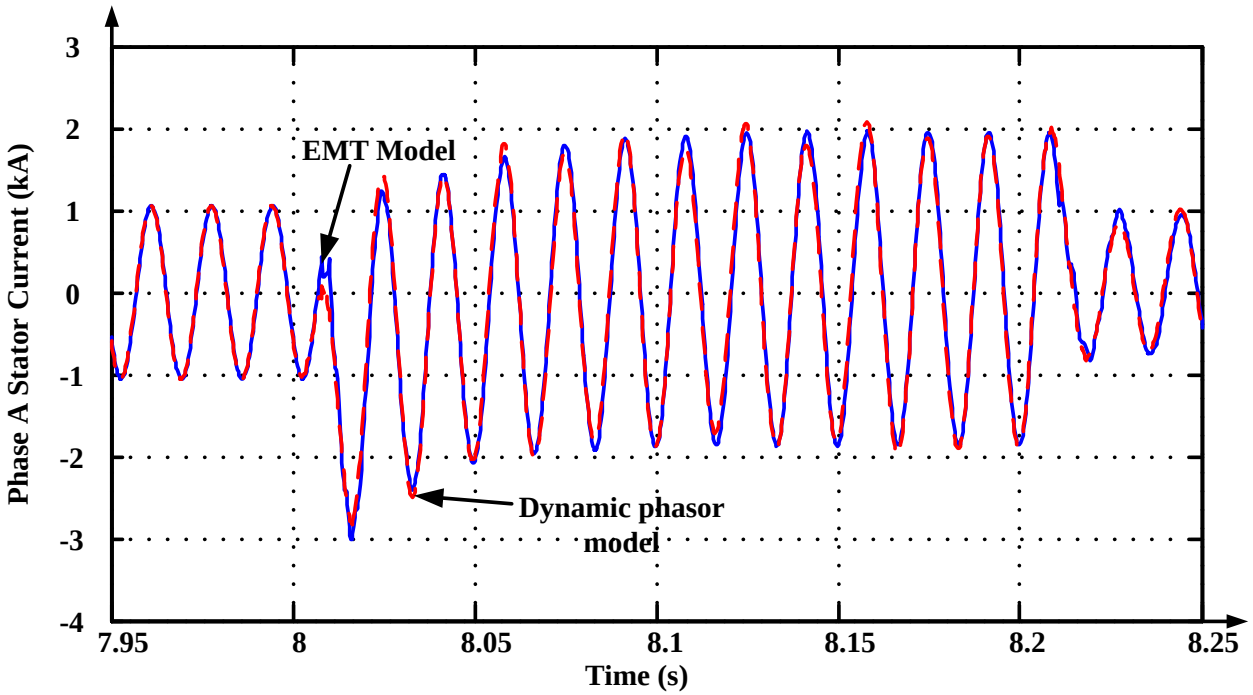

Figure 5.9: Comparison of EMT and dynamic phasor modeling for Type 3 wind farm unsymmetrical fault application with Y-Y grounded transformer

5.4.3 Fault Behavior with a Series Compensated Transmission Line

Chapter 4 discussed the scenario of a Type 3 wind farm connected to a series compensated transmission line. The interaction between the series compensated line and the Type 3 wind generator with the converters led to SSCI and the presence of sub-synchronous frequencies in the fault current waveform. In order to test the accuracy of the proposed dynamic phasor model to represent such a fault behavior, the correct choice of the appropriate dynamic phasors (Fourier coefficients) is critical.

5.4.3.1 Symmetrical Fault Behavior

The fault current behavior of the Type 3 wind farm with a 50 percent series compensated line for a 200 ms 3 phase fault at the point of interconnection of the wind farm with the grid

is shown below in Figure 5.10.

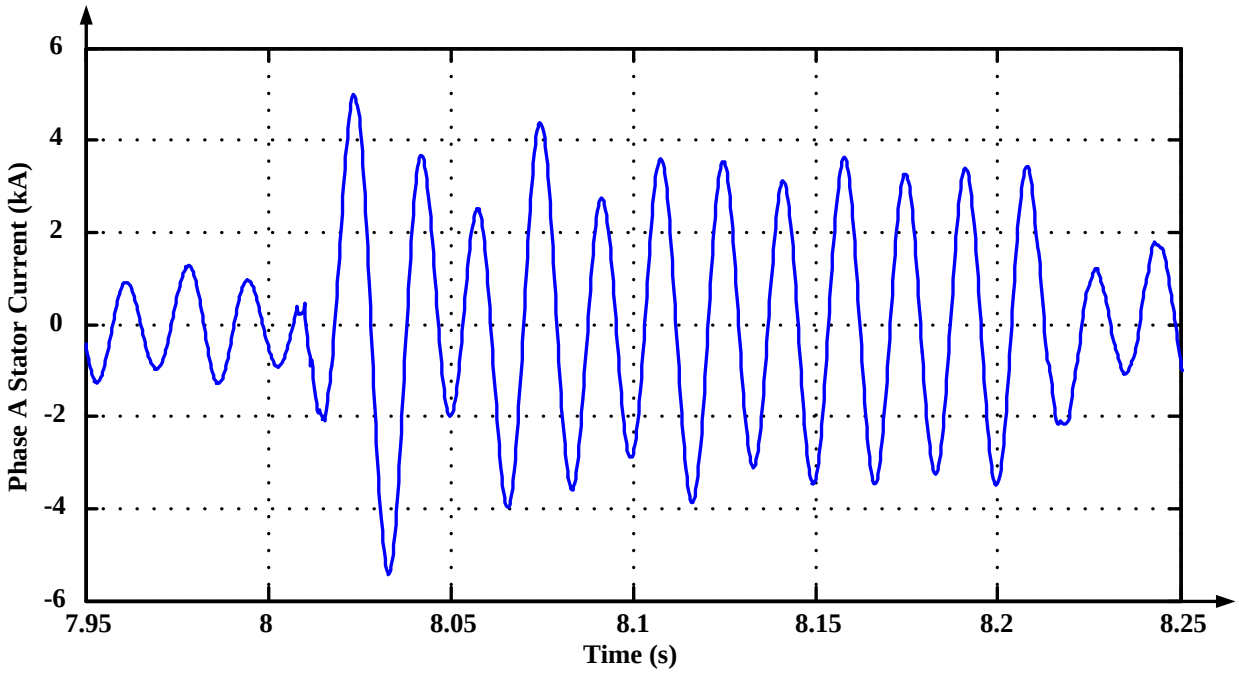

Figure 5.10: Type 3 wind farm phase A fault current for symmetrical fault with 50 percent series compensation - EMT model

In Section 4.3, FFT analysis and prony analysis of the fault current waveform were used to show that, apart from the fundamental frequency component, a sub-synchronous frequency component with an approximate frequency of 36.5 Hz was also present for 50 percent compensated line. This value was verified by the frequency scanning technique in Section 4.4. Also, the sub-synchronous frequency component present for test systems with 30 and 70 percent compensated line were identified.

For accurate representation of this type of a fault, as shown in Table 5.1, the positive sequence and sub-synchronous component dynamic phasors are to be chosen. The negative sequence dynamic phasor is not included as this is a symmetrical fault. Figure 5.11 below shows the relative magnitudes of the positive sequence and sub-synchronous component dynamic phasors for a 200 ms three phase fault for a Type 3 wind farm with a 50 percent compensated transmission line.

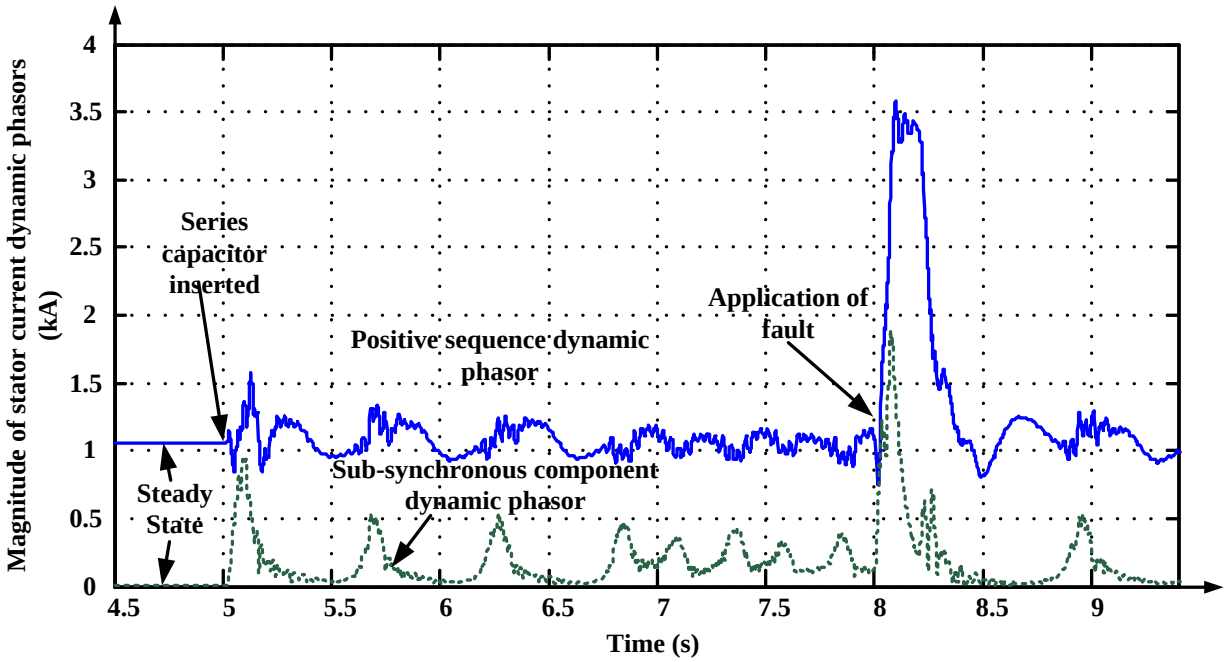

Figure 5.11: Relative magnitude of positive, negative sequence and sub-synchronous component dynamic phasors for a symmetrical fault in a 50 percent series compensated Type 3 wind farm

Figures 5.12, 5.13, and 5.14 show the comparison of the phase A fault current obtained from the EMT and the dynamic phasor modeling for 30, 50 and 70 percent compensated systems respectively. Both the fundamental and the appropriate sub-synchronous frequency Fourier coefficients are considered. The accuracy of the dynamic phasor model is high, even for scenarios with sub-synchronous oscillations and different percentage compensations.

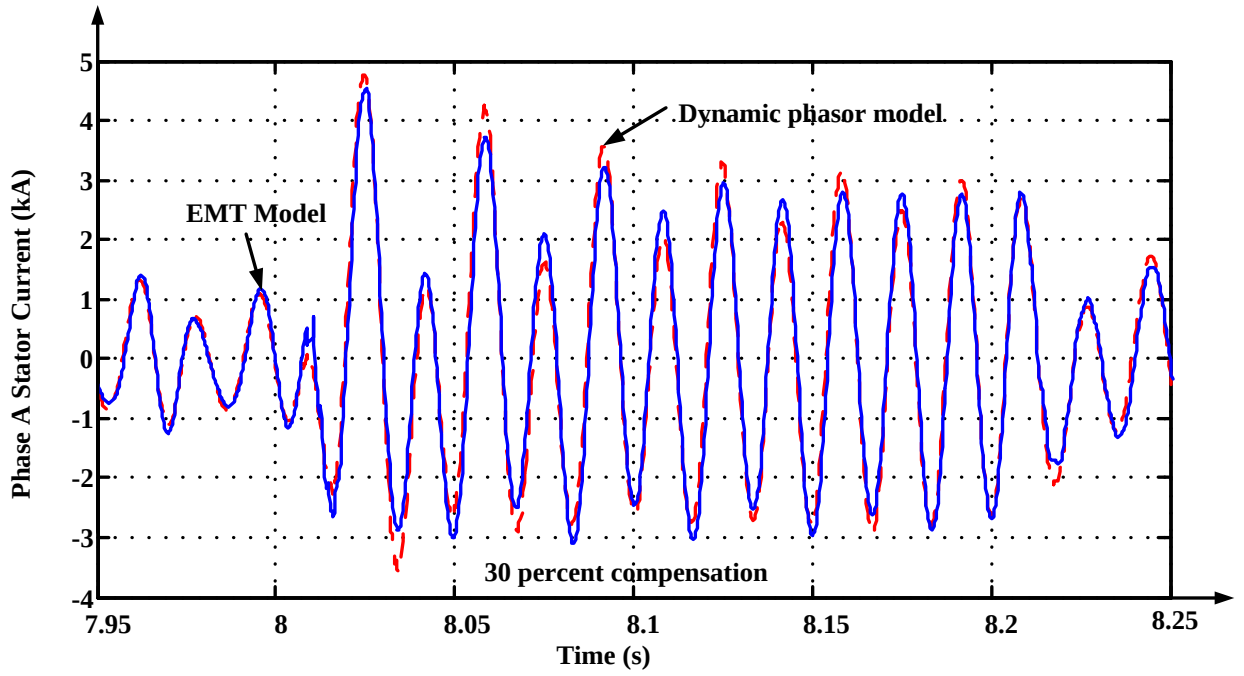

Figure 5.12: Comparison of EMT and dynamic phasor modeling for 30 percent series compensated Type 3 wind farm symmetrical fault application

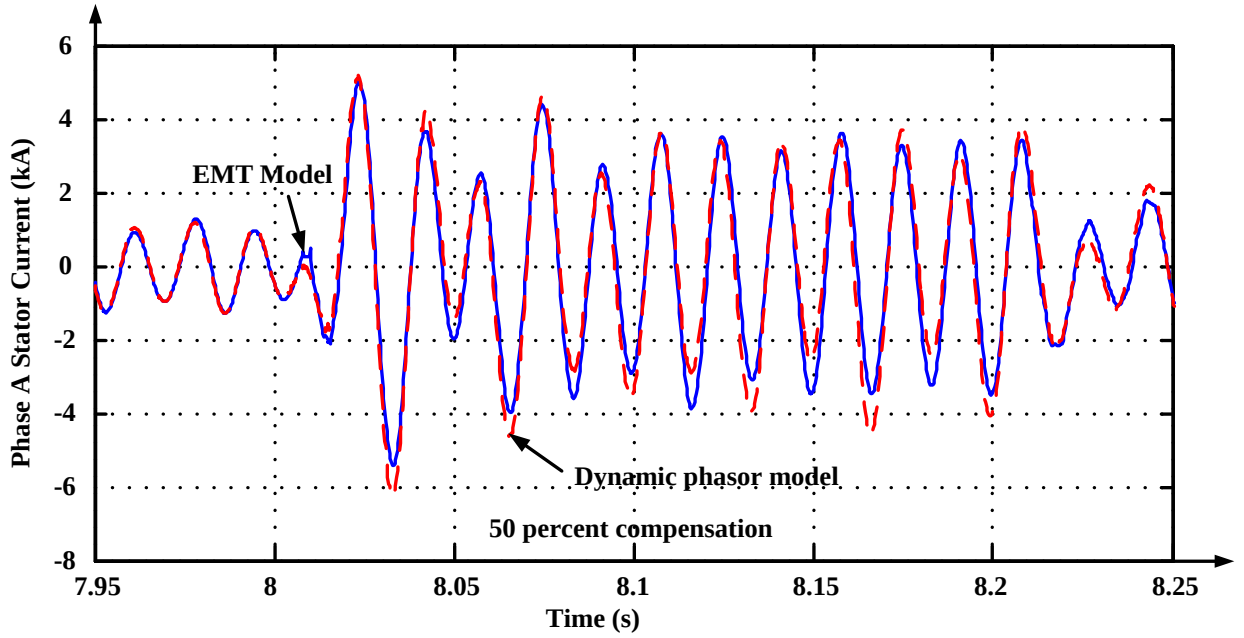

Figure 5.13: Comparison of EMT and dynamic phasor modeling for 50 percent series compensated Type 3 wind farm symmetrical fault application

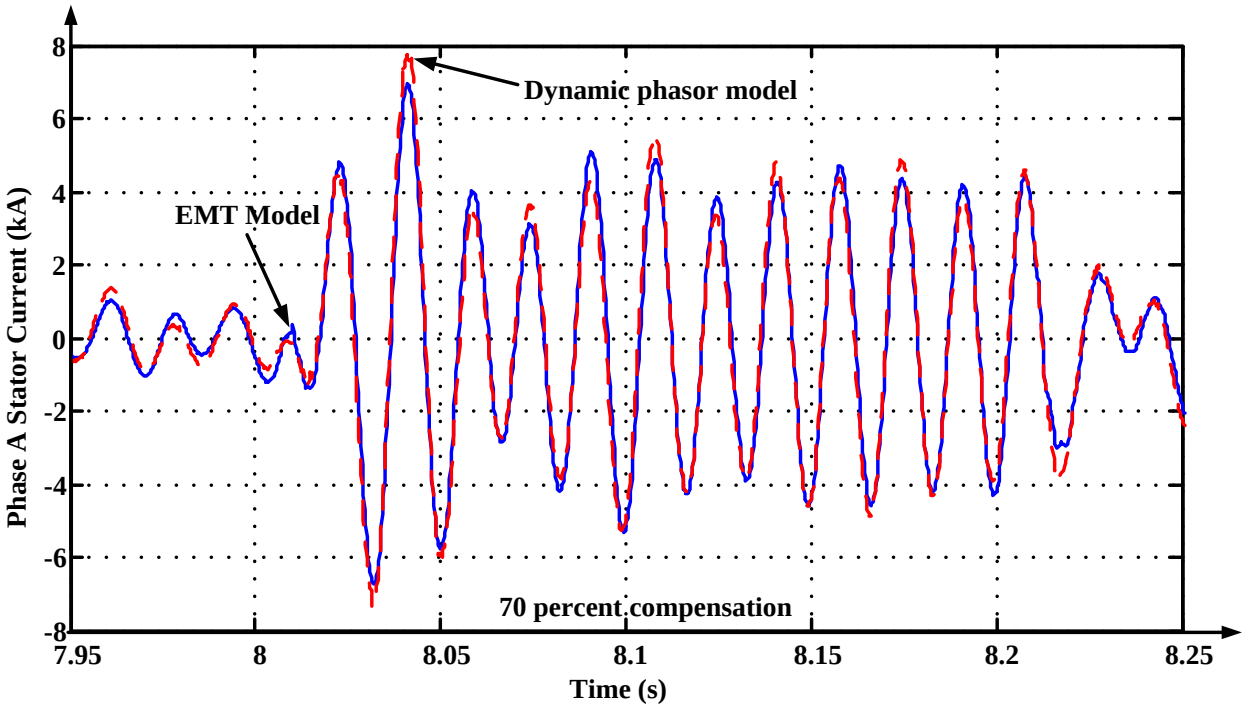

Figure 5.14: Comparison of EMT and dynamic phasor modeling for 70 percent series compensated Type 3 wind farm symmetrical fault application

5.4.3.2 Unsymmetrical Fault Behavior

The dynamic phasor model is also tested for accuracy for representing unsymmetrical fault behavior of a series compensated Type 3 wind farm. A 200 ms phase A to ground fault is applied at the point of interconnection of the wind farm to the grid. The phase A fault current obtained for a 50 percent compensated line with a Y-Y grounded transformer used in the test system is shown in Figure 5.15 below.

The dynamic phasor model for the Type 3 wind farm is developed by choosing the appropriate Fourier coefficients, which are the positive sequence, negative sequence, zero sequence and sub-synchronous component dynamic phasors as explained in Table 5.1. The zero sequence dynamic phasor is included as the Y-Y grounded transformer configuration allows the flow of zero sequence currents for an unsymmetrical fault. Figure 5.16 below shows the relative magnitudes of the dynamic phasors.

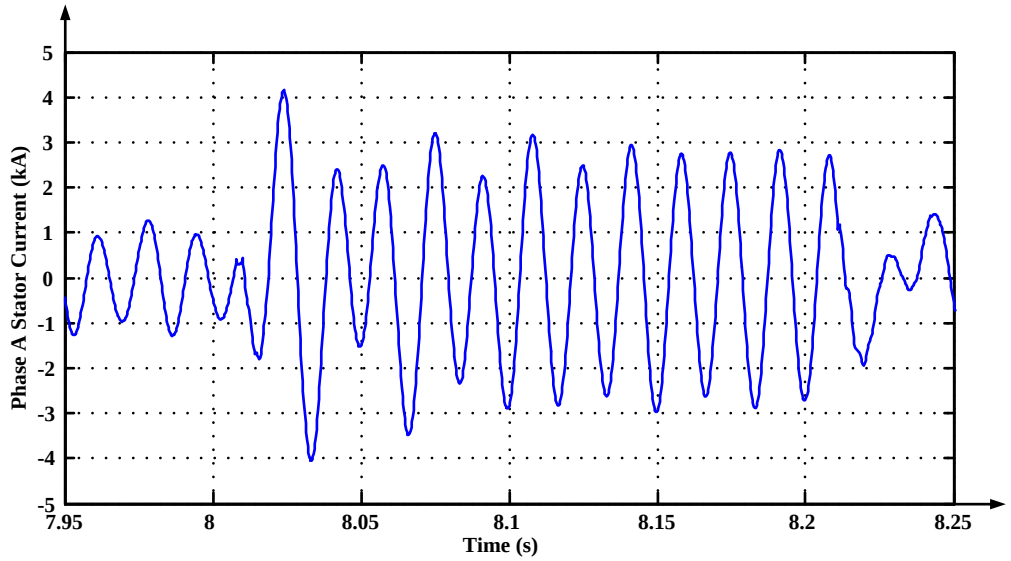

Figure 5.15: Type 3 wind farm phase A fault current for unsymmetrical fault with series compensation - EMT model

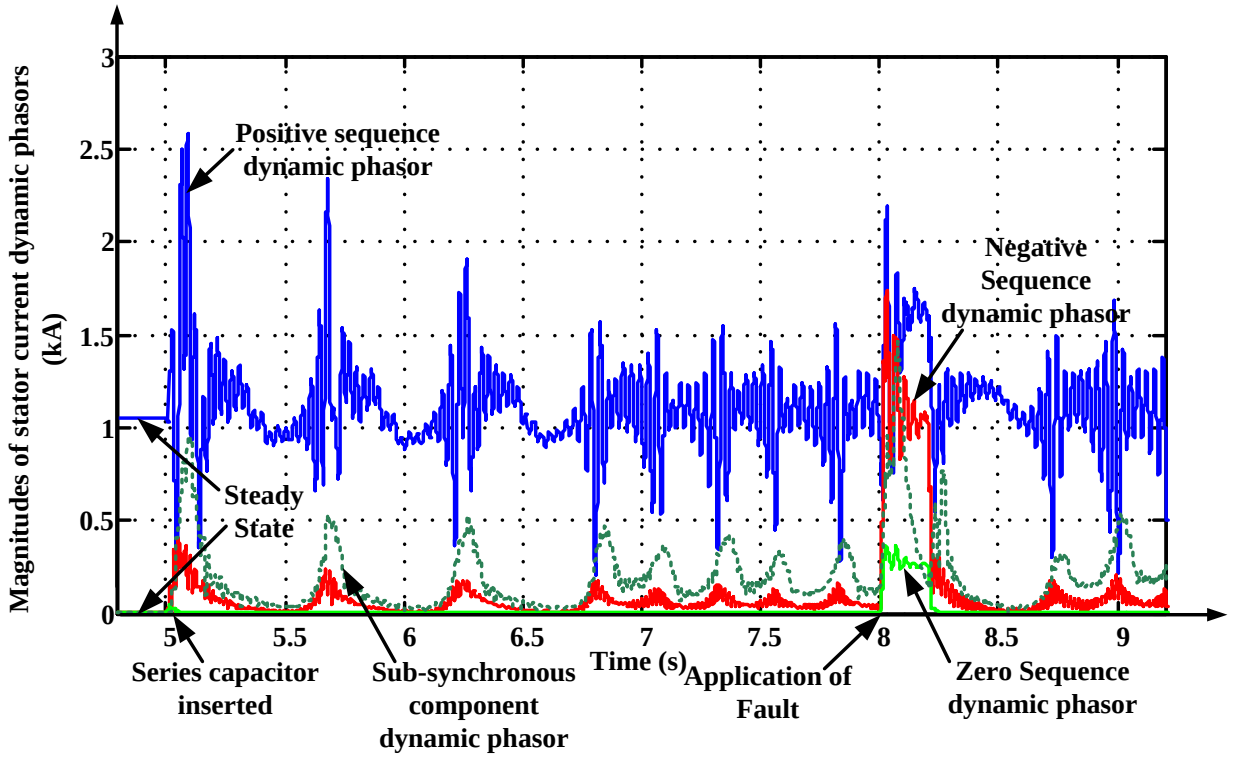

Figure 5.16: Relative magnitude of positive sequence, negative sequence, zero sequence and sub-synchronous component dynamic phasors for an unsymmetrical fault in a series compensated Type 3 wind farm

Using this selection of dynamic phasors, the model was developed and Figure 5.17 shows the high level of accuracy achieved with the developed model as compared to EMT simulation results. The dynamic phasor model was also found to be highly accurate for phase A to ground fault application for a test system with a Δ-Y transformer configuration. In such a case, the zero sequence dynamic phasor was not included as this transformer configuration does not allow zero sequence currents to flow through. Only the positive sequence, negative sequence and sub-synchronous frequency component dynamic phasors were included. In case of a different degree of series compensation, the appropriate sub-synchronous frequency component as explained in Section 5.4.3.1 is included.

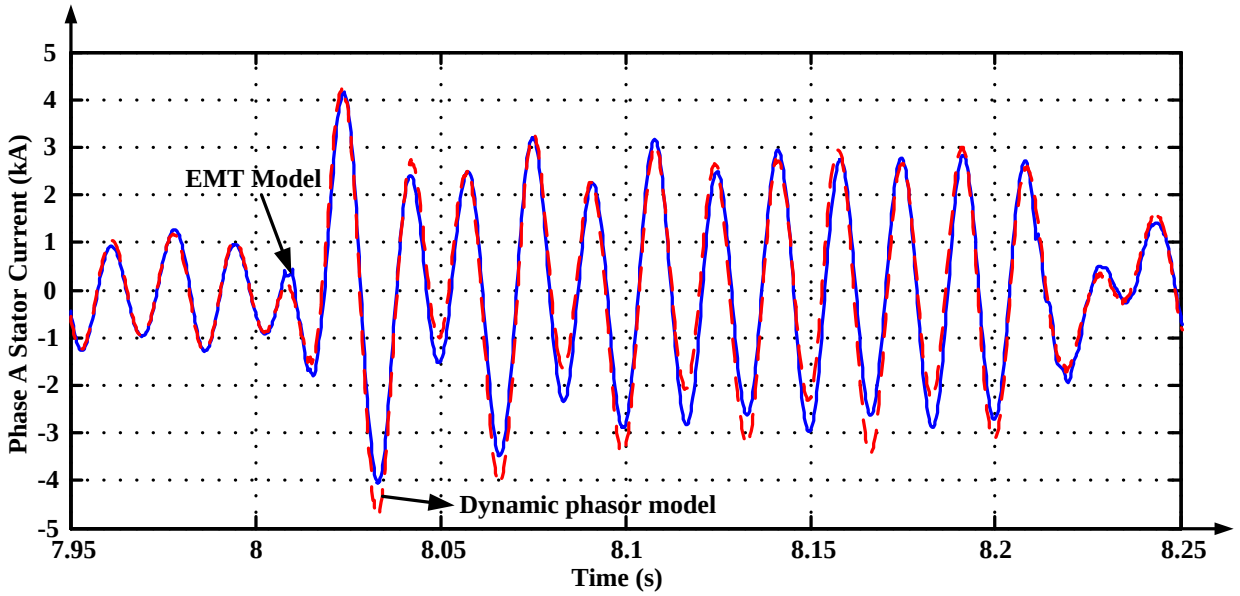

Figure 5.17: Comparison of EMT and dynamic phasor modeling for 50 percent series compensated Type 3 wind farm unsymmetrical fault application

5.5 Summary

This chapter introduced the generalized averaging theory of modeling power system variables as time-varying Fourier coefficients called dynamic phasors. The motivation behind proposing such a modeling approach for a complex system, such as a Type 3 wind farm connected to a series compensated transmission line, was explained along with its advantages, followed by developing the model itself. Using this modeling approach allows selective inclusion of only the appropriate dynamic phasors based on the fault behavior to be represented, making it computationally efficient. Unlike fundamental frequency approximations, this modeling method is capable of including non-fundamental sub-synchronous frequency dynamic phasors for accurately representing SSCI effects. The methodology for the appropriate choice of these dynamic phasors was explained and the proposed modeling technique shown to be capable of accurately representing symmetrical and unsymmetrical faults with and without the occurrence of SSCI.

Chapter 6

Summary and Conclusions

6.1 Summary

In recent years, the power grid has seen an ever growing integration of more wind farms. Wind generators have evolved from conventional Type 1 squirrel cage induction generators and Type 2 wound rotor induction generators to highly complex power electronic converter based Type 3 DFIG and Type 4 full power converter wind generators, with Type 3 having the highest market penetration.

Power system short circuit faults result in the flow of a large fault current, and protection equipment must isolate the faulted part of the system quickly enough so as to prevent equipment damage. Short circuit modeling of power system components is a critical exercise performed by power utilities worldwide to determine the protective relay settings, protection coordination, and equipment ratings. Short circuit modeling of wind generators is a complex and challenging task due to the many factors that influence their short circuit behavior and this has led to disagreement and ambiguity about the techniques to be used for modeling.

The study of the short circuit behavior of wind generators in Chapter 2 showed that the response of Type 1 and Type 2 wind generators to faults is relatively less complex. The fault current contribution of a Type 4 full converter based wind generator is limited by the rating of its converter and can be modeled by a current source. However, a Type 3 wind generator's short circuit behavior is much more complicated compared to the other types of wind generators due to the relatively large number of factors that determine its behavior. This research work analyzed these factors and proposed a modeling technique to develop an

accurate and generic short circuit model of a Type 3 wind farm.

Grid code and LVRT requirements necessitate Type 3 wind farms stay connected to the grid during low voltage conditions at the terminal of the wind farm and also provide reactive power support. This research work provided considerable clarity on the functionality of this feature. The ability to stay connected to the grid without damaging its sensitive power electronic equipment is enabled by using crowbar protection. The actual activation sequence of the crowbar and the LVRT based unit breaker protection was modeled as opposed to the assumption that the crowbar is triggered throughout the fault duration. This functionality was tested for fault applications as well as for voltage sags.

Chapter 3 discussed the different modeling techniques used to represent the short circuit behavior of wind generators. Type 1 and Type 2 wind generators can be accurately represented using the voltage behind transient reactance model. A fundamental frequency based model can accurately model their symmetrical fault behavior. However, such simplified modeling techniques are not accurate enough to represent the fault behavior of Type 3 wind generators due to their inherent assumptions. Even though the voltage dependent current source model is accurate, it is a black box approach and is not a standalone model as it depends on other modeling techniques for the fault current values.

Type 3 wind farms connected to series compensated transmission lines are prone to subsynchronous control interactions that could be triggered by faults. Chapter 4 discussed this very important modeling complexity of Type 3 wind farms. An aggregate model of a 450 MW Type 3 wind farm connected to a 50 percent compensated line was used as a test system and SSCI oscillations were demonstrated. Further analysis of the fault current waveforms was done to determine the frequency of these oscillations in order to model this behavior. Fundamental frequency approximations were incapable of modeling such behavior.

A modeling technique that can accurately represent SSCI effects in a Type 3 wind farm and at the same time is not as cumbersome to build as a detailed EMT model was proposed in Chapter 5. This modeling was based on the generalized averaging theory of representing power system variables using dynamic phasors or time-varying Fourier coefficients.

This technique achieved a middle ground between conventional fundamental frequency based electromechanical models and detailed EMT models with the ability to also represent non-fundamental frequencies accurately. This model can selectively model only those frequency components required for the fault behavior under study, making it efficient. The model was shown to be capable of accurately representing both symmetrical and unsymmetrical fault behavior as well as sub-synchronous interactions with a high degree of accuracy by comparing its results against benchmark EMT models.

6.2 Thesis Contributions

The following are the contributions of this thesis :

- *A comprehensive analysis of sub-synchronous interactions, LVRT and crowbar action in Type 3 wind generators and their impact on short circuit behavior:* This thesis discussed and analyzed the aspect of sub-synchronous control interactions in a Type 3 wind farm from a short circuit modeling perspective and its impact on short circuit behavior. Also described in detail is the Type 3 wind generator protection based on LVRT requirements and the corresponding active or passive crowbar action. The IEEE Power System Relaying Committee (PSRC) report, "Fault Current Contributions from Wind Plants" [48], which was recently completed, does not discuss these aspects.

- *Developing a generic short circuit model (dynamic phasor based model) of a Type 3 wind farm taking into account both fundamental and non-fundamental frequency behavior:* As discussed previously, detailed EMT models are capable of accurately representing a Type 3 wind farm's short circuit behavior but are cumbersome and computationally demanding. In this thesis, a dynamic phasor modeling technique, based on a generalized averaging method and which has the ability to represent both fundamental and non-fundamental frequency behavior, has been proposed and implemented. This modeling approach allows the user to selectively add frequency components other than the fundamental frequency representation, namely the sub-synchronous frequency

components. This method was tested for symmetrical fault, unsymmetrical fault, and sub-synchronous interaction scenarios of Type 3 wind farms. The sub-synchronous interactions were tested by adding series compensation in the transmission line connected to the Type 3 wind farm test system.

6.3 Future Work

- *Developing the voltage behind transient reactance and analytical expression models for a wind farm:* This research work considers these models only for a single wind generator connected to the grid. It will be required to extend these methods to be applied to a wind farm with multiple generator units connected together.

- *Developing a synchronous generator based equivalent model for a Type 3 wind farm:* The practice in the industry has been to perform field tests on wind farms and utilize the recorded waveform characteristics to develop an equivalent model using a synchronous generator and its controls. Future work will be develop such a model and validate it against the dynamic phasor model developed in this research work.

- *Validating the results of the dynamic phasor model against real fault data records:* The short circuit behavior of the Type 3 wind farm obtained from the dynamic phasor model needs to be validated against real fault data records obtained from utilities. This will ensure additional validation of the accuracy of the model which has already been validated against benchmark EMT models.

- *Developing the dynamic phasor model in a real time digital simulator to design and test protection functions of relays:* The dynamic phasor model of a Type 3 wind farm has to be developed in a real time simulator so that hardware in the loop test of relays can be performed. This would allow the design of protection coordination and also test their working in real time.

- *Studying the impact of fault location and internal faults in wind farms:* The fault studies on Type 3 wind farms have so far been done for faults occurring outside the

wind farm at the point of interconnection of the wind farm to the grid. However, faults internal to the wind farm, i.e., faults occurring on the feeders connecting the individual wind generators to the substation, are also possible. Such faults would not only comprise the respective wind generator's fault contribution but also that from the other units in the wind farm. Thus, an aggregate model of the wind farm cannot be used. For these reasons, these kinds of faults must be studied to develop short circuit models that are inclusive of such behavior.

- *Studying the impact of a multi-mass model:* In this thesis, the generator, the turbine, and the shaft have been lumped together and modeled as a single mass model. This modeling is sufficient for studying sub-synchronous control interactions between the generator controls and the series compensated line. However, a multi-mass model is required to study possible sub-synchronous resonance conditions, where the series compensated line interacts with the turbine generator shaft system at frequencies below the synchronous frequency of the system. Such a model would represent the low-speed turbine and the high-speed generator as a two mass model and the shaft as a spring and a damper.

- *Improving accuracy of the analytical expression method:* The analytical expression used to determine the short circuit behavior of wind generators in this thesis work does not take into account the decrement of the voltage, i.e., of the flux linkage. This is an approximation based on the constancy of flux linkages which is valid only for a very short duration after initiation of the fault. Computing the voltage using an additional differential equation representing the flux decrement would increase the accuracy and the utility of this modeling approach.

References

[1] "Global Wind Report - Annual Market Update 2012," Global Wind Energy Council, Brussels, Tech. Rep., 2012.

[2] "Renewables 2012 Global Status Report," Renewable Energy Policy Network for the 21st Century (REN21), Tech. Rep., June 2012.

[3] "Renewable Energy Essentials: Wind," International Energy Agency, Tech. Rep., 2008.

[4] A. D. Hansen and L. H. Hansen, "Market penetration of wind turbine concepts over 10 years (1995-2004)," *Wind Energy - Issue 1, Wiley Interscience*, vol. 10, pp. 81–97, 2006.

[5] Shun Hsien Huang, D. Maggio, K. McIntyre, V. Betanabhatla, J. Dumas, and J. Adams, "Impact of wind generation on system operations in the deregulated environment: ERCOT experience," in *Power & Energy Society General Meeting, IEEE*, Calgary, Alberta, Canada, July 2009, pp. 1–8.

[6] G. D. Irwin, A. K. Jindal, and A. L. Isaacs, "Sub-synchronous control interactions between Type 3 wind turbines and series compensated AC transmission systems," in *Power and Energy Society General Meeting, IEEE*, Detroit, Michigan, USA, 2011, pp. 1–6.

[7] C. Karawita and U. Annakkage, "A hybrid network model for small signal stability analysis of power systems," in *Power and Energy Society General Meeting, IEEE*, Minneapolis, Minnesota, USA, July 2010, pp. 25–29.

[8] A. Luna, F. K. A. Lima, D. Santos, P. Rodriguez, E. H. Watanabe, and S. Arnaltes, "Simplified Modeling of a DFIG for Transient Studies in Wind Power Applications," *IEEE Transactions on Industrial Electronics*, vol. 58, pp. 9–20, 2011.

[9] M. Kayikci and J. V. Milanovic, "Assessing Transient Response of DFIG-Based Wind Plants - The Influence of Model Simplifications and Parameters," *IEEE Transactions on Power Systems*, vol. 23, pp. 545–554, May 2008.

[10] E. Muljadi, N. Samaan, V. Gevorgian, Jun Li, and S. Pasupulati, "Different Factors Affecting Short Circuit Behavior of a Wind Power Plant," *IEEE Transactions on Industry Applications*, vol. 49, no. 1, pp. 284–292, 2013.

[11] T. Ackermann, Ed., *Wind Power in Power Systems*. John Wiley & Sons, Ltd, 2005.

[12] W. P. Wagner, "Short circuit contribution of large induction motors," *Proceedings of the Institution of Electrical Engineers*, vol. 116, no. 6, pp. 985–990, 1969.

[13] S. S. Kalsi, B. Adkins, and D. D. Stephen, "Calculation of system fault currents due to induction motors," *Proceedings of the Institution of Electrical Engineers*, vol. 118, no. 1, pp. 201–215, 1971.

[14] J. Morren and S. W. H. de Haan, "Short Circuit Current of Wind Turbines With Doubly Fed Induction Generator," *IEEE Transactions on Energy Conversion*, vol. 22, pp. 174–180, 2007.

[15] E. Muljadi and V. Gevorgian, "Short circuit modeling of a wind power plant," in *Power and Energy Society General Meeting, IEEE*, Detroit, Michigan, USA, 2011.

[16] P. Karaliolios, A. Ishchenko, E. Coster, J. Myrzik, and W. Kling, "Overview of short circuit contribution of various distributed generators on the distribution network," in *43rd International Universities Power Engineering Conference*, 2008, pp. 1–6.

[17] D. F. Howard, J. Restrepo, T. Smith, M. Starke, J. Dang, and R. G. Harley, "Calculation of Fault Current Contribution of Type 1 Wind Turbine Generators," in *Power and Energy Society General Meeting, IEEE*, Detroit, Michigan, USA, 2011, pp. 1–7.

[18] S. Brahma, M. Chaudhary, and S. Ranade, "Some findings about equivalencing windfarms with Type 1 and Type 2 induction generators," in *North American Power Symposium*, Boston, Massachusetts, USA, 2011, pp. 1–6.

[19] M. Chaudhary, S. M. Brahma, and S. J. Ranade, "Short circuit analysis of Type II induction generator and wind farm," in *IEEE PES Transmission and Distribution Conference and Exposition*, Montevideo, Uruguay, 2012, pp. 1–5.

[20] C. Abbey, J. Morneau, J. Mahseredjian, and G. Joos, "Modeling requirements for transient stability studies for wind parks," in *Power Engineering Society General Meeting, IEEE*, Montreal, Quebec, Canada, 2006, p. 6.

[21] J. G. Slootweg and W. L. Kling, "Aggregated modelling of wind parks in power system dynamics simulations," in *Power Tech Conference Proceedings, IEEE*, vol. 3, Bologna, Italy, 2003, p. 6.

[22] Markus Poller and S. Achilles, "Aggregated Wind Park Models for Analyzing Power System Dynamics," in *4th Int. Workshop Large-Scale Integration of Wind Power and Transmission Networks for Offshore Wind Farms*, Billund, Denmark, Oct 2003.

[23] L. Fan, R. Kavasseri, Z. L. Miao, and C. Zhu, "Modeling of DFIG Based Wind Farms for SSR Analysis," *IEEE Transactions on Power Delivery*, vol. 25, no. 4, pp. 2073–2082, 2010.

[24] J. Morren and S. de Haan, "Ridethrough of wind turbines with doubly-fed induction generator during a voltage dip," *IEEE Transactions on Energy Conversion*, vol. 20, pp. 435–441, 2005.

[25] I. J. Gabe, H. Grundling, and H. Pinheiro, "Design of a voltage sag generator based on impedance switching," in *37th Annual Conference on IEEE Industrial Electronics Society*, Melbourne, Australia, 2011, pp. 3140–3145.

[26] I. Erlich and F. Shewarega, "Interaction of Large Wind Power Generation Plants with the Power System," in *IEEE International Power and Energy Conference*, Malaysia, 2006, pp. 12–18.

[27] D. H. R. Suriyaarachchi, U. D. Annakkage, C. Karawita, and D. A. Jacobson, "A Procedure to Study Sub-Synchronous Interactions in Wind Integrated Power Systems," *IEEE Transactions on Power Systems*, vol. 28, no. 1, pp. 377–384, Feb 2013.

[28] N. Johansson, L. Angquist, and H. P. Nee, "A Comparison of Different Frequency Scanning Methods for Study of Subsynchronous Resonance," *IEEE Transactions on Power Systems*, vol. 26, no. 1, pp. 356–363, 2011.

[29] M. Sahni, D. Muthumuni, B. Badrzadeh, A. Gole, and A. Kulkarni, "Advanced screening techniques for sub-synchronous interaction in wind farms," in *Transmission and Distribution Conference and Exposition (T D), 2012 IEEE PES*, Orlando, Florida, USA, 2012, pp. 1–9.

[30] B. Badrzadeh, M. Sahni, D. Muthumuni, Y. Zhou, and A. Gole, "Sub-synchronous interaction in wind power plants part I: Study tools and techniques," in *Power and Energy Society General Meeting, IEEE*, San Diego, CA, USA, 2012, pp. 1–9.

[31] E. V. Larsen, "Wind generators and series-compensated AC transmission lines," in *IEEE PES Transmission and Distribution Conference and Exposition*, Orlando, Florida, USA, 2012, pp. 1–4.

[32] "Lesson Learned - Sub-Synchronous Interaction between Series-Compensated Transmission Lines and Generation," North American Electric Reliability Corporation, Tech. Rep., July 2011.

[33] M. S. El Moursi, B. Bak Jensen, and M. H. Abdel Rahman, "Novel STATCOM Controller for Mitigating SSR and Damping Power System Oscillations in a Series Compensated Wind Park," *Power Electronics, IEEE Transactions on*, vol. 25, no. 2, pp. 429–441, 2010.

[34] D. H. R. Suriyaarachchi, U. D. Annakkage, C. Karawita, D. Kell, R. Mendis, and R. Chopra, "Application of an SVC to damp sub-synchronous interaction between wind farms and series compensated transmission lines," in *Power and Energy Society General Meeting, IEEE*, San Diego, CA, USA, 2012, pp. 1–6.

[35] R. K. Varma, S. Auddy, and Y. Semsedini, "Mitigation of Subsynchronous Resonance in a Series-Compensated Wind Farm Using FACTS Controllers," *IEEE Transactions on Power Delivery*, vol. 23, no. 3, pp. 1645–1654, 2008.

[36] P. C. Krause and C. H. Thomas, "Simulation of Symmetrical Induction Machinery," *IEEE Transactions on Power Apparatus and Systems*, vol. 84, pp. 1038 – 1053, Nov 1965.

[37] E. Gursoy and R. A. Walling, "Representation of variable speed wind turbine generators for short circuit analysis," in *Electrical Power and Energy Conference (EPEC), IEEE*, Winnepeg, Manitoba, Canada, Oct 2011, pp. 444–449.

[38] S. R. Sanders, J. M. Noworolski, X. Z. Liu, and G. C. Verghese, "Generalized averaging method for power conversion circuits," *IEEE Transactions on Power Electronics*, vol. 6, pp. 251–259, 1991.

[39] Aleksandar M. Stankovic, Bernard C. Lesieutre, and T. Aydin, "Applications of Generalized Averaging to Synchronous and Induction Machines," in *28th North American Power Symposium, M.I.T*, Nov 1996.

[40] P. Mattavelli, G. C. Verghese, and A. Stankovic, "Phasor dynamics of thyristor-controlled series capacitor systems," *IEEE Transactions on Power Systems*, vol. 12, no. 3, pp. 1259–1267, 1997.

[41] P. C. Stefanov and A. M. Stankovic, "Modeling of UPFC operation under unbalanced conditions with dynamic phasors," *IEEE Transactions on Power Systems*, vol. 17, no. 2, pp. 395–403, 2002.

[42] M. A. Hannan, A. Mohamed, and A. Hussain, "Modeling and power quality analysis of STATCOM using phasor dynamics," in *IEEE International Conference on Sustainable Energy Technologies*, Kathmandu, Nepal, 2008, pp. 1013–1018.

[43] L. Piyasinghe, Z. Miao, and L. Fan, "Dynamic phase based model of Type 1 wind generator for unbalanced operation," in *Power Electronics and Machines in Wind Applications, IEEE*, Denver, USA, 2012, pp. 1–5.

[44] T. Demiray, F. Milano, and G. Andersson, "Dynamic Phasor Modeling of the Doubly-fed Induction Generator under Unbalanced Conditions," in *Power Tech, IEEE*, Lausanne, Switzerland, 2007, pp. 1049–1054.

[45] Turhan Hilmi Demiray, "Simulation of Power System Dynamics using Dynamic Phasor Models," Ph.D. dissertation, Swiss Federal Institute of Technology, Zurich, 2008.

[46] E. Muljadi, N. Samaan, V. Gevorgian, Jun Li, and S. Pasupulati, "Short circuit current contribution for different wind turbine generator types," in *Power and Energy Society General Meeting, IEEE*, Minneapolis, Minnesota, USA, 2010, pp. 1–8.

[47] N. Z. BinWu, Yongqiang Lang and Samir Kouro, *Power Conversion and Control of Wind Energy Systems.* John Wiley & Sons, Inc., 2011.

[48] Joint Working Group on Fault Current Contributions from Wind Plants, "Fault Current Contributions from Wind Plants - Draft 7.1," IEEE Power Systems Relaying Committee, Tech. Rep., 2012.

[49] A. M. Gole, U. Annakage, F.Mosallat, and D. Muthumani, "A proposed benchmark system for wind energy incorporation in a large electric network," Dept. of Electrical and Computer Eng., University of Manitoba and Manitoba HVDC Research Centre, Winnipeg, Canada, Tech. Rep.

[50] G. Abad, J. Lopez, M. Rodriguez, P.guez, L. Marroyo, and G. Iwanski, *Doubly Fed Induction Machine: Modeling and Control for Wind Energy Generation.* Wiley-IEEE Press, 2011.

[51] George J. Wakileh, *GE 1.5 MW, 60 Hz Wind Turbine General Data*, GE Wind Energy, California, USA.

[52] N. Stringer, "The effect of DC offset on current-operated relays," *IEEE Transactions on Industry Applications*, vol. 34, no. 1, pp. 30–34, 1998.

[53] Joint Working Group on Fault Current Contributions from Wind Plants, "Current Contribution from Wind Plant for a System Fault," IEEE Power Systems Relaying Committee, Tech. Rep., 2010.

[54] Lingling Fan, R. Kavasseri, Zhixin Lee Miao, and Chanxia Zhu, "Modeling of DFIG Based Wind Farms for SSR Analysis," *IEEE Transactions on Power Delivery*, vol. 25, pp. 2073–2082, 2010.

[55] L. F. W. Souza, T. M. L. Assis, and I. F. Visconti, "On the assessment of voltage ride-through needs of the power transmission Grid," in *Bulk Power System Dynamics and Control Symposium*, Rio de Janeiro, Brazil, Aug 2010, pp. 1–10.

[56] V. Akhmatov, "Analysis of dynamic behavior of electric power systems with large amount of wind power," Ph.D. dissertation, Technical University of Denmark, 2003.

[57] J. F. Hauer, C. J. Demeure, and L. L. Scharf, "Initial results in Prony analysis of power system response signals," *IEEE Transactions on Power Systems*, vol. 5, pp. 80–89, 1990.

[58] J. Hauer, "Identification of power system models for large scale damping control," in *Proceedings of the 28th IEEE Conference on Decision and Control*, vol. 2, Tampa, Florida, USA, 1989, pp. 1841–1846.

[59] R. P. S. Leo, J. B. Almada, P. A. Souza, R. J. Cardoso, R. F. Sampaio, F. K. A. Lima, J. G. Silveira, and L. E. P. Formiga, "The Implementation of the Low Voltage Ride-Through Curve on the Protection System of a Wind Power Plant," in *International Conference on Renewable Energies and Power Quality*, Spain, April 2010.

[60] P. Kundur, *Power System Stability and Control*. New York: McGraw-Hill, 1994.

Appendix A

System data

A.1 Type 1 GE Wind Generator Test System Parameters

Table A.1: Type 1 wind generator test system data

Generator data	$1.717\,MVA$, $1.545\,MW$, $0.575\,kV$, $60\,Hz$, $Poles = 6$, $H = 4.55\,s$, $R_{stator} = 0.00727\,p.u$, $R_{rotor} = 0.00514\,p.u$, $L_m = 2.9922\,p.u$, $L_{stator} = 0.1766\,p.u$, $L_{rotor} = 0.1610\,p.u$
Transmission line data	$R_{Line} = 0.002\,\Omega$, $L_{line} = 2.36e-5\,H$
Transformer data	$2\,MVA$, $60\,Hz$, $Y-\Delta$, $0.575/34.5\,kV$, $X_t = 0.05\,pu$

A.2 Type 2 Suzlon Wind Generator Test System Parameters

Table A.2: Type 2 wind generator test system data

Generator data	$2.283\ MVA,\ 0.6\ kV,\ 60\ Hz,\ H = 4.7\ s,\ R_{stator} = 0.017\ p.u,$ $R_{rotor} = 0.0215\ p.u,\ L_m = 16.497\ p.u,\ L_{stator} = 0.340\ p.u,$ $L_{rotor} = 0.3577\ p.u$
Transmission line data	$R_{Line} = 0.002\,\Omega,\ L_{line} = 2.36e-5\ H$
Transformer data	$2.5\ MVA,\ 60\ Hz,\ Y-\Delta,\ 0.6/34.5\ kV,\ X_t = 0.05\ pu$

A.3 Type 3 Wind Generator Test System Parameters

Table A.3: Type 3 wind generator test system data

Generator data	$3.4\,MVA$, $0.69\,kV$, $60\,Hz$, $J = 1.856\,s$, $R_{stator} = 0.0054\,p.u$, $R_{rotor} = 0.00607\,p.u$, $L_m = 4.362\,p.u$, $L_{stator} = 0.102\,p.u$, $L_{rotor} = 0.11\,p.u$
Crowbar circuit	$R_{crowbar} = 0.1\,\Omega$, $R_{IGBT-ON} = 0.01\,\Omega$, $R_{IGBT-OFF} = 1.0e6\,\Omega$, $V_{dc-UL} = 1.3\,p.u$, $V_{dc-LL} = 1.05\,p.u$
Back to back converter	$R_{IGBT-ON-GSC} = 0.0005\ \Omega$, $R_{IGBT-ON-RSC} = 0.01\ \Omega$, $R_{IGBT-OFF} = 1.0e6\,\Omega$.
Rotor side controller	$K_{P,Q_s} = 1.0$, $K_{I,Q_s} = 1.0\ s$, $K_{P,P_s} = 1.0$, $K_{I,P_s} = 1.0\ s$, $K_{P,i_{r,d}} = 1.0$, $K_{I,i_{r,d}} = 2.0\ s$, $K_{P,i_{r,q}} = 1.0$, $K_{I,i_{r,q}} = 2.0\ s$
Grid side controller	$K_{P,Q_g} = 1.0$, $K_{I,Q_g} = 0.02\ s$, $K_{P,V_{dc}} = 1.0$, $K_{I,V_{dc}} = 0.02\ s$, $K_{P,i_{g,q}} = 0.1$, $K_{I,i_{g,q}} = 0.1\ s$, $K_{P,i_{g,d}} = 1.0$, $K_{I,i_{g,d}} = 0.02\ s$
Transmission line data	$240kms$, $R_{Line} = 0.3107e{-}7p.u/m$, $X_{Line} = 0.3479e{-}6p.u/m$, $B_{Line} = 5.1885e-6\,p.u/m$
Transformer data	$3.4\,MVA$, $60\,Hz$, $Y-Y-Y$, $0.482/33/0.688\,kV$, $X_{1-2} = 0.0888\,p.u$, $X_{1-3} = 0.1663\,p.u$, $X_{2-3} = 0.0875\,p.u$